

“You are required to assist on the Atmospheric Structure Reconstruction using the Beagle 2 Entry, Descent, and Landing Accelerometer”

Final Report to
The Planetary and Space Sciences Research Institute,
The Open University
For Consultancy Contract 01249983\001

Date: 2001-08-17

Paul Withers
withers@lpl.arizona.edu

Lunar and Planetary Laboratory
University of Arizona
Tucson, Arizona 85721, USA
Phone: +1 520 621 1507
Fax: +1 520 621 4933

Summary

A theoretical model for reconstructing a planetary entry trajectory and atmospheric structure is developed using measured accelerations. This is a reproduction of work done at NASA-Ames by Seiff and colleagues. Several options for modelling spacecraft attitude are discussed – a drag-only model, a gyroscopic model, and a model using ratios of accelerations.

This model is tested on the Mars Pathfinder Accelerometer data, publicly available from the PDS. There may be an error in the entry state quoted with this data. Using another entry state at 132 km altitude, I reconstruct the atmospheric trajectory to within a few hundredths of a degree in latitude and longitude. I reconstruct the atmospheric density and pressure to within 2% below 120 km. I reconstruct the atmospheric structure, compared to the PDS results, to better than 5 K above 40 km and to better than 8 K below this. The discrepancy is largest at low altitudes where my aerodynamic knowledge is poorest. There is no significant discrepancy at the highest altitudes. My entire knowledge of the spacecraft aerodynamics is a scanned figure. In practice, one would use an extensive database generated by experiment and numerical simulation.

The effects of uncertainties in entry state and aerodynamic properties on the reconstructed trajectory and atmospheric structure are studied. The effects of instrument digitisation, sampling rate, and systematic offset on the reconstructed trajectory and atmospheric structure are studied.

A bibliography has been compiled and a simple search procedure provides an interface. The main references are briefly discussed.

All computer programs used in this work have been commented, archived, and are discussed in detail in this report. A flowchart depicts the main trajectory and atmospheric structure reconstruction programs.

Recommendations to build upon these results and to prepare for the planetary entries of Beagle 2 and Huygens are made.

Contents

- 1 Introduction
- 2 General Solution Procedure
 - 2.1 Frame Definitions
 - 2.1.1 Inertial Cartesian and Spherical Frames
 - 2.1.2 Momentary Inertial and Spherical Frames
 - 2.1.3 Transformations between Frames
 - 2.1.4 Caveats
 - 2.2 Rigid Body Dynamics
 - 2.3 Initial Conditions
 - 2.4 Gravity-Only Solution Algorithm
 - 2.5 The Spacecraft Frame
 - 2.6 [I can't count...]
 - 2.7 Basic Solution Algorithm with Black Box Aerodynamics
 - 2.8 Aerodynamic Options
 - 2.8.1 Drag-only
 - 2.8.2 Gyroscopes
 - 2.8.3 Acceleration ratios
 - 2.8.4 Pros and cons
 - 2.9 Solution Procedure for Drag-only Option
 - 2.10 Solution Procedure for Gyroscopes Option
 - 2.10.1 Euler angles
 - 2.10.2 Algorithm
 - 2.11 Solution Procedure for Acceleration Ratios Option
 - 2.11.1 Aerodynamics as I understand it
 - 2.11.2 Acceleration Ratios and Angle-Of-Attack
 - 2.11.3 Algorithm
 - 2.12 Atmospheric structure reconstruction
 - 2.13 Additional Constraints
 - 2.14 Effects of Errors and Uncertainties
- 3 Mars Pathfinder Test Case
 - 3.1 Mars Pathfinder Mission Summary
 - 3.2 Necessary Data and Entry State
 - 3.3 Reconstructed Mars Pathfinder Trajectory
 - 3.4 Mars Pathfinder Aerodynamic Properties
 - 3.5 Reconstructed Mars Pathfinder Atmospheric Structure
 - 3.6 Reconstructing the Reconstruction
- 4 Error and Uncertainty
 - 4.1 Uncertainty in Entry State Parameters
 - 4.2 Uncertainty in Aerodynamic Properties
 - 4.3 Digitisation of acceleration measurements
 - 4.4 Reduced Sampling Rate
 - 4.5 Systematic offset in acceleration measurements
 - 4.6 Effect of the Atmosphere on the Trajectory

- 5 Recommendations

- 6 Bibliography and Resources
 - 6.1 Early Work and Overview
 - 6.2 Viking
 - 6.3 Pioneer Venus
 - 6.4 Galileo
 - 6.5 Mars Pathfinder
 - 6.6 Others
 - 6.7 Correspondence

- 7 Detailed Look at Archived Computer Programs
 - 7.1 E:/
 - 7.2 E:/idl/
 - 7.3 E:/idl/mpf_nominal/
 - 7.3.1 Flowchart
 - 7.4 E:/idl/effects_of_errors/
 - 7.5 E:/idl/gyroscopes/

- 8 References

1- Introduction

[Seiff, 1990, 1991]

Given the initial position and velocity of a planetary entry spacecraft, knowledge of a planet's gravitational field, and regular measurements of the aerodynamic forces experienced by the spacecraft, the planetary entry trajectory may be reconstructed from atmospheric entry to landing. This is a trivial statement. What is less obvious is that the aerodynamic forces acting on the spacecraft can be analysed to provide measurements of atmospheric density, pressure, and temperature along the entry trajectory.

This insight seems to have originated with, or at least was rapidly developed by, staff at NASA-Ames led by Al Seiff in the early 1960s. Earlier work on intercontinental ballistic missiles that would survive terrestrial re-entry at typical planetary entry speeds provided the basic framework for Seiff's work.

$$\rho C_D A V_r^2 = -2ma_v \quad (1)$$

ρ is atmospheric density

C_D is a dimensionless fudge factor called the drag force coefficient

A is a reference area for the spacecraft

V_r is the speed of the spacecraft relative to the surrounding atmosphere

m is the spacecraft mass

a_v is the linear acceleration of the spacecraft, due to aerodynamic forces, in the direction of the velocity of the spacecraft relative to the surrounding atmosphere

This equation is the key to converting measurements of linear acceleration into atmospheric density. Grossly oversimplifying, C_D is known from preflight modelling and experiments, A is known from the spacecraft design, V_r is known from the trajectory integration thus far, m is known from the spacecraft design and fuel consumption, and a_v is measured by onboard accelerometers. Hence, equation (1) may be solved for ρ at each point along the entry trajectory. Complications that arise in practice will be discussed in excruciating depth later.

Given ρ , the equation of hydrostatic equilibrium can be integrated to give the atmospheric pressure, p , along the trajectory.

$$\frac{dp}{dh} = -\rho g \quad (2)$$

h is altitude

g is the linear acceleration due to gravity

Given ρ , p , and the relevant atmospheric composition, an equation of state gives the atmospheric temperature, T , along the trajectory. The ideal gas equation is often used.

$$pV = NkT \quad (3)$$

V is the volume of a given amount of gas

N is the number of molecules in that given amount of gas

k is Boltzmann's constant

which rearranges to

$$pm_m = \rho RT \quad (4)$$

m_m is the mean molecular mass of the gas per mole

R is the universal gas constant

The techniques developed in the literature to reconstruct the trajectory and atmospheric structure often come from a time before computers. They tend to work in just one frame, one that rotates with the planet. This requires integration of the equations of motion in a rotating frame, which can be complicated in the fully general case. I preferred to integrate in an inertial frame and use other frames as needed.

Theoretical discussions in the 1960s culminated in 1971 in a test-flight, PAET, into the Earth's atmosphere. This verified instruments and analysis techniques.

Planetary flight heritage includes:

1976	Viking landers	2	Mars
1978	Pioneer Venus probes	4	Venus
1995	Galileo probe	1	Jupiter
1997	Mars Pathfinder	1	Mars
1999	Mars Polar Lander	1	Mars (failed)
	May or may not have had accelerometers onboard		
1999	Deep Space 2	2	Mars (failed)
2003	Mars Exploration Rovers	2	Mars (upcoming)
2003	Beagle 2	1	Mars (upcoming)
2005	Huygens	1	Saturn (upcoming)
1961 - present	Venera and Vega	many	Venus
	Soviet landers of varying success		
	May or may not have had accelerometers onboard		
	See nssdc.gsfc.nasa.gov		
1971 – present	Mars 2, 3, 6, 7, Phobos, Mars 96	many	Mars
	Soviet landers of varying success		
	May or may not have had accelerometers onboard		
	See nssdc.gsfc.nasa.gov		

Earth re-entry examples include PAET and the Shuttle. No doubt there are many more, including Mercury, Gemini, and Apollo.

It is reasonable to assume that almost every spacecraft that passes through an atmosphere is equipped with accelerometers for atmospheric structure reconstruction.

Atmospheric aerobraking and aerocapture are very similar processes.

1978 – 1992	Pioneer Venus orbiter OAD experiment (Keating) was almost an accelerometer	1	Venus
1990 – 1994	Magellan Windmill experiment was almost an accelerometer	1	Venus
1997 – present	Mars Global Surveyor Aerobraking	1	Mars
1999	Mars Climate Orbiter Aerobraking	1	Mars (failed)
2001	Mars Odyssey Aerobraking	1	Mars (upcoming)

Nozomi, Mars Express, and future Mars spacecraft may include aerobraking and aerocapture. Aerocapture is extremely desirable for sample-return missions.

2 - General Solution Procedure

2.1 – Frame Definitions

First we need some coordinate systems.

2.1.1 – Inertial Cartesian and Spherical Frames

[Bradbury, 1968]

[E:/idl/mpf_nominal/getaltlatlon.pro]

Suppose there is a nearby planet and let \underline{r} be a position vector.

Construct a righthanded cartesian coordinate system with origin at the centre of mass of the planet and z-axis aligned with the planetary rotation axis. Define the positive x-axis to pass through the rotating planet's zero longitude line at time $t = 0$. The y-axis completes a righthanded set. This is the inertial cartesian frame. It is labelled with the subscript *inert*.

t is time since arbitrary start

x_{inert} , y_{inert} , z_{inert} are the inertial cartesian axes

Construct the usual spherical polar coordinate system about this set, with radius, r_{inert} , being the magnitude of \underline{r} ; colatitude, θ_{inert} , being the angle between the z_{inert} -axis and \underline{r} ; and longitude, ϕ_{inert} , being the angle between the x_{inert} -axis and the projection of \underline{r} into the $x_{inert}y_{inert}$ -plane. ϕ_{inert} is measured in the sense of a positive rotation about the z_{inert} -axis rotating the x_{inert} -axis onto the projection of \underline{r} into the $x_{inert}y_{inert}$ -plane. This is the inertial spherical frame. It is labelled with the subscript *inert*.

\underline{r} is a position vector

r_{inert} is the magnitude of \underline{r}

θ_{inert} is the colatitude of position \underline{r}

ϕ_{inert} is the angle between the x_{inert} -axis and the projection of \underline{r} into the $x_{inert}y_{inert}$ -plane

Bradbury (1968), or any other introductory mechanics or applied mathematics textbook, has diagrams of these frames and their coordinates.

2.1.2 – Momentary Inertial and Spherical Frames

[Bradbury, 1968]

Use the magnitude of \underline{r} , r_{mom} ; a colatitude referenced to the surface of the planet, θ_{mom} ; and an east longitude referenced to the surface of the planet, ϕ_{mom} , as a spherical coordinate frame. At any time t , it is non-rotating and transformations between it and the inertial cartesian frame do not need to consider fictitious forces (coriolis and centrifugal). An instant later, as the planet has rotated slightly, this frame

is ripped up and redefined so that colatitudes and east longitudes once again match up with surface features. It is not a rotating frame. It is a frame that only exists for an instant and so only instantaneous transformations between it and other frames can be made. No integration with time can be done in this frame because it does not exist for the duration of a timestep. This is the momentary spherical frame. It is labelled with the subscript *mom*.

r_{mom} is the magnitude of \underline{r}

θ_{mom} is the colatitude of position \underline{r} referenced to the surface of the planet

ϕ_{mom} is the east longitude of position \underline{r} referenced to the surface of the planet

Use the rotating spherical frame to construct an cartesian coordinate system (with the usual conventions). This also only exists for an instant and no integration with time can be done in this frame. This is the momentary cartesian coordinate system. It is labelled with the subscript *mom*.

x_{mom} , y_{mom} , z_{mom} are the momentary cartesian axes

2.1.3 – Transformations between Frames

[E:/idl/mpf_nominal/get_grav.pro, E:/idl/mpf_nominal/get_entry_state.pro]

There are many different conventions for defining latitude and longitude on the surface of a planet. Geographic, geodetic, and geocentric (as applied to the Earth) are some of the more well-known ones. I shall assume that all latitudes and longitudes referenced to the surface of the planet are in a planetocentric system. This means that the cartesian and spherical polar coordinate systems are related as follows

$$\begin{aligned} x &= r \sin \theta \cos \phi \\ y &= r \sin \theta \sin \phi \\ z &= r \cos \theta \end{aligned} \tag{5}$$

These equations can be inverted to give spherical polar coordinates as a function of cartesian coordinates. This applies to both the momentary and inertial pairs of frames. Positions can be converted between cartesian and spherical frames using IDL's CV_COORD function.

Given the planetocentric assumption,

$$\begin{aligned} r_{inert} &= r_{mom} \\ \theta_{inert} &= \theta_{mom} \\ \phi_{inert} &= \phi_{mom} + \omega t \end{aligned} \tag{6}$$

ω is the planetary rotation rate

Positions may be converted between the rotating spherical frame and the inertial spherical frame using the above equations. Hence positions may be transformed between all four frames with the minimum of fuss.

$$\underline{A} = A_x \underline{\hat{x}} + A_y \underline{\hat{y}} + A_z \underline{\hat{z}} = A_r \underline{\hat{r}} + A_\theta \underline{\hat{\theta}} + A_\phi \underline{\hat{\phi}}$$

Other vector quantities, such as \underline{A} , need reasonably standard transformations that do not have an IDL command. Knowledge of the unit vectors of one frame in terms of another frame's unit vectors is needed.

$$\begin{aligned} \underline{\hat{r}} &= \sin \theta \cos \phi \underline{\hat{x}} + \sin \theta \sin \phi \underline{\hat{y}} + \cos \theta \underline{\hat{z}} \\ \underline{\hat{\theta}} &= \cos \theta \cos \phi \underline{\hat{x}} + \cos \theta \sin \phi \underline{\hat{y}} - \sin \theta \underline{\hat{z}} \\ \underline{\hat{\phi}} &= -\sin \phi \underline{\hat{x}} + \cos \phi \underline{\hat{y}} \end{aligned} \quad (7)$$

or, equivalently,

$$\begin{aligned} \underline{\hat{x}} &= \sin \theta \cos \phi \underline{\hat{r}} + \cos \theta \cos \phi \underline{\hat{\theta}} - \sin \phi \underline{\hat{\phi}} \\ \underline{\hat{y}} &= \sin \theta \sin \phi \underline{\hat{r}} + \cos \theta \sin \phi \underline{\hat{\theta}} + \cos \phi \underline{\hat{\phi}} \\ \underline{\hat{z}} &= \cos \theta \underline{\hat{r}} - \sin \theta \underline{\hat{\theta}} \end{aligned} \quad (8)$$

These apply to both the momentary and inertial pairs of frames. Now we need a transformation between the momentary and inertial frames.

The rotating and inertial frames are related as follows

$$\begin{aligned} \underline{\hat{x}}_{inert} &= \underline{\hat{x}}_{mom} \cos(\omega t) - \underline{\hat{y}}_{mom} \sin(\omega t) \\ \underline{\hat{y}}_{inert} &= \underline{\hat{x}}_{mom} \sin(\omega t) + \underline{\hat{y}}_{mom} \cos(\omega t) \\ \underline{\hat{z}}_{inert} &= \underline{\hat{z}}_{mom} \end{aligned} \quad (9)$$

Now vector quantities may be transformed between all four frames.

2.1.4 – Caveats

The centre of mass of the planet is assumed to be at rest. Its motion around the Sun and so on will be neglected. This error may be quantified if desired.

The familiar coordinates of radius, surface-referenced latitude, and surface-referenced longitude are called the momentary spherical frame. My comments in computer programs often use this terminology, which might be unexpected.

2.2 - Rigid Body Dynamics

[Smith et al, 1993]

[E:/idl/mpf_nominal/recon_traj.pro, E:/idl/mpf_nominal/get_grav.pro]

In an inertial frame, the equations of motion of the centre of mass of a rigid body are:

$$\dot{\underline{r}} = \underline{v} \quad (10)$$

$$\dot{\underline{v}} = \underline{a} \quad (11)$$

\underline{r} is the position vector of the centre of mass of the rigid body

\underline{v} is the velocity vector of the centre of mass of the rigid body

\underline{a} is the linear acceleration vector of the centre of mass of the rigid body

In practice, the rigid body is more commonly called a spacecraft. I will use the more general terminology in the development of this general solution procedure and call a spacecraft a spacecraft when addressing specific cases.

If the only force acting on the centre of mass of the rigid body is gravity due to the nearby planet

$$\underline{a} = \underline{g}(\underline{r}) \quad (12)$$

$\underline{g}(\underline{r})$ is the linear acceleration vector due to gravity at position \underline{r} . It does not include any centrifugal component since we are working in an inertial frame.

$$\underline{g}(\underline{r}) = \nabla V(\underline{r}) \quad (13)$$

$$V(\underline{r}) = V(r_{mom}, \theta_{mom}, \phi_{mom}) = \frac{GM}{r_{mom}} \left(1 + \left(\frac{r_{ref}}{r_{mom}} \right)^2 P_{20}(\cos \theta_{mom}) C_{20} \right) \quad (14)$$

$$\nabla = \nabla(r_{mom}, \theta_{mom}, \phi_{mom}) = \frac{\partial}{\partial r_{mom}} \hat{r}_{mom} + \frac{1}{r_{mom}} \frac{\partial}{\partial \theta_{mom}} \hat{\theta}_{mom} \quad (15)$$

∇ is the gradient operator

$V(\underline{r})$ is the gravitational potential at position \underline{r} in this sign convention. It is expanded to second degree and order and S_{20} is neglected as small

GM is the product of the gravitational constant and the mass of the planet

r_{ref} is a reference radius associated with the spherical harmonic coefficients. It is

often, but not necessarily, the mean or mean equatorial planetary radius. It has meaning only in association with the spherical harmonic coefficients. If your favourite data resource has a newer, better equatorial radius than that quoted in the resource you're using for the spherical harmonic coefficients, do not update r_{ref} without changing all the spherical harmonic coefficients.

$P_{20}(x)$ is the normalised associated Legendre function of degree 2 and order 0.

$$P_{20}(x) = \frac{1}{2}(3x^2 - 1)$$

C_{20} is the tesseral (?) normalised spherical harmonic coefficient of degree 2 and order 0. It contains exactly the same information as J_2 , which you may see used in formulae. $C_{20} = -J_2$

Hence

$$\begin{aligned} \underline{g}(\underline{r}) &= \underline{g}(r_{mom}, \theta_{mom}, \phi_{mom}) = \\ &= \frac{-GM}{r_{mom}^2} \left(1 + \frac{3}{2} \left(\frac{r_{ref}}{r_{mo}} \right)^2 (3 \cos^2 \theta_{mom} - 1) C_{20} \right) \hat{r}_{mom} \\ &\quad - \frac{GM}{r_{mom}^2} \left(\frac{r_{ref}}{r_{mom}} \right)^2 \frac{1}{2} (6 \cos \theta_{mom} \sin \theta_{mom}) C_{20} \hat{\theta}_{mom} \end{aligned}$$

(16)

2.3 - Initial Conditions

[Magalhaes et al, 1999]

[E:/idl/mpf_nominal/get_entry_state.pro]

Initial conditions of the centre of mass of the rigid body (position, velocity, and a time) will rarely be provided in the format you will work in. They need to be transformed into a useful frame. For example, Mars Pathfinder initial conditions are available in two formats.

Time needs to be re-expressed as time elapsed since your chosen, arbitrary start time.

Radius from centre of Mars, aerocentric latitude, aerocentric east longitude, entry speed (v_{entry}), flight path angle below horizontal (γ), and flight path azimuth measured clockwise from north (ψ) – either in a Mars-fixed (rotating) or an inertial frame.

Position already given in one of the four frames. Velocity is not. Draw yourself a diagram to understand the necessary transformations.

If the values are given in an inertial frame, then

$$\begin{aligned}v_{r,mom} &= -v_{entry} \sin \gamma \\v_{\theta,mom} &= -v_{entry} \cos \gamma \cos \psi \\v_{\phi,mom} &= v_{entry} \cos \gamma \sin \psi\end{aligned}\tag{17}$$

If the values are given in a Mars-fixed frame, then

$$\begin{aligned}v_{r,mom} &= -v_{entry} \sin \gamma \\v_{\theta,mom} &= -v_{entry} \cos \gamma \cos \psi \\v_{\phi,mom} &= v_{entry} \cos \gamma \sin \psi + \omega r \sin \theta\end{aligned}\tag{18}$$

It is possible that these equations are slightly incorrect. I haven't been completely convinced by my derivations here.

2.4 – Gravity-Only Solution Algorithm

[Peterson, 1965a; Magalhaes et al, 1999]

[E:/idl/mpf_nominal/recon_traj.pro]

With no aerodynamic forces on the centre of mass of the rigid body, its trajectory can be reconstructed as follows

Transform time of initial conditions into a value of t

Transform initial position and velocity into the inertial cartesian frame

Start loop

Transform position from the inertial cartesian frame to the rotating spherical frame

$$x_{inert}, y_{inert}, z_{inert} \rightarrow r_{mom}, \theta_{mom}, \phi_{mom}$$

Use this position to obtain the linear acceleration due to gravity at this position in the rotating spherical frame

$$r_{mom}, \theta_{mom}, \phi_{mom} \rightarrow g_{r,mom}, g_{\theta,mom}, g_{\phi,mom}$$

Transform the linear acceleration due to gravity from the rotating spherical frame to the inertial cartesian frame

$$g_{r,mom}, g_{\theta,mom}, g_{\phi,mom} \rightarrow g_{x,inert}, g_{y,inert}, g_{z,inert}$$

Increment time, position and velocity, using a fancier integrator if desired

$$dx_{inert} = v_{x,inert} dt$$

$$dy_{inert} = v_{y,inert} dt$$

$$dz_{inert} = v_{z,inert} dt$$

$$dv_{x,inert} = g_{x,inert} dt$$

$$dv_{y,inert} = g_{y,inert} dt$$

$$dv_{z,inert} = g_{z,inert} dt$$

Stop loop

Have we hit the planet's surface yet?

$$|z_{inert}| < \textit{Planetary Radius} ?$$

If yes, stop

If no, start loop again

2.5 – The Spacecraft Frame

If aerodynamic forces are now allowed to act on the centre of mass of the rigid body, additional terms must be included in the integration. Suppose that the linear accelerations of the centre of mass of the rigid body due to aerodynamic forces are measured by accelerometers onboard the rigid body in three orthogonal directions. Gravitational forces are not measured by these accelerometers since the rigid body is falling freely. We introduce another frame consisting of right-handed cartesian axes along the three directions along which the accelerometers operate. This is the spacecraft frame. It is labelled with the subscript *sct*.

x_{sct} , y_{sct} , z_{sct} are the spacecraft cartesian axes

$a_{aero,x,sct}$, $a_{aero,y,sct}$, $a_{aero,z,sct}$ are the linear accelerations of the centre of mass of the rigid body due to aerodynamic forces measured in the spacecraft frame.

Suppose that a black box exists that transforms $a_{aero,x,sct}$, $a_{aero,y,sct}$, $a_{aero,z,sct}$ into the inertial cartesian frame, $a_{aero,x,inert}$, $a_{aero,y,inert}$, $a_{aero,z,inert}$.

$a_{aero,x,inert}$, $a_{aero,y,inert}$, $a_{aero,z,inert}$ are the linear accelerations of the centre of mass of the rigid body due to aerodynamic forces measured in the inertial cartesian frame.

2.7 – Basic Solution Algorithm with Black Box Aerodynamics

[E:/idl/mpf_nominal/recon_traj.pro]

The trajectory reconstruction algorithm is modified to

Transform time of initial conditions into a value of t

Transform initial position and velocity into the inertial cartesian frame

Start loop

Transform position from the inertial cartesian frame to the rotating spherical frame

$$x_{inert}, y_{inert}, z_{inert} \rightarrow r_{mom}, \theta_{mom}, \phi_{mom}$$

Use this position to obtain the linear acceleration due to gravity at this position in the rotating spherical frame

$$r_{mom}, \theta_{mom}, \phi_{mom} \rightarrow g_{r,mom}, g_{\theta,mom}, g_{\phi,mom}$$

Transform the linear acceleration due to gravity from the rotating spherical frame to the inertial cartesian frame

$$g_{r,mom}, g_{\theta,mom}, g_{\phi,mom} \rightarrow g_{x,inert}, g_{y,inert}, g_{z,inert}$$

Transform the linear accelerations of the spacecraft centre of mass due to aerodynamic forces from the spacecraft frame to the inertial cartesian frame, using the black box

$$a_{aero,x,sct}, a_{aero,y,sct}, a_{aero,z,sct} \rightarrow a_{aero,x,inert}, a_{aero,y,inert}, a_{aero,z,inert}$$

Increment time, position and velocity, using a fancier integrator if desired

$$dx_{inert} = v_{x,inert} dt$$

$$dy_{inert} = v_{y,inert} dt$$

$$dz_{inert} = v_{z,inert} dt$$

$$dv_{x,inert} = (g_{x,inert} + a_{aero,x,inert}) dt$$

$$dv_{y,inert} = (g_{y,inert} + a_{aero,y,inert}) dt$$

$$dv_{z,inert} = (g_{z,inert} + a_{aero,z,inert}) dt$$

Stop loop

Have we hit the planet's surface yet?

$$|z_{inert}| < \textit{Planetary Radius} ?$$

If yes, stop

If no, start loop again

2.8 – Aerodynamic Options

[Peterson, 1965a; Spencer et al, 1999; Gnoffo et al, 1998]

Making a real black box is one of the more complicated aspects of this reconstruction procedure. It boils down to the problem of tracking the spacecraft attitude.

There are several options:

2.8.1 – Drag-only

[E:/idl/mpf_nominal/get_acc.pro]

Option 1 - Assume that the rigid body aerodynamics and attitude are such that the only aerodynamic forces acting on the centre of mass of the rigid body are directed opposite to the relative velocity vector between the rigid body and the atmosphere. In this case, there is no lift, there are no side forces, there is only drag. These terms will be defined carefully later. Mars Pathfinder was designed so that this condition was reasonably well satisfied. Viking was not. Viking had lots of lift.

2.8.2 - Gyroscopes

[E:/idl/gyroscopes/recon_gyro.pro]

Option 2 - Track the rigid body attitude using, for example, onboard gyroscopes. This will enable the transformation of measured linear accelerations of the centre of mass of the rigid body between the spacecraft frame and the inertial cartesian frame. Viking carried such gyroscopes. I am unaware of any other spacecraft that has used gyroscopes in this way. You can do without them, so they are usually omitted.

2.8.3 – Acceleration ratios

Option 3 - The ratios of x_{sct} , y_{sct} , and z_{sct} linear accelerations of the centre of mass of the rigid body can be analysed to give the attitude of the rigid body.

2.8.4 – Pros and cons

Option 1 requires minimal knowledge of the rigid body aerodynamics. If the rigid body aerodynamics are appropriate, then this is a quick and convenient way of tackling the problem.

Option 2 requires the rigid body to actually have gyroscopes. If it does, wonderful, if not, this option is not available.

Option 3 is the usual method of choice if the rigid body's aerodynamics are well known. I will outline the procedure, but have not been able to test it myself owing to a lack of a good aerodynamic database.

2.9 – Solution Procedure for Drag-only Option

[E:/idl/mpf_nominal/recon_traj.pro, E:/idl/mpf_nominal/get_acc.pro]

Option 1 of section 2.8

The black box works as follows:

Calculate the velocity of the atmosphere due to planetary rotation at position \underline{r} . In the inertial cartesian frame, this is

$$\underline{v}_{wind,inert} = \underline{\omega}_{\hat{z}_{inert}} \times \underline{r} \quad (19)$$

Include more realistic winds from a climate model if you like.

Calculate the velocity of the centre of mass of the rigid body relative to the atmosphere. In the inertial cartesian frame, this is

$$\underline{v}_{rel,inert} = \underline{v}_{inert} - \underline{v}_{wind,inert} \quad (20)$$

Calculate the magnitude of the velocity of the centre of mass of the rigid body relative to the atmosphere and the magnitude of the aerodynamic linear accelerations. These are the same in all four frames. A practical complication, for Mars Pathfinder at least, is that the x and y axis accelerometers were far enough away from the centre of mass to pick up rotational terms that overwhelmed the linear aerodynamic terms high in the atmosphere. Careful examination of your pre-entry and early entry data will reveal if this is a problem for you. My solution for Mars Pathfinder was to ignore the x and y accelerations in this step.

They can be calculated from

$$\begin{aligned} |\underline{v}_{rel}| &= \sqrt{(v_{x,inert}^2 + v_{y,inert}^2 + v_{z,inert}^2)} \\ (A) \quad |\underline{a}_{aero}| &= \sqrt{(a_{aero,x,sct}^2 + a_{aero,y,sct}^2 + a_{aero,z,sct}^2)} \\ (B) \quad |\underline{a}_{aero}| &= \sqrt{(a_{aero,z,sct}^2)} \end{aligned} \quad (21)$$

Where (A) is perhaps better formally but (B) might be best in reality. (B) requires that the z-axis be closely aligned with the flow direction always.

Calculate the aerodynamic linear accelerations of the centre of mass of the rigid body in the inertial cartesian frame assuming that this vector is directed opposite to the velocity of the centre of mass of the rigid body relative to the atmosphere.

$$\underline{a}_{aero,inert} = -1 \times \frac{|\underline{a}_{aero}|}{|\underline{v}_{rel}|} \underline{v}_{rel,inert} \quad (22)$$

2.10 – Solution Procedure for Gyroscopes Option

[Goldstein, 1980]

[E:/idl/gyroscopes/recon_gyro.pro]

Option 2 of section 2.8

This is more complicated than simply fitting a black box into the pre-existing algorithm, so I will outline the entire algorithm.

2.10.1 – Euler angles

[E:/idl/gyroscopes/recon_gyro.pro, E:/idl/gyroscopes/get_em.pro]

Express the attitude of the rigid body in terms of Euler angles in Goldstein's xyz convention (page 608 of the second edition, 1980). Goldstein's unprimed coordinate system is the inertial cartesian frame, Goldstein's primed coordinate system is the spacecraft frame. See Goldstein's figure 4.2 on page 130 of the second edition for clarification. There are many conventions for Euler angles. This one makes it easy to track the rigid body attitude by means of its angular velocity. Goldstein's x-convention, used in his main text, does not. Euler angles can cause problems in actual calculations as one of the angles might be indeterminate for a given attitude. This is basically the same issue as trying to describe the longitude of the north pole. Quaternions or some other system that I know nothing about are more generally used in actual calculations. I will stick with Euler angles because it keeps the formulation simple.

$\phi_{Euler}, \psi_{Euler}, \theta_{Euler}$ are the Euler angles

The Euler matrix, constructed from these Euler angles, enables the conversion of vectors between the inertial cartesian frame and the spacecraft frame.

EM is the Euler matrix

Expand the initial condition to include the three Euler angles and the angular velocity of the rigid body about its axes at the appropriate time. For example, the angular velocity might be a predetermined spin. Whatever it is, it should stay constant during the spacecraft's journey through the vacuum of space and is knowable. We're going to need it.

$\Omega_{x,scf}, \Omega_{y,scf}, \Omega_{z,scf}$ are the three components of the angular velocity of the spacecraft about the three spacecraft cartesian axes.

The Euler angles change with time due to the rotation of the spacecraft about its axes. Rearrangement of Goldstein's equations B-14xyz on page 609 of the second edition gives:

$$\begin{aligned}
\dot{\phi} &= \frac{\Omega_{y,scf} \sin \psi + \Omega_{z,scf} \cos \psi}{\cos \theta} \\
\dot{\psi} &= \Omega_{x,scf} + \tan \theta \times (\Omega_{y,scf} \sin \psi + \Omega_{z,scf} \cos \psi) \\
\dot{\theta} &= \Omega_{y,scf} \cos \psi - \Omega_{z,scf} \sin \psi
\end{aligned} \tag{23}$$

The gyroscopes measure the angular acceleration of the rigid body about its axes. These angular accelerations are caused by torques acting on the rigid body. In the limit that the rigid body is a point mass, there are no angular accelerations.

$\dot{\Omega}_{x,scf}, \dot{\Omega}_{y,scf}, \dot{\Omega}_{z,scf}$ are the three components of the angular acceleration of the spacecraft about the three spacecraft cartesian axes.

2.10.2 - Algorithm

[E:/idl/gyroscopes/recon_gyro.pro, E:/idl/gyroscopes/get_acc_genl.pro]

The trajectory reconstruction algorithm is

Transform time of initial conditions into a value of t

Transform initial position and velocity into the inertial cartesian frame

Transform initial attitude and rate of change of attitude into Euler angles and angular velocity about the three spacecraft axes

Start loop

Construct Euler matrix, \underline{EM} , from the Euler angles for transforming vectors between the inertial cartesian frame and the spacecraft frame

$$\phi_{Euler}, \psi_{Euler}, \theta_{Euler} \rightarrow \underline{EM}$$

Transform position from the inertial cartesian frame to the rotating spherical frame

$$x_{inert}, y_{inert}, z_{inert} \rightarrow r_{mom}, \theta_{mom}, \phi_{mom}$$

Use this position to obtain the linear acceleration due to gravity at this position in the rotating spherical frame

$$r_{mom}, \theta_{mom}, \phi_{mom} \rightarrow g_{r,mom}, g_{\theta,mom}, g_{\phi,mom}$$

Transform the linear acceleration due to gravity from the rotating spherical frame to the inertial cartesian frame

$$g_{r,mom}, g_{\theta,mom}, g_{\phi,mom} \rightarrow g_{x,inert}, g_{y,inert}, g_{z,inert}$$

Transform the linear accelerations of the spacecraft centre of mass due to aerodynamic forces from the spacecraft frame, using the Euler matrix

$$a_{aero,x,sct}, a_{aero,y,sct}, a_{aero,z,sct} \rightarrow a_{aero,x,inert}, a_{aero,y,inert}, a_{aero,z,inert}$$

Increment time, position and velocity, attitude and angular velocity using a fancier integrator if desired

$$dx_{inert} = v_{x,inert} dt$$

$$dy_{inert} = v_{y,inert} dt$$

$$dz_{inert} = v_{z,inert} dt$$

$$dv_{x,inert} = (g_{x,inert} + a_{aero,x,inert}) dt$$

$$dv_{y,inert} = (g_{y,inert} + a_{aero,y,inert}) dt$$

$$dv_{z,inert} = (g_{z,inert} + a_{aero,z,inert}) dt$$

$$d\phi = \left(\frac{\Omega_{y,sct} \sin \psi + \Omega_{z,sct} \cos \psi}{\cos \theta} \right) dt$$

$$d\psi = \left(\Omega_{x,sct} + \tan \theta \times (\Omega_{y,sct} \sin \psi + \Omega_{z,sct} \cos \psi) \right) dt$$

$$d\theta = (\Omega_{y,sct} \cos \psi - \Omega_{z,sct} \sin \psi) dt$$

$$d\Omega_{x,sct} = \dot{\Omega}_{x,sct} dt$$

$$d\Omega_{y,sct} = \dot{\Omega}_{y,sct} dt$$

$$d\Omega_{z,sct} = \dot{\Omega}_{z,sct} dt$$

Stop loop

Have we hit the planet's surface yet?

$$|z_{inert}| < \textit{Planetary Radius} ?$$

If yes, stop

If no, start loop again

2.11 – Solution Procedure for Acceleration Ratios Option

[Peterson, 1965a; Magalhaes et al, 1999; Braun et al, 1995]

Option 3 of section 2.8

2.11.1 – Aerodynamics as I understand it

Immerse and fix a rigid body [spacecraft] in a fluid [atmosphere]. Suppose the fluid moves with a known far-field bulk velocity relative to the rigid body. Three numbers constrain this vector quantity. Specify the composition of the fluid. The behaviour of the fluid is fixed by thermodynamics. In general, two parameters are necessary to specify the equilibrium thermodynamic state of any system. These can be pressure and temperature, density and temperature, or just about anything else.

Aerodynamicists tend to use two dimensionless numbers for this purpose. They are often the Mach, Ma , and Knudsen, Kn , numbers. The Mach number is the ratio of a speed to the speed of sound in the fluid. The Knudsen number is the ratio of the molecular mean free path in the fluid to some reference length, typically a linear dimension of the rigid body. I've seen the Reynolds number, Re , used as well. Despite the fact that these two numbers are referenced to the rigid body in some way, their actual purpose is to specify the thermodynamic state of the fluid. Scaling relations that apply in the absence of chemistry make them useful representations. We have now completely constrained the behaviour of the system.

Constraints:

- Rigid body (size, shape, mass distribution)
- Flow velocity (3 parameters)
- Thermodynamic state of the fluid (2 parameters)

Constrained quantities:

- Forces acting on the centre of mass of the rigid body (3 parameters)
- Torques acting about the centre of mass of the rigid body (3 parameters)

An axisymmetric rigid body needs only 2 parameters to specify the flow velocity, has no forces out of the plane containing the flow velocity vector and the axis of symmetry, and probably has one of the torques equal to zero.

These forces and torques are usually expressed in terms of dimensional quantities and a dimensionless fudge-factor or coefficient. I don't know much about the torque formalism. I expect that these results are expressed as follows:

Torque about a given axis fixed in the rigid body =
(Moment coefficient) (Fluid density) (Fluid velocity)² (Reference area) (Reference length)

In this formalism, ratios of torques about different axes are equal to ratios of moment coefficients. You need to see a diagram, an equation, and a sign convention before understanding and being able to use any moment coefficient. You need the moments of inertia of the rigid body to convert torques into angular accelerations.

Force coefficients are more commonly seen and are expressed as follows:

Force along an axis fixed in the rigid body, along the flow direction, or perpendicular to the flow direction =
(Spacecraft mass) (Linear Acceleration in same direction) =
(+/-) (1/2) (Force coefficient) (Fluid density) (Fluid velocity)² (Reference area)

2.11.2 - Acceleration Ratios and Angle-Of-Attack

In this formalism, ratios of forces are equal to ratios of force coefficients. You need to see a diagram, an equation, and a sign convention before understanding and being able to use any force coefficient. You need the mass of the rigid body to convert forces into linear accelerations.

The force coefficients corresponding to different axes have typical symbols. For x, y, and z axes fixed in the rigid body, the symbols C_x , C_y , and C_z are typical. For an axisymmetric rigid body, the symbol C_n is typical for forces normal to the symmetry axis and the symbol C_A is typical for forces parallel to the symmetry axis. For a force parallel to the flow direction (drag) the symbol C_D is typical. Drag acts in the direction opposite to the velocity of the centre of mass of the rigid body relative to the atmosphere. Drag tends to make the fluid and the rigid body move together. For a force perpendicular to the flow direction (lift) the symbol C_L is typical. Hence, lift is perpendicular to drag. Lift is perpendicular to the axis of symmetry, if one exists. This restricts the lift force to two possible directions, which are antiparallel to each other. Choose and make clear a convention for a positive direction for lift. In an aircraft, lift is parallel to whatever is the vertical axis when the aircraft is on the ground. For a force perpendicular to the flow direction but also perpendicular to whatever convention has defined as the lift direction (side force?) the symbol C_Y is typical.

L is the lift force

D is the drag force

I define the angle-of-attack to be the angle between the axis of symmetry and the relative velocity vector. Aerodynamics texts may talk about the angle-of-attack and sideslip angle being combined to give a total angle-of-attack. Insist on seeing a diagram and definitions when someone mentions these. Bearing in mind the confusion that east and west longitude can cause, know in which directions the angles are increasing.

α is the angle-of-attack

For a known fluid composition and pressure and temperature (or Ma and Kn), a known axisymmetric rigid body and a specified fluid velocity, only the angle-of-attack, α , is required to completely specify the forces acting on the centre of mass of the rigid body. We can obtain an expression for lift as a function of α . We can do the same for drag and hence obtain an expression for the lift-to-drag ratio as a function of α . This expression is surprisingly well-behaved. The lift-to-drag ratio is often simply proportional to α . The constant of proportionality changes as function of everything in the first sentence of this paragraph.

The lift-to-drag ratio is related to the ratio of normal to axial linear accelerations via α . A diagram shows the following relation:

$$\frac{L}{D} = \frac{\left(\frac{A_{normal}}{A_{axial}} \right) - \tan \alpha}{1 + \left(\frac{A_{normal}}{A_{axial}} \right) \tan \alpha} \quad (24)$$

This is also given in Blanchard et al (1989). There is immense potential for sign confusion here. Know your conventions for positive and negative directions for lift, drag, normal, and axial forces and derive this yourself. Your equation may easily be different in some signs to the above.

Given everything in the first sentence of the earlier paragraph, we can obtain the angle-of-attack, α , from aerodynamic linear acceleration measurements made in the spacecraft frame.

Look up the appropriate function for the lift-to-drag ratio in a pre-prepared aerodynamic database, substitute it in the angle-of-attack equation (24), and solve for the angle-of-attack.

The drag and lift forces can now be calculated. The direction of the drag force is opposite to that of $\underline{v}_{rel,inert}$. The direction of the lift force is perpendicular to this, but that only constrains the lift force vector to lie in a plane whose normal is parallel to $\underline{v}_{rel,inert}$. If the spacecraft is rotating about its axis of symmetry, then the direction of the lift force will rotate with it, and contributions to the trajectory from lift will be nullified. In actual trajectory reconstructions, the lift force is neglected for this reason. The errors introduced into the trajectory and atmospheric structure reconstruction can be evaluated in simulations in which you control the spacecraft attitude.

There's nothing else you can do with it unless you have some additional attitude information. Somewhat surprisingly, a non-axisymmetric spacecraft is better off here as you can, in theory, use x/z and y/z linear acceleration ratios to constrain the two angles necessary to completely define the spacecraft attitude. See Peterson (1965a, b).

If the axis of symmetry of the rigid body is the z-axis, then

$$\begin{aligned} a_{normal,sct} &= \sqrt{a_{aero,x,sct}^2 + a_{aero,y,sct}^2} \\ a_{axial,sct} &= a_{aero,z,sct} \end{aligned} \quad (25)$$

Note that some directional information has been lost in the calculation of the normal acceleration.

2.11.3 - Algorithm

The trajectory reconstruction algorithm is modified to

Generate aerodynamic database that states the values of the lift and drag force coefficients as a function of angle-of-attack, fluid velocity, atmospheric pressure and temperature.

[Run this procedure with a simulated pressure and temperature profile, and then use the results to obtain an estimate of the pressure and temperature profile. The calculation of density, pressure, and temperature profiles from the results of this procedure will be outlined later. Iterate. Keep passing the pressure and temperature profile back and forth until the pressure and temperature profile input into this procedure agrees with those that are calculated from its results.]

Transform time of initial conditions into a value of t

Transform initial position and velocity into the inertial cartesian frame

Start loop

Transform position from the inertial cartesian frame to the rotating spherical frame

$$x_{inert}, y_{inert}, z_{inert} \rightarrow r_{mom}, \theta_{mom}, \phi_{mom}$$

Use this position to obtain the linear acceleration due to gravity at this position in the rotating spherical frame

$$r_{mom}, \theta_{mom}, \phi_{mom} \rightarrow g_{r,mom}, g_{\theta,mom}, g_{\phi,mom}$$

Transform the linear acceleration due to gravity from the rotating spherical frame to the inertial cartesian frame

$$g_{r,mom}, g_{\theta,mom}, g_{\phi,mom} \rightarrow g_{x,inert}, g_{y,inert}, g_{z,inert}$$

Calculate the velocity of the atmosphere due to planetary rotation at position \underline{r} . In the inertial cartesian frame, this is

$$\underline{v}_{wind,inert} = \underline{\omega}_{inert} \times \underline{r} \quad (26)$$

Include more realistic winds from a climate model if you like.

Calculate the velocity of the centre of mass of the rigid body relative to the atmosphere. In the inertial cartesian frame, this is

$$\underline{v}_{rel,inert} = \underline{v}_{inert} - \underline{v}_{wind,inert} \quad (27)$$

Obtain the lift-to-drag ratio as a function of angle-of-attack using the aerodynamic database

$$p, T, |\underline{v}_{rel,inert}| \rightarrow \frac{L}{D}(\alpha)$$

Take the linear accelerations of the spacecraft centre of mass due to aerodynamic forces and form the normal and axial accelerations. Solve the angle-of-attack equation for α

$$\frac{L}{D}(\alpha) = \frac{\left(\frac{A_{normal}}{A_{axial}} \right) - \tan \alpha}{1 + \left(\frac{A_{normal}}{A_{axial}} \right) \tan \alpha} \quad (28)$$

Obtain the lift and drag forces using the angle-of-attack, α

$$p, T, \left| \underline{v_{rel, inert}} \right|, \alpha \rightarrow L, D$$

Neglect the lift force due to rotation. The drag force is directed opposite to the velocity of the centre of mass of the rigid body relative to the atmosphere. It is divided by the rigid body mass, m , to give the total aerodynamic acceleration.

$$\underline{a_{aero, inert}} = -1 \times \frac{D/m}{\left| \underline{v_{rel}} \right|} \underline{v_{rel, inert}} \quad (29)$$

Increment time, position and velocity, using a fancier integrator if desired

$$dx_{inert} = v_{x, inert} dt$$

$$dy_{inert} = v_{y, inert} dt$$

$$dz_{inert} = v_{z, inert} dt$$

$$dv_{x, inert} = (g_{x, inert} + a_{aero, x, inert}) dt$$

$$dv_{y, inert} = (g_{y, inert} + a_{aero, y, inert}) dt$$

$$dv_{z, inert} = (g_{z, inert} + a_{aero, z, inert}) dt$$

Stop loop

Have we hit the planet's surface yet?

$$\left| z_{inert} \right| < \text{Planetary Radius} ?$$

If yes, stop

If no, start loop again

2.12 - Atmospheric structure reconstruction

[Magalhaes et al, 1999; Spencer et al, 1999]
[E:/idl/mpf_nominal/recon_atm.pro]

This takes place separately from the trajectory reconstruction. It uses the results of the trajectory reconstruction.

$$\rho C_D A V_r^2 = -2ma_v \quad (30)$$

ρ is fluid density

C_D is the drag force coefficient

A is a reference area for the rigid body

V_r is the speed of the rigid body relative to the surrounding fluid

m is the rigid body mass

a_v is the linear acceleration of the centre of mass of the rigid body due to aerodynamic forces in the direction of the velocity of the rigid body relative to the surrounding fluid

This equation is solved for ρ on a point-by-point basis. Alternatively, the force balance equation along any other axis can be used. All should give exactly the same results for ρ . This equation is used in practice because a_v will be known better than the smaller normal accelerations. a_v is approximately equal to a_z in the limit of small angle-of-attack, in which case a_z will be better known than a_x, a_y

A is constant along the trajectory. It is whatever reference area C_D is referenced to. It may or not be similar to what you think is an appropriate area.

m must be allowed to change along the trajectory. However, in the spacecraft case, m will be well constrained by mission plans, known fuel burns, telemetry, and so on. It may change due to heat shield ablation. m will be known as a function of time for all but the most pathological of cases.

In option 1 of section 2.8, a_v is tracked by assuming that it is the only aerodynamic acceleration. In option 2 of section 2.8, $a_{aero,inert}$ is known and $v_{rel,inert}$ can be calculated by incorporating the wind calculation from options 1 or 3 of section 2.8. In option 3 of section 2.8, a_v is tracked using the angle-of-attack and neglecting the lift force.

V_r is calculated as part of the trajectory reconstruction procedure for options 1 and 3 of section 2.8. Given our need to track a_v , as detailed above, it is also done in option 2 of section 2.8 as well.

For a known fluid composition and pressure and temperature (or Ma and Kn), a known rigid body and a specified fluid velocity, only the rigid body attitude is

required to specify C_D . Assume a pressure and temperature profile along the trajectory or use the results from a previous iteration. Know the fluid composition along the trajectory in some way. V_r is tracked along the trajectory. In option 1 of section 2.8, C_D is either insensitive to attitude or the rigid body attitude is assumed to keep the relative velocity aligned along one of the rigid body axes. C_D can be extracted from the aerodynamic database. In option 2 of section 2.8, attitude is tracked along the trajectory and C_D can be extracted from the aerodynamic database. In option 3 of section 2.8, ratios of accelerations in the spacecraft frame constrain the rigid body attitude and C_D can be extracted from the aerodynamic database.

Everything thus far in section 2 applies to the general case of a rigid body moving through a fluid under the influence of a gravitational field. What follows applies only to the restricted case of a spacecraft entering an atmosphere

The above equation is now solved at each point along the trajectory to give $\rho(h)$ h is height above the surface of the planet.

$$\frac{dp}{dh} = -\rho g \text{ can be integrated to give } p(h) \quad (31)$$

This is the equation of hydrostatic equilibrium. I am unsure just how valid it is over the large horizontal distances covered by the typical planetary entry. I am unsure how you would use anything more complicated than a spherically symmetric gravitational field in this equation.

A constant of integration must be specified. The easiest solution is to say that pressure is zero at the highest altitude for which you have density measurements, h_0 . A better solution follows:

If both the atmospheric mean molecular mass and temperature vary slowly with altitude compared with the variation of density with altitude, then using equation (4), the ideal gas equation of state

$$d(\ln \rho) = d(\ln p) \quad (32)$$

and hence

$$p \frac{d}{dh}(\ln \rho) = -\rho g \quad (33)$$

$$p(h_0) = -\rho(h_0)g(h_0) \times \left(\frac{d}{dh}(\ln \rho) \Big|_{h_0} \right)^{-1} \quad (34)$$

$$p(h) = -\rho(h_0)g(h_0) \times \left(\frac{d}{dh}(\ln \rho) \Big|_{h_0} \right)^{-1} - \int_{h_0}^h \rho(h)g(h)dh \quad (35)$$

Since pressure increases exponentially as the spacecraft descends, the constant of integration eventually becomes irrelevant. It does not do so very quickly. Suppose you set the pressure to zero at a given altitude in your calculation. All future pressure calculations at lower altitudes are underestimates by an offset of whatever the actual pressure is at this altitude. One scale height lower, pressure calculations are offset by a factor of e^{-1} , or 37%. Two scale heights lower, pressure calculations are offset by a factor of e^{-2} , or 14%. Four scale heights lower, pressure calculations are offset by a factor of e^{-4} , or 2%. For a simple ideal gas equation of state, temperatures are underestimated by the same factor. Errors in temperature introduced by lack of a constant of integration will exceed 2% for the first four scale heights of your trajectory, a huge vertical range. Correct choice of the altitude at which you calculate the density scale height and the altitude range over which you do so assumes great importance and the reconstruction is sensitive to these parameters. It must be understood.

Illustration:

Let z_1 be one scale height below z_0

Actual pressure at z_0 is 1

Estimate of pressure at z_0 is 0

Actual pressure at z_1 is e^1

Estimate of pressure at z_1 is $e^1 - 1$

Absolute error in pressure estimate at z_1 is $e^1 - (e^1 - 1) = 1$

Relative error in pressure estimate at z_1 is $1/e^1 = e^{-1}$

A good choice for the constant of integration will require complete understanding of the returned dataset and its uncertainties.

An equation of state, such as the ideal gas equation, can then be solved for $T(h)$

$$p(h)m_m(h) = \rho(h)RT(h) \quad (36)$$

2.13 – Additional Constraints

[Magalhaes et al, 1999; Spencer et al, 1999; Seiff, 1968; Seiff and Kirk, 1977]

Space missions involve redundancy. There may be additional information available to you that will constrain your trajectory and atmospheric structure reconstruction.

The Doppler shift of telemetry during descent constrains the descent speed.

Any radar altimetry during descent (nominally a trigger for events during entry, descent, and landing) constrains the altitude and descent speed if the underlying topography is well-behaved.

The Doppler shift of transmissions after landing enable the landing site position (3 parameters) to be located to very high precision and accuracy.

Direct pressure and temperature measurements may be made by other instruments during the super- and subsonic portions of the trajectory.

The acceleration due to gravity at the landing site can be used to constrain the accuracy of the accelerometers.

Viking's Upper Atmosphere Mass Spectrometer somehow derived a temperature profile.

Spencer et al (1999) has a good description of how more refined numerical methods can be used in the reconstructions and how the additional constraints were incorporated.

The use of higher-order integration routines is complicated by the fact that the transformation of linear accelerations between the spacecraft and inertial cartesian frames depends on both position and velocity in the inertial cartesian frame (using options 1 or 3 of section 2.8). IDL's automatic RK4 procedure can't deal with this easily and the "derivs" function, E:/idl/mpf_nominal/derivs.pro/, that RK4 requires becomes a lot messier than you would like.

2.14 - Effects of Errors and Uncertainties

These are discussed in Peterson (1965b) and scattered throughout the 1960s-era references. Look out for anything that quantitatively discusses accelerometers that are located away from the centre of mass or with strange alignments of axes.

3 - Mars Pathfinder Test Case

[E:/idl/mpf_nominal/]

It is important to test your understanding of the above theoretical formalism by actually coding it all up and testing it against pre-existing results. Mars Pathfinder proved a suitable test case.

Many upcoming plots show fractional or relative differences. Such results are calculated as $(\text{nominal value} - \text{my estimate of value}) / (\text{nominal value})$.

Many of the plots which show differences between two datasets at a given altitude actually evaluate the difference at a given time, then plot the difference as a function of altitude in one dataset. Look at E:/idl/mpf_nominal/plot_results.pro for an example of this.

3.1 – Mars Pathfinder Mission Summary

[Extracted from the PDS files]

“The Mars Pathfinder Project was one of the first of the NASA Discovery class missions. Discovery Program missions are defined as low cost missions, (with a \$150M FY'92 development cost cap), and a fast schedule (less than 3 years development period). They have focused, but significant, science objectives. Mars Pathfinder placed a single vehicle on the surface of Mars, the Mars Pathfinder Lander, which then deployed a microrover, called variously 'Sojourner', the 'Microrover Flight Experiment', or the 'Mars Pathfinder Rover'. Several instruments were included on the two spacecraft. The Sojourner carried three cameras, (two black & white cameras on the front and one color camera in the rear), and the Alpha Proton X-Ray Spectrometer (APXS). Sojourner's mobility provided the capability of 'ground truthing' a landing area over hundreds of square meters on Mars. The Lander investigated the surface of Mars with two additional science instruments, a stereoscopic imager with spectral filters on an extensible mast (Imager for Mars Pathfinder or IMP), and the Atmospheric Structure Instrument / Meteorology package (ASI/MET). Mars Pathfinder paved the way for a cost effective implementation of future Mars lander missions as part of a comprehensive Mars exploration program augmented by additional Discovery Program missions.

The launch occurred December 4, 1996 on a McDonnell Douglas Delta II 7925 launch vehicle. The Earth-Mars trajectory was a Type 1 transfer with a Mars arrival date of July 4, 1997. The landing site for Mars Pathfinder was in the Ares Vallis region of Chryse Planitia at 19.17 degrees North latitude, 33.21 degrees West longitude. The Earth elevation angle at landing was 11 degrees and rising, and the Sun was 30 degrees below the local horizon and rising. The Earth-Mars range at arrival was 191,000,000 km (and increasing).

Required guidance, navigation, attitude control, telemetry, and power generation functions during the 7 month cruise were provided by the cruise stage. At Mars

arrival, the cruise stage was jettisoned from the entry capsule. The entry capsule entered the Martian atmosphere directly from the Earth-Mars transfer orbit at a velocity of 7.6 km/s. The lander velocity was reduced from this high entry speed through the sequential application of aerodynamic braking by a Viking heritage aeroshell and parachute, propulsive deceleration using small solid tractor rockets, and airbags to nullify the remaining vertical and horizontal velocity components at surface impact. Key engineering status information was collected and returned in near real time to the extent possible during entry and descent. In addition, all engineering and science data obtained during the critical entry, descent, and landing phase were recorded for playback at the initiation of lander surface operations.

The principal surface operations activities were return of engineering data characterizing the performance of the lander system in the Martian environment, return of science data obtained from the imaging, meteorology, and spectroscopy instruments, and operation of the rover to deploy instruments and conduct science and technology experiments.”

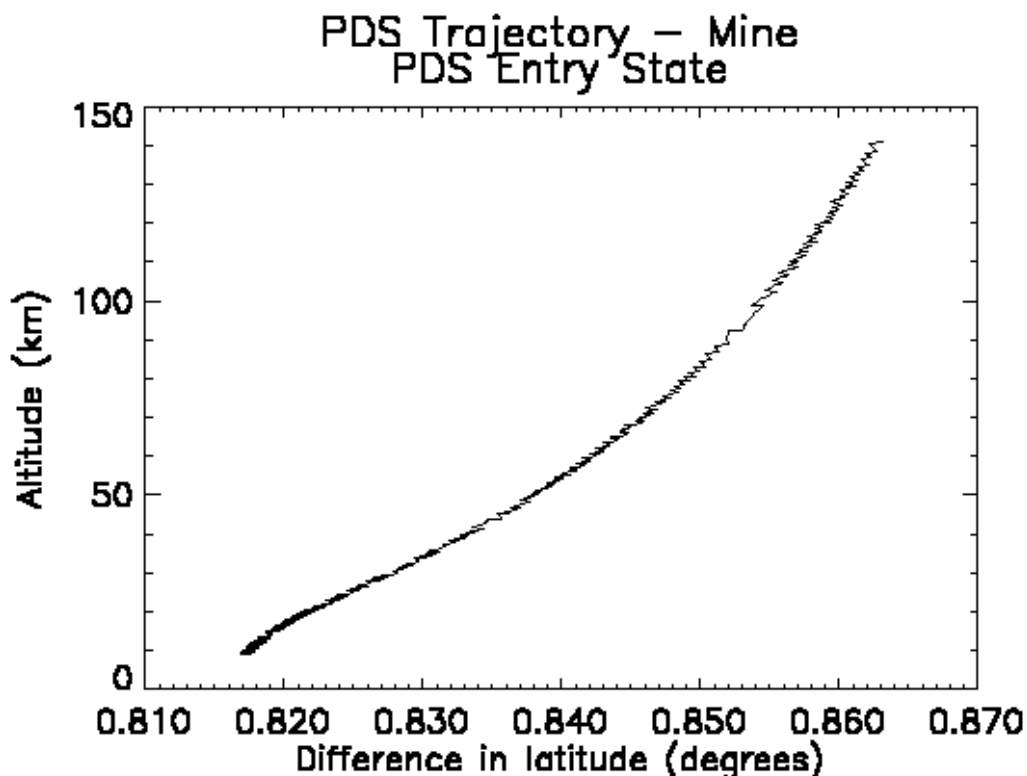
3.2 – Necessary Data and Entry State

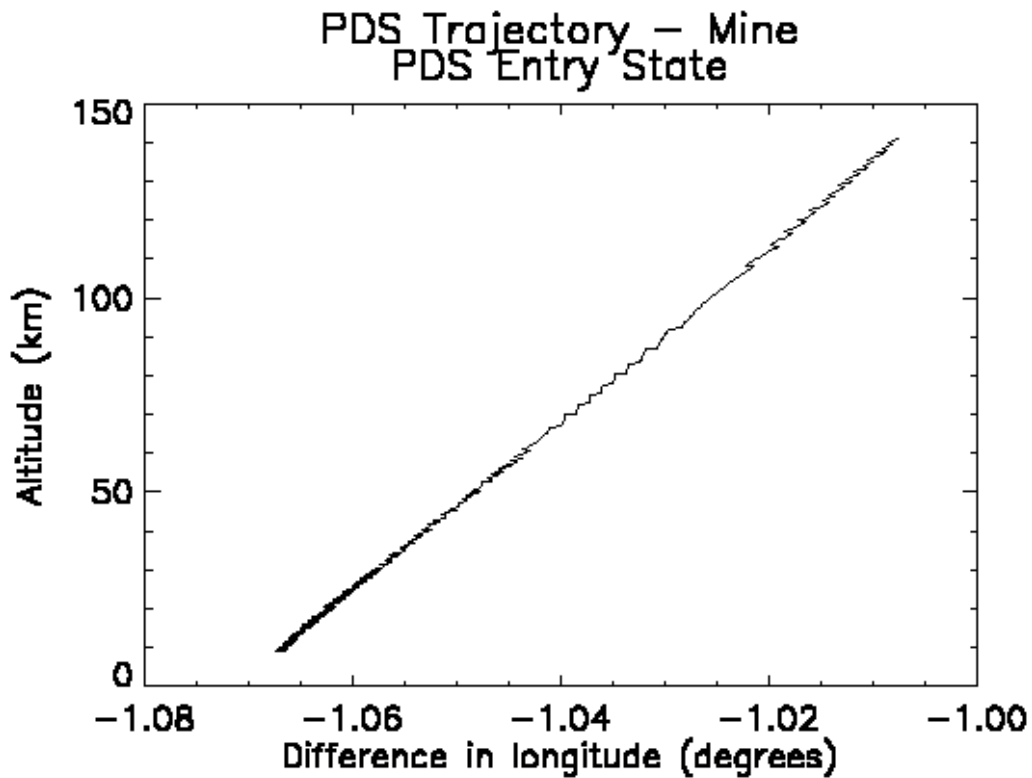
[Magalhaes et al, 1999; Spencer et al, 1999; Braun et al, 1995, Smith et al, 1993]
[E:/idl/mpf_nominal/extract_data.pro, E:/idl/mpf_nominal/recon_traj.pro,
E:/idl/mpf_nominal/get_entry_state.pro]

Much of the information necessary to reconstruct the Mars Pathfinder trajectory and atmospheric structure are available from the Planetary Data System (PDS) in volume MPAM_0001 (Mars Pathfinder Atmospheric Structure Instrument / Meteorology Package). The computer programs used for the reconstruction are discussed later.

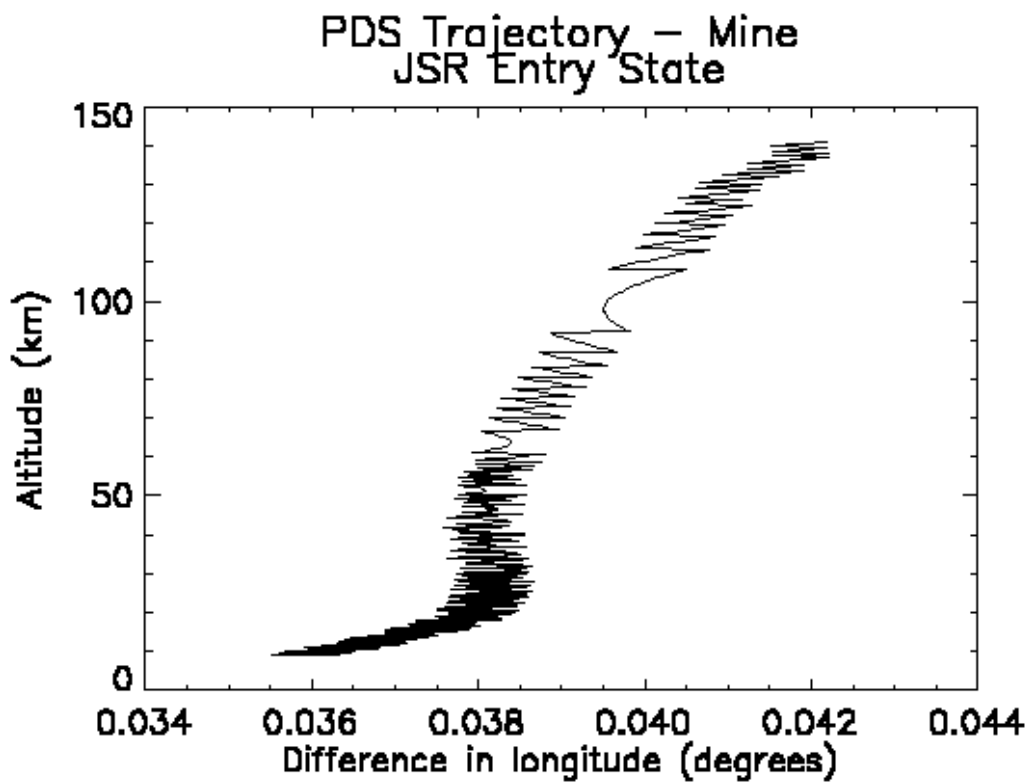
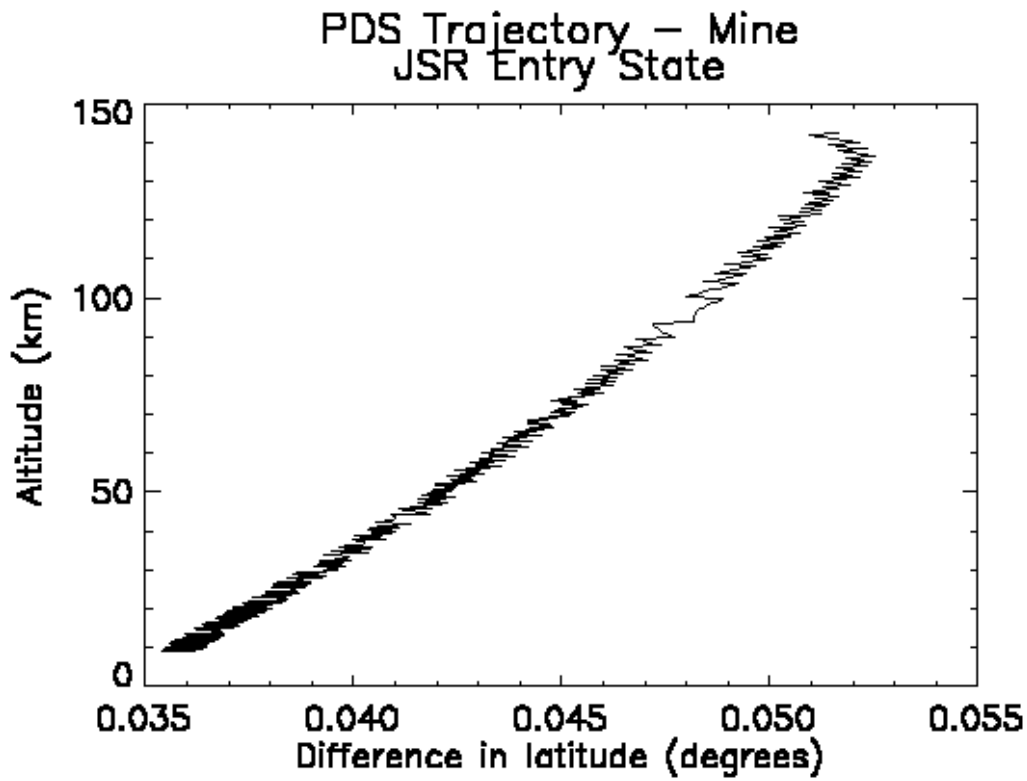
The initial UTC time, position and velocity of the spacecraft are given in:
E:/mpam_0001/document/edler_ds.htm and Magalhaes et al (1999)

This is the “PDS Entry State”. These two different sources, compiled by the same authors, give identical values and uncertainties. However, this entry state disagrees with figure 2 of Magalhaes et al (1999) at 200 km altitude by about 1 degree in latitude and longitude, many times greater than the quoted uncertainty of 0.04 degrees in latitude and 0.01 degrees in longitude. I have no idea why. When I compare my trajectory reconstruction from these initial conditions with the PDS trajectory, available only below about 150 km, I am systematically in error by about 1 degree in both latitude and longitude.





A different entry state, without any uncertainties, is given in Spencer et al (1999). This is the “JSR Entry State”. When I compare my trajectory reconstruction from these initial conditions with the PDS trajectory, available only below about 150 km, I am systematically in error by about 0.04 degrees in latitude and longitude.



The entry state of Spencer et al (1999) is at about 132.5 km altitude and should agree with the portion of the PDS trajectory that passes through this level. Instead, there is a disagreement of about 0.15 degrees in longitude and 0.1 degrees in latitude. No uncertainties for latitude and longitude along the profile are quoted in the PDS data.

I have not tried integrating the PDS trajectory backwards up beyond 150 km to 200 km with no aerodynamic forces, but that might be a useful test.

Since the PDS entry state at 200 km, compiled by Magalhaes et al (1999), disagrees with a figure by the same authors and that same figure agrees with the PDS trajectory below 150 km as far as my eye can tell, I believe that either there is an error in the PDS entry state or I am misinterpreting the PDS entry state in some way. In either case, all further reconstructions used the Spencer et al (1999) entry state.

I chose 16:00:00.000UTC as my $t = 0$ mark and expressed all times as seconds from this. Atmospheric entry is at approximately 16:50 UTC.

Measurements of the linear acceleration of the centre of mass of the spacecraft along the spacecraft x, y, and z axes as a function of time during entry, descent, and landing are given in:

E:/mpam_0001/edl_erdr/r_sacc_s.tab

There are many data files in the above directory. The explanation for why the 32 Hz RAM Science Accelerometer Science Data is the best is given in:

E:/mpam_0001/document/edler_ds.htm

These data need to be multiplied by a reference value for the Earth's gravity. This is 9.795433 ms^{-2} , given in:

E:/mpam_0001/edl_erdr/r_sacc_s.tbl

Next, the data needs to be cleaned up.

Two data values are 0.0 for no good reason, one in the x-axis data and the other in the z-axis data. These are mentioned in Magalhaes et al (1999) but not in

E:/mpam_0001/document/edler_ds.htm. I've averaged neighbouring points to fill the gaps. There are about ten data points in the y-axis data that are zero. Neighbouring points show that they are correctly zero.

When an accelerometer changes gain state, there is a brief acceleration pulse which is an artifact of the electronic time constant of the sensor. These need to be removed and interpolated through. E:/mpam_0001/document/edlhdrs.htm states that 1 second's worth of data should be replaced. I interpolated linearly to fill in the gap. The group generating the PDS atmospheric reconstruction used a logarithmic interpolation. This may cause my results to disagree with those of the PDS in restricted intervals. Any suspicious spikes in the results should be checked to see if they occur at these known times. Minor spikes visible in the difference between my $T(h)$ and the PDS $T(h)$ at 65 and 85 km are due to this.

Acceleration measurements in the data file continue beyond landing, which messes up your atmospheric trajectory. Discard all measurements taken after impact. The atmospheric structure reconstruction is garbage after a mortar fires and a parachute opens at about 8 km altitude. This is because the aerodynamics of a capsule are a lot easier to model than those of a capsule on the end of a parachute. You may wish to discard all measurements after this point as well.

Acceleration measurements in the data file are given before the quoted entry state. Comparing the timestamp of the entry state with those of the data tells you which to discard.

Finally, the first few acceleration measurements that remain are made at 1 Hz, not 32 Hz. I found it easiest to interpolate those to 32 Hz and have a single timestep throughout the rest of my programs. The first few interpolated timesteps were discarded to bring the first acceleration measurements as close as possible to the quoted entry state.

There are now four clean arrays with the time since 1600UTC in seconds and spacecraft x, y, and z-axis acceleration measurements in ms^{-2} beginning at the time of the initial conditions.

The planetary sidereal day of 24.6229 hours, obtained from the National Space Science Data Center at NASA's Goddard Space Flight Center (<http://nssdc.gsfc.nasa.gov/>), is necessary for all the frame transformations. NSSDC is a useful resource for planetary science data in general.

The planet's gravitational field is specified by GM , r_{ref} , and C_{20} as discussed in section 2.2. These values are updated regularly in light of improved data. The original reconstructions of the Mars Pathfinder trajectory and atmospheric structure were pre-MGS and used GMM-1 values. See Smith et al (1993). To verify my programs, I also used this model. Better ones are available from the MGS Radio Science experiment, but the changes are hardly significant for our purposes.

The initial conditions refer to distance from the centre of mass of Mars, not altitude above the surface. For convenience, most results are presented in terms of altitude above the well-known landing site position. The distance of the landing site from the centre of mass of Mars is 3389.715 km. This is given in E:/mpam_0001/document/edladdrds.htm (to six significant figures only) and in Magalhaes et al (1999). This number is not strictly necessary for the reconstruction procedure.

I do not have a good aerodynamic database for Mars Pathfinder. I have the data used to make figure 3 of Braun et al (1995) from Walt Engelund (see section 6.7) but I have no idea what Ma and Kn it is valid at. Figure 3 of Magalhaes et al (1999) shows that Braun's data is not valid above 80 km at all. Consequently, I have to use option 1 of section 2.8 for tracking the spacecraft's attitude. Examination of the data reveals that the high altitude results for the spacecraft x and y-axis accelerometers is contaminated by rotational contributions due to their off-centre position. I used only the z-axis accelerations in my reconstructions. See equation (21) in section 2.9.

I then integrate my trajectory forward in time using IDL's RK4 procedure and a very messy function for "derivs". I haven't checked to see what improvement it gives over a first-order integration procedure. The first few and last few timesteps are integrated using a first-order integration procedure. I needed a reasonable stretch of data to interpolate between timesteps and modifying "derivs" to use a shorter stretch of data near the ends would have been more trouble than it was worth. It also means that I can simply switch to the first-order integrator if desired.

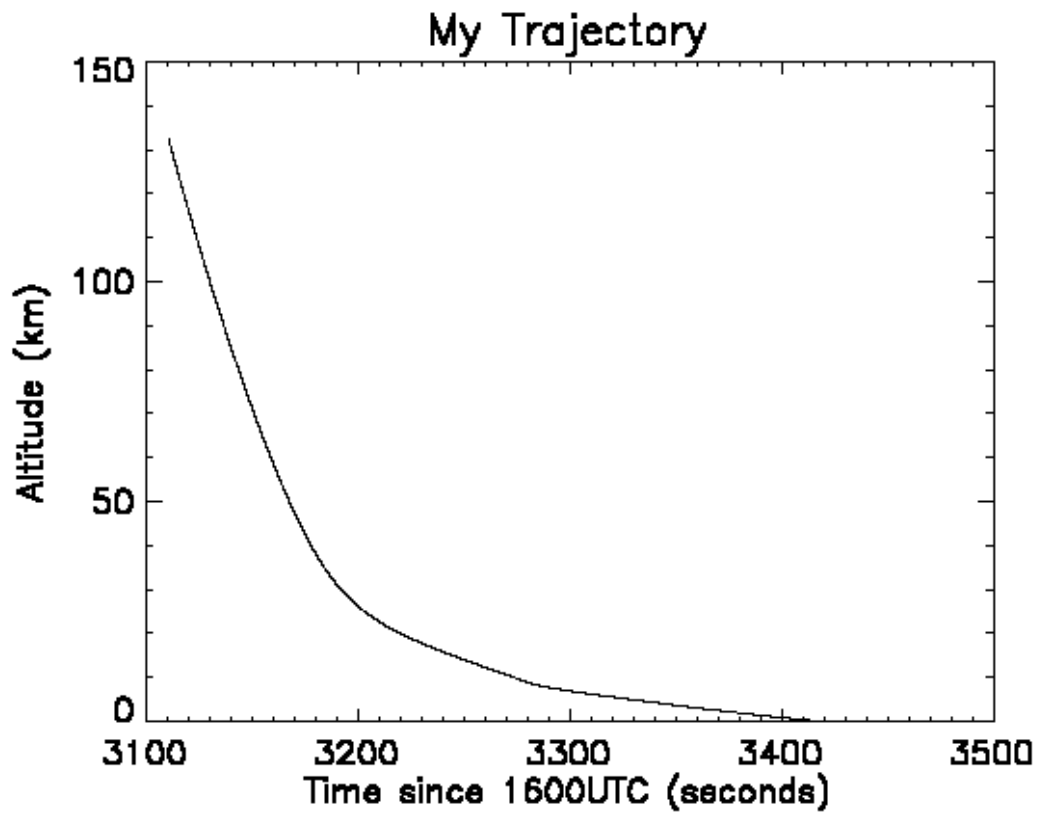
This is all the information necessary to reconstruct the trajectory of Mars Pathfinder.

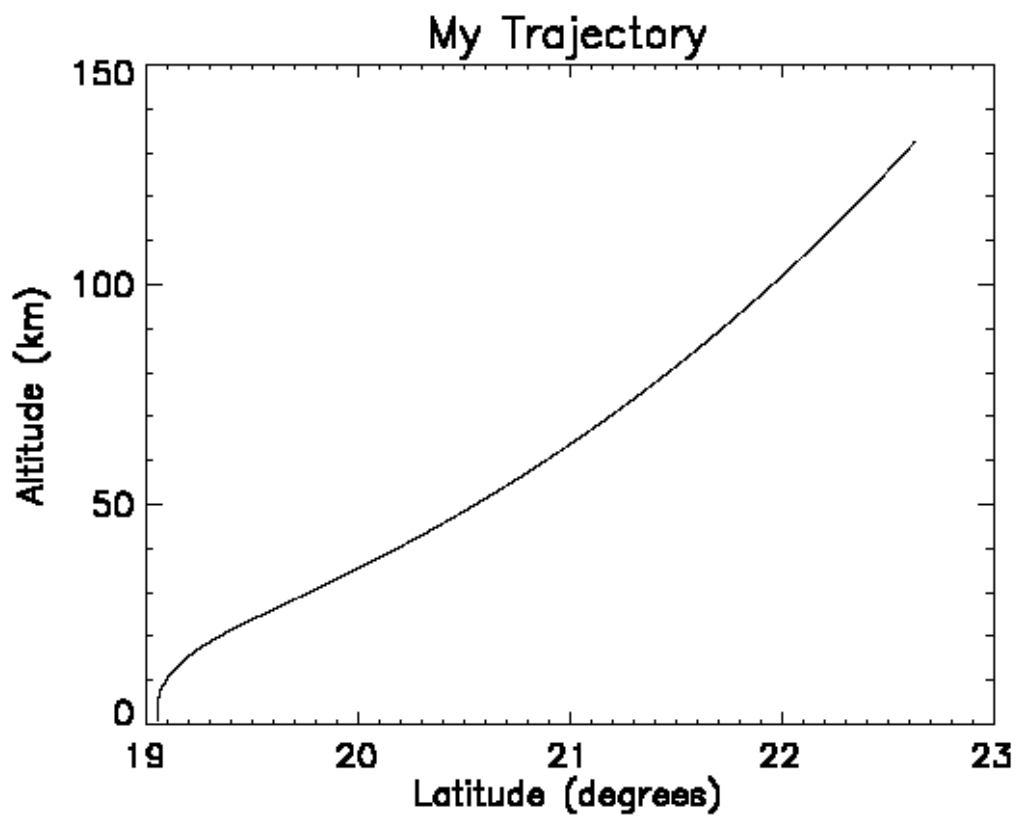
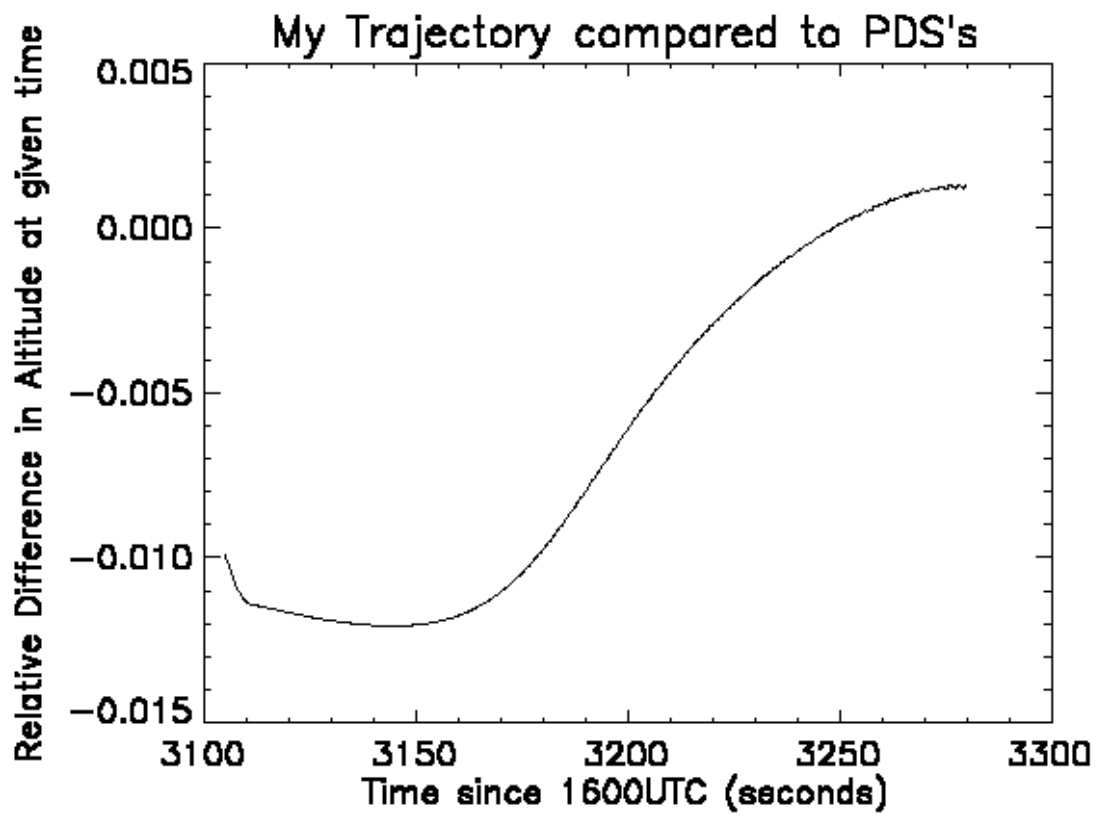
3.3 Reconstructed Mars Pathfinder Trajectory

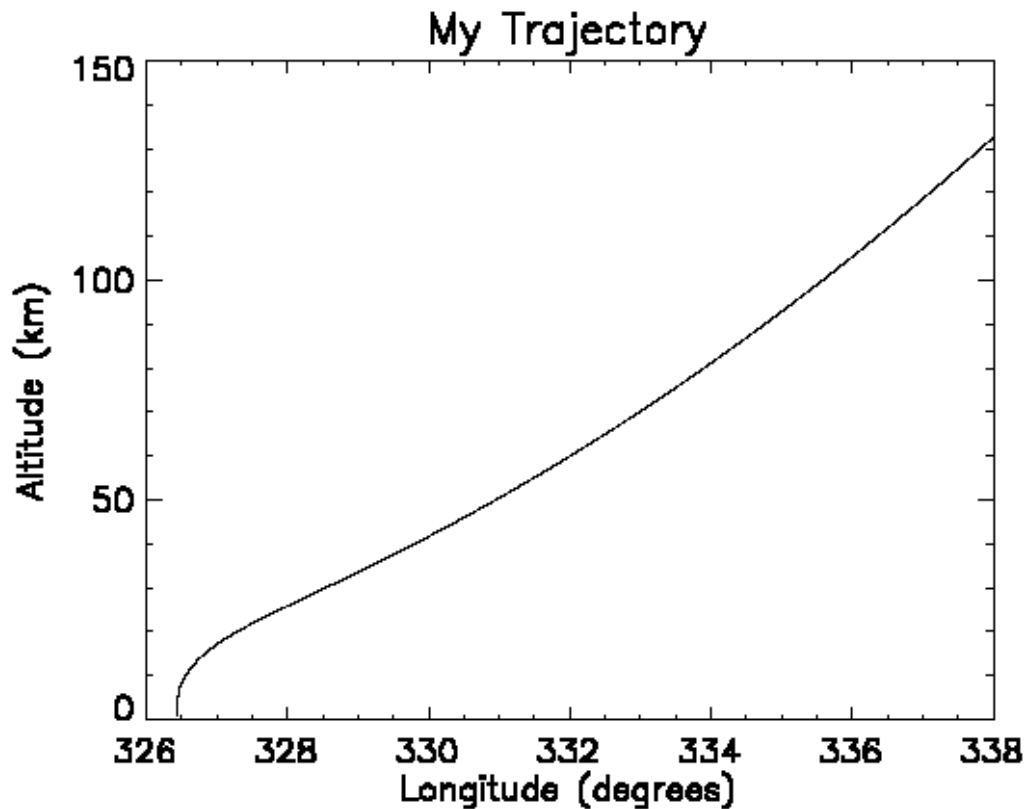
[Magalhaes et al, 1999; Spencer et al, 1999]

[E:/idl/mpf_nominal/extract_data.pro, E:/idl/mpf_nominal/recon_traj.pro,
E:/idl/mpf_nominal/plot_results.pro]

My trajectory is shown below. This may be compared with Figure 2 of Magalhaes et al (1999) if you are interested in the high altitude results not given by the PDS. My trajectory is compared with the PDS trajectory in the region where they overlap.







Differences in latitude and longitude have been shown in section 3.2 for both the PDS and the JSR entry states.

The results are good. Differences in latitude and longitude are on the order of a few hundredths of a degree. Differences in altitude are on the order of a percent. There appears to be both a systematic offset and an offset that grows more or less linearly with distance in all three fields. I attribute the systematic offset to the fact that the PDS trajectory is generated from a different entry state and then shifted to reproduce the landed position. The changing offset is probably due to uncertainties accumulating in my trajectory reconstruction that are minimised in the PDS reconstruction by additional constraints and better numerical techniques.

My landed position is:

406.3 m altitude below reference radius of 3389.715 km

19.055 degrees north latitude

326.446 degrees east longitude

The PDS landed position is:

At the reference radius of 3389.715 km

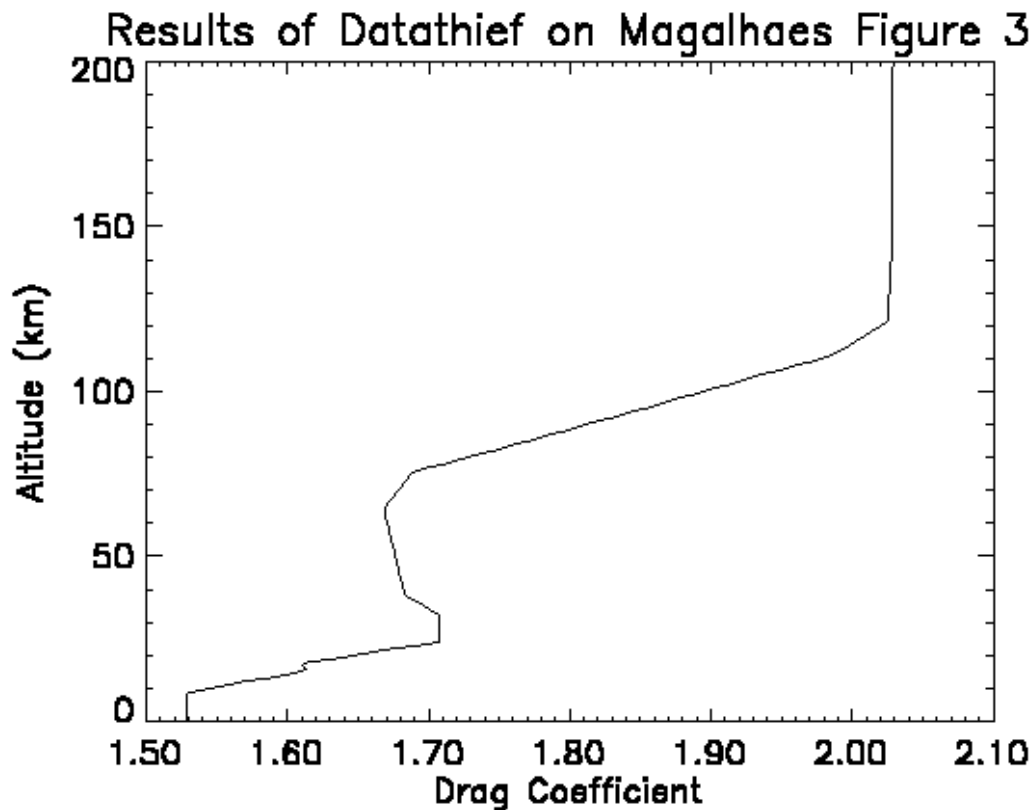
19.09 degrees north latitude

326.48 degrees east longitude

3.4 – Mars Pathfinder Aerodynamic Properties

[Magalhaes et al, 1999; Spencer et al, 1999; Braun et al, 1995]
[E:/idl/mpf_nominal/datathief.pro, E:/idl/mpf_nominal/thief.dat,
E:/idl/mpf_nominal/steal_mpfcd.pro, E:/idl/mpf_nominal/mpfcd.dat,
E:/idl/mpf_nominal/Mpfcd.jpg, E:/idl/mpf_nominal/mpfcd_rot.tif,
E:/idl/mpf_nominal/mpfcd_rot.gif]

Having done that, let's move on to reconstructing the atmospheric structure. Without any aerodynamic information at all, this is going to be difficult. However, figure 3 of Magalhaes et al (1999) gives the drag coefficient that they used as a function of altitude. I scanned this in and used Ralph Lorenz's handy datathief program to crudely reproduce the information that it contains. See the end of section 7.3. The single biggest cause of error in my reconstruction is likely to be poor knowledge of the drag coefficient.



This figure should be compared to Figure 3 of Magalhaes et al (1999). Roughly speaking, a 1% uncertainty in the drag coefficient causes exactly the same uncertainty in the derived temperature. A drag coefficient of 1.72 rather than 1.70 means, roughly, a temperature change of 2 K.

The spacecraft reference area necessary to do anything useful with the drag coefficient is 5.526 m² and the spacecraft mass is 585.3 kg. Both are given in E:/mpam_0001/document/edlhdrs.htm. When the mortar fires, the parachute opens, and the heatshield is jettisoned, the spacecraft mass changes. Spencer et al (1999)

mention the heatshield and backshell masses and when these are jettisoned. However, since the spacecraft aerodynamic characteristics are not well-known after the parachute opens, these details are moot.

This is all the information necessary to reconstruct the atmospheric density profile.

3.5 – Reconstructed Mars Pathfinder Atmospheric Structure

[Magalhaes et al, 1999; Spencer et al, 1999]

[E:/idl/mpf_nominal/recon_atm.pro, E:/idl/mpf_nominal/plot_results.pro]

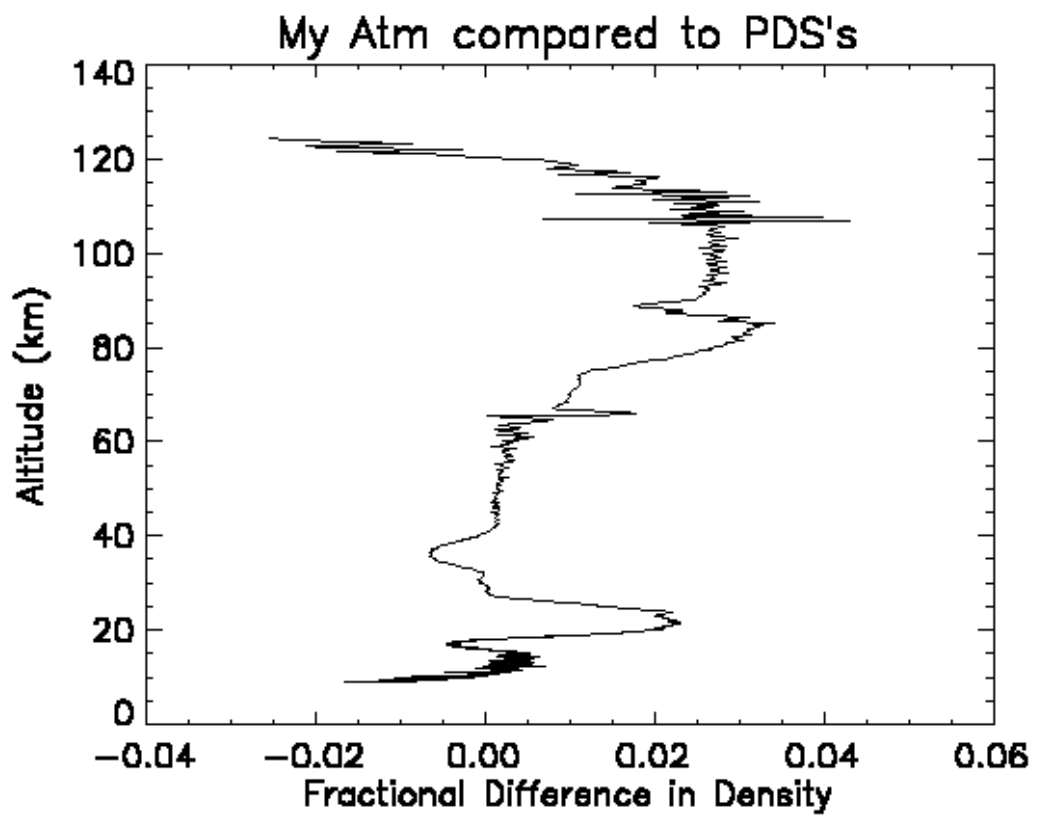
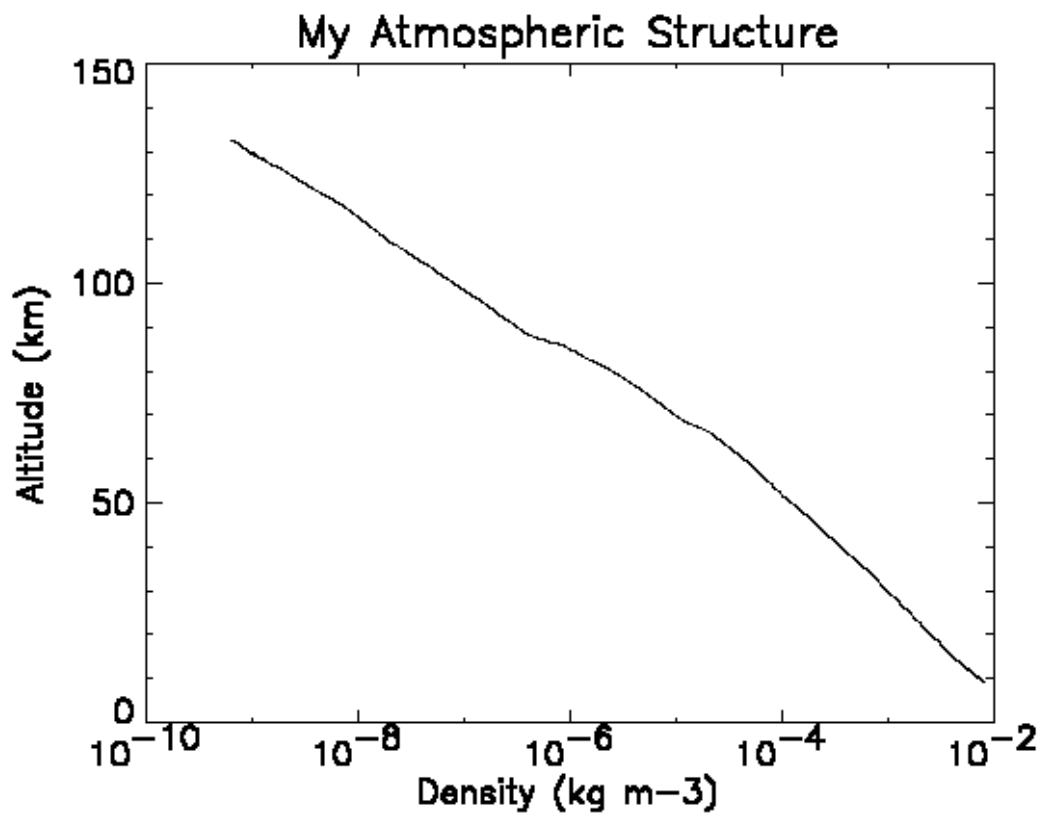
For simplicity, I use a spherically symmetric martian gravitational field and integrate the density profile to obtain the pressure profile. I fit densities in the highest 5 km of the data to get a density scale height applied at the highest altitude to use in my constant of integration. See section 2.12. The results are very sensitive to changes in these parameters. My integration routine is slow and should be improved. IDL's INT_TABULATED command will only integrate from one end to the other of an array. It won't integrate from one end to the other spitting out the result of the integration so far at each element of the array. So I have to integrate from the first to the second element in the array, from the first to the third, from the first to the fourth, ..., and from the first to the last. This is inelegant.

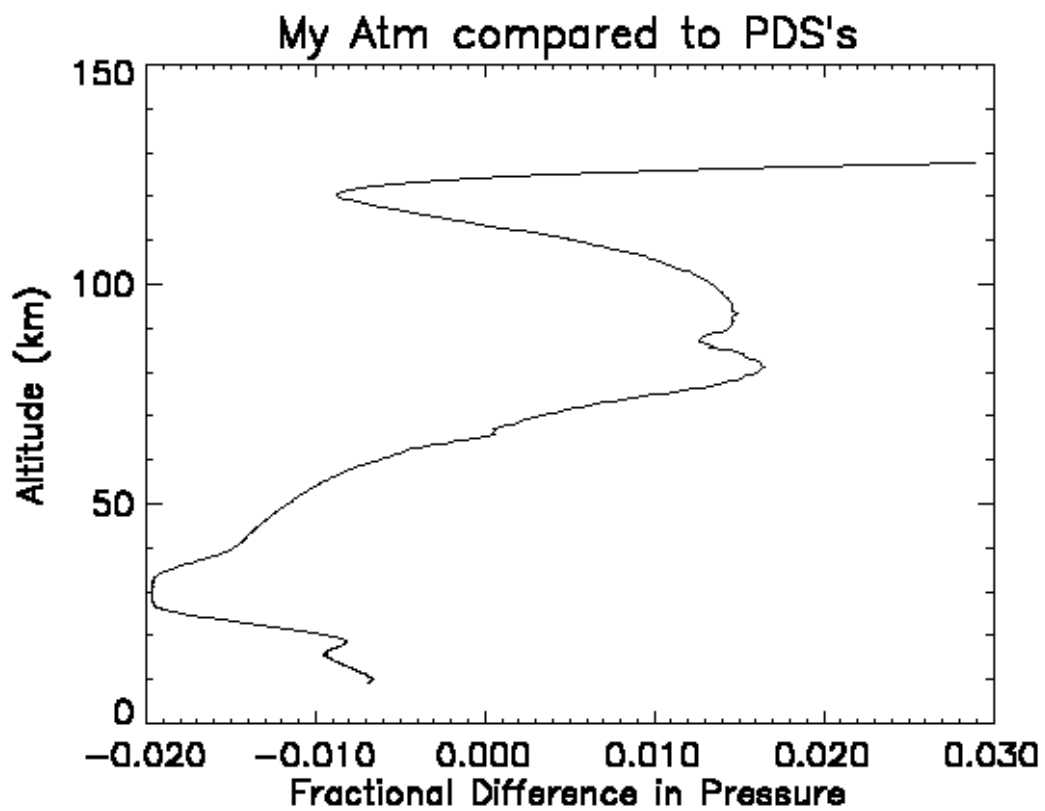
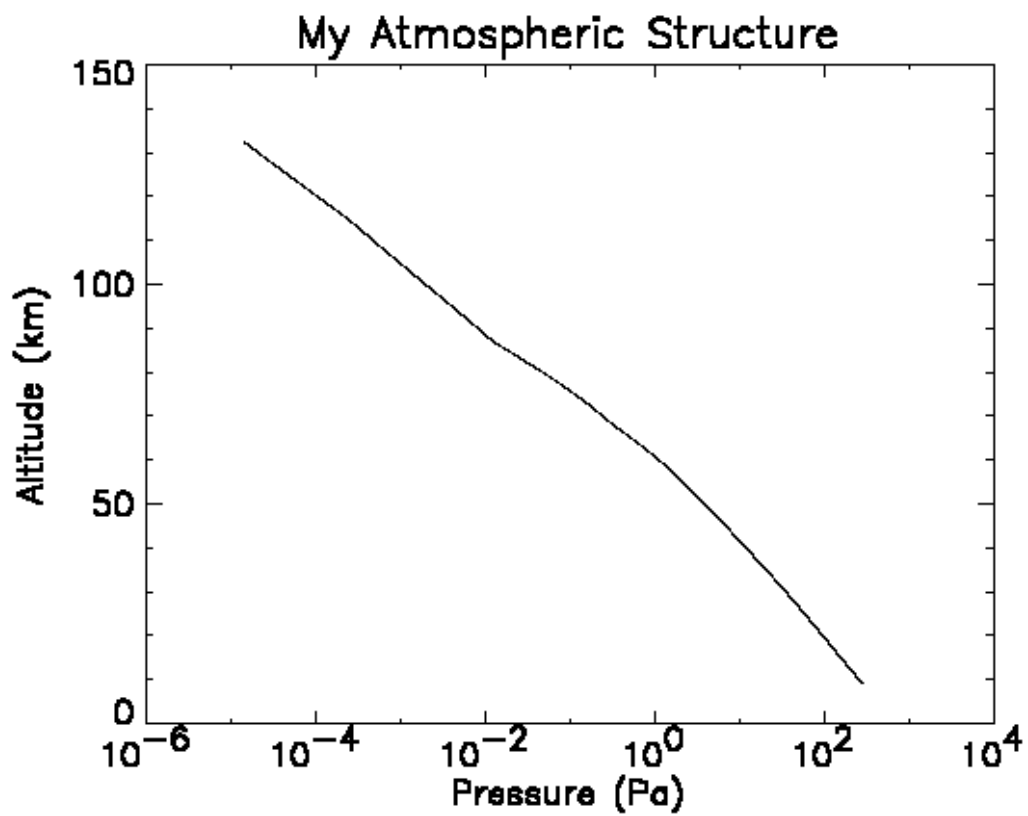
To calculate the temperature, I use the ideal gas law. I would really like to know how accurate that is for CO₂ in the conditions of interest to us. I use a constant mean molecular mass of 43.49 g mol⁻¹ which is given by

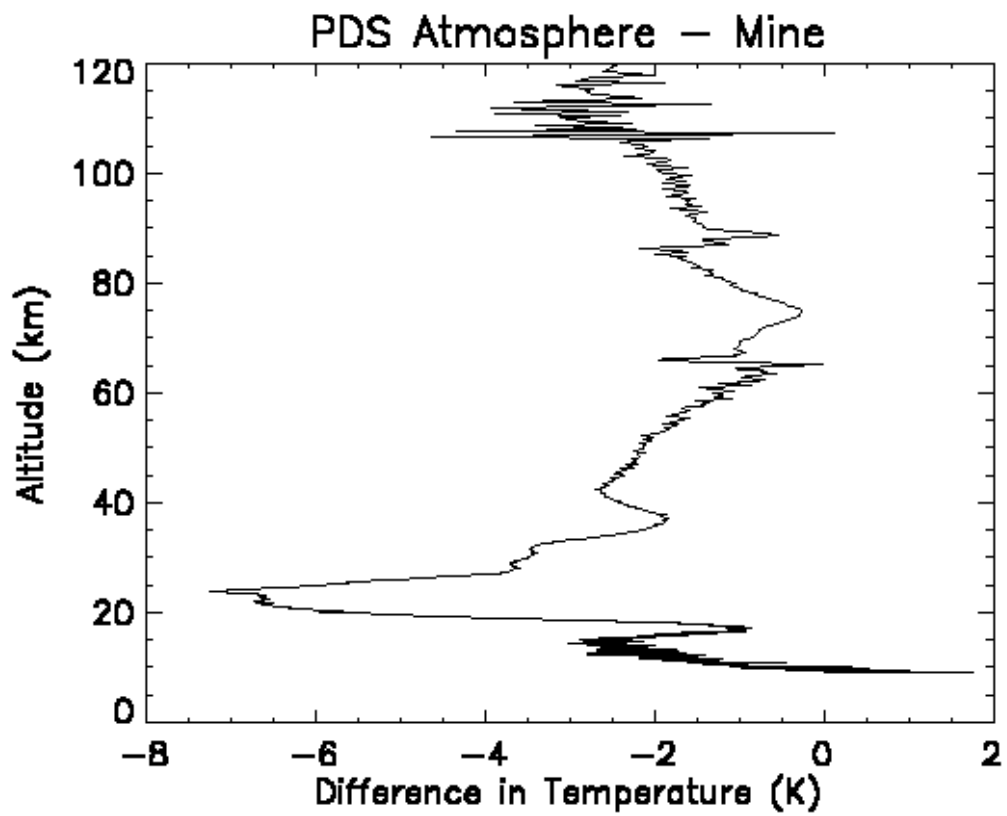
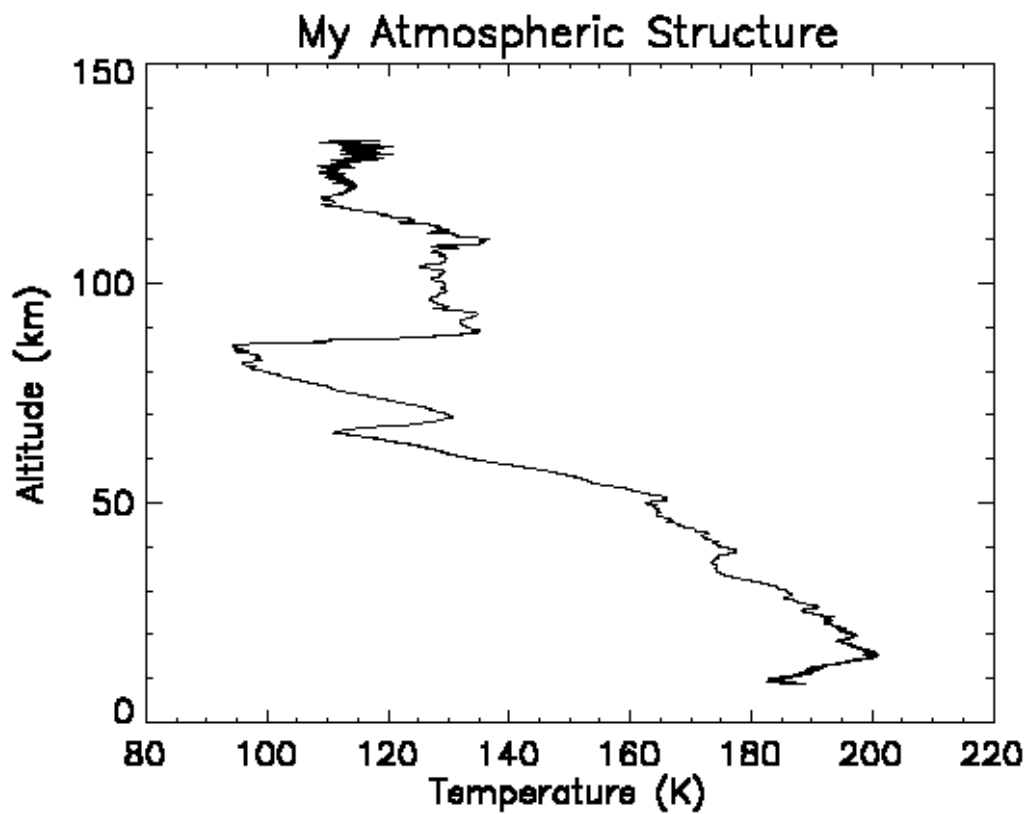
E:/mpam_0001/document/edladdrds.htm. Figure 4 of Magalhaes et al (1999) shows that that is a good approximation below 100 km and my temperature results above 100 km are not going to be improved by minor changes in the mean molecular mass.

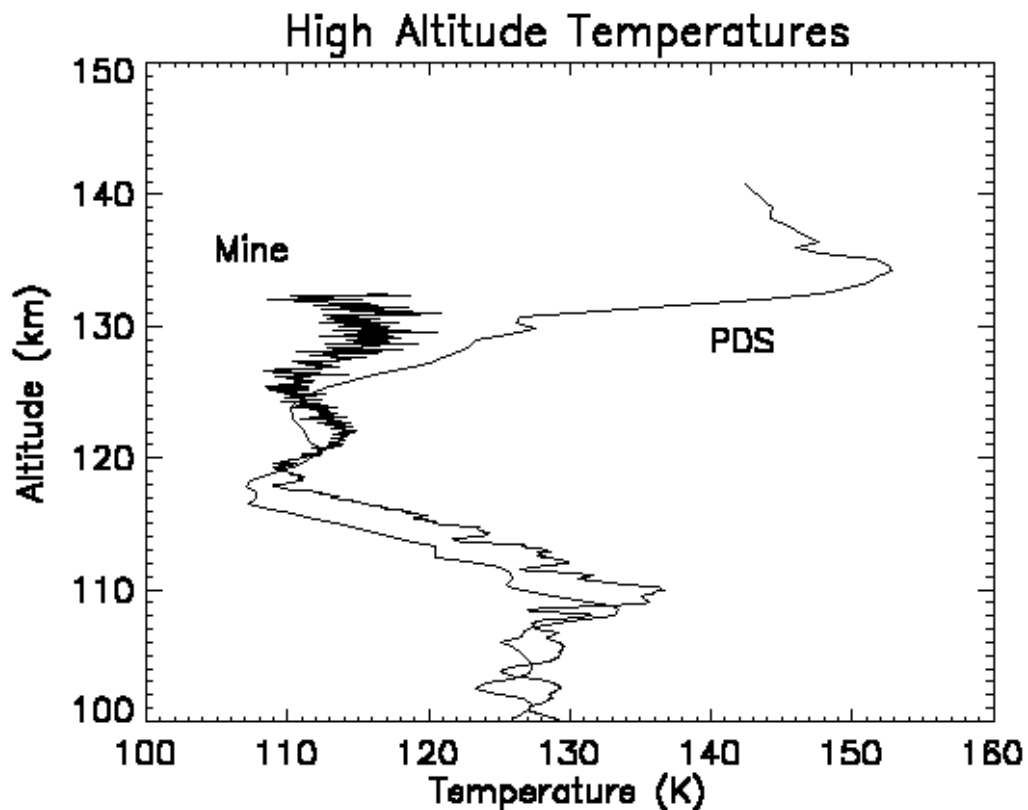
I use a universal gas constant of 8.31451 J K⁻¹ mol⁻¹ from Lodders and Fegley (1998).

The plot of $T(h)$ is the easiest result to interpret. It is the most useful for further scientific study.









Plots of fractional differences in density and pressure have omitted the very highest few kilometres as the interpolations necessary to translate one set of density (or pressure) measurements onto the set of height measurements appropriate for the other set didn't seem to do a good job with the smallest (hence highest) quantities.

The density, pressure, and temperature results are excellent at all altitudes. Density and pressure results are maybe 10% too low in the highest few kilometres. This is possibly due to corrections I have neglected to make to the data that only make a difference when the signal is barely above the noise. For instance, I have not made any corrections based on what the first few seconds of data look like.

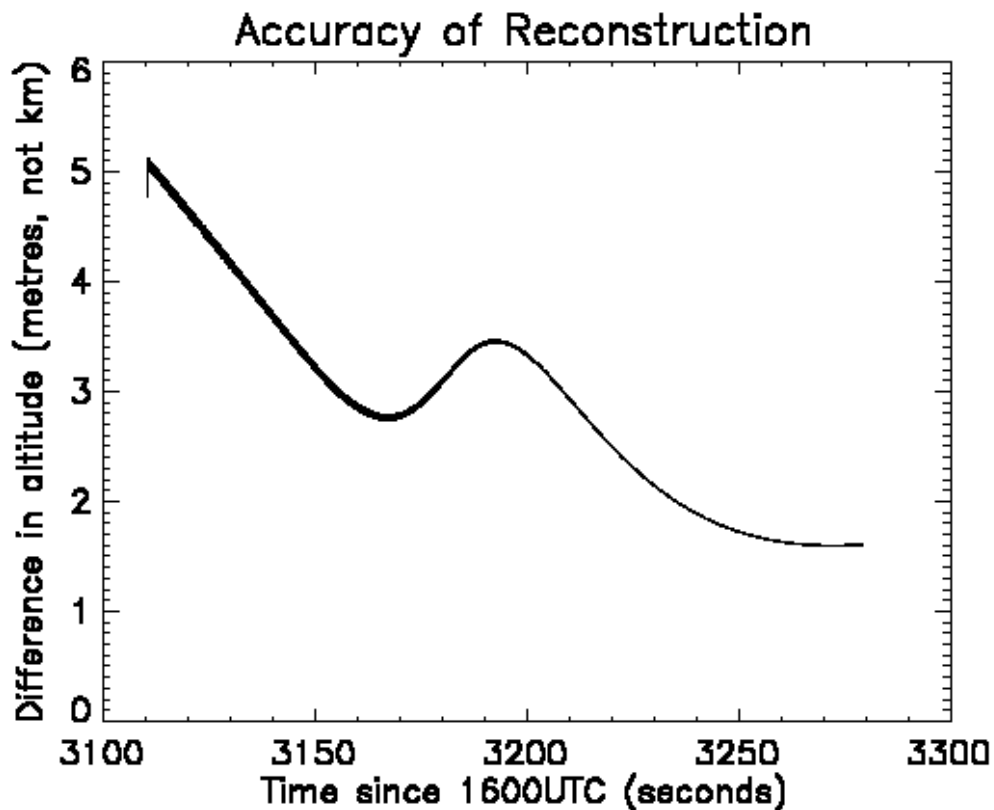
My temperature results at high altitude fluctuate a lot since the data is affected by digitisation at low signal levels. I haven't smoothed them at all. Sudden jumps in the difference between my temperatures and the PDS temperatures at 85 and 65 km altitude are due to our different techniques for interpolating through corrupted data at gain state changes. Below about 40 km my temperatures deviate more from the PDS temperatures. This is because the drag coefficient is varying significantly in this region and I have a very poor aerodynamic database to refer too.

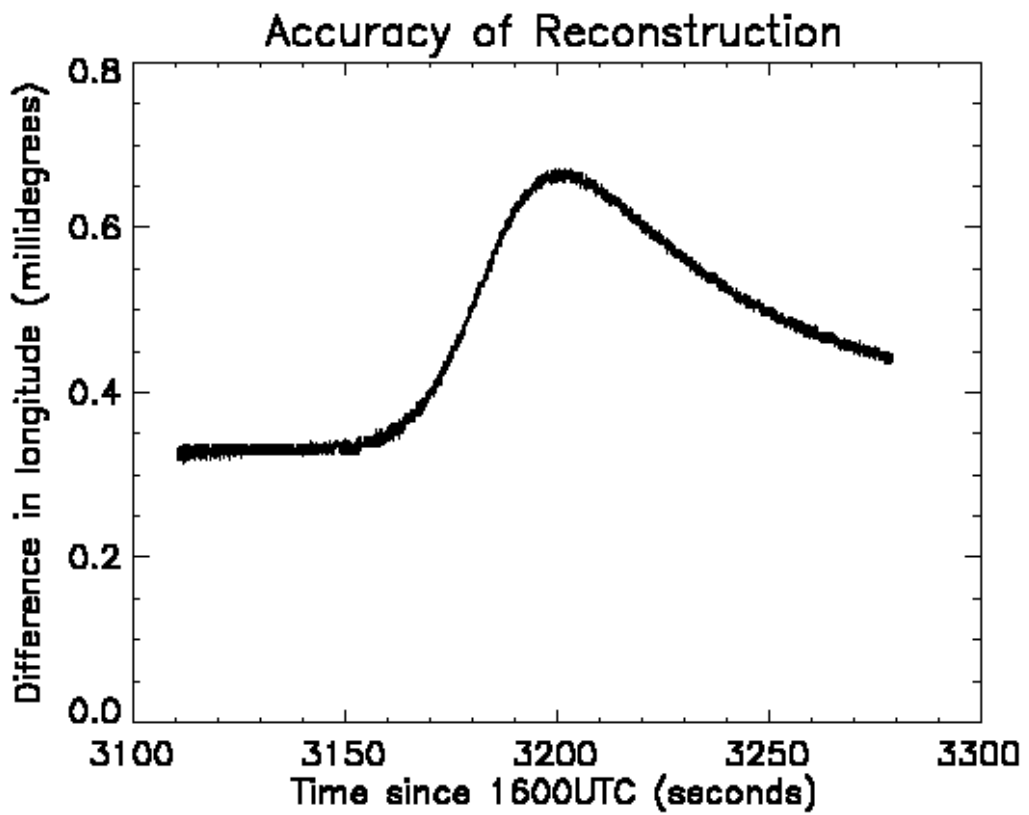
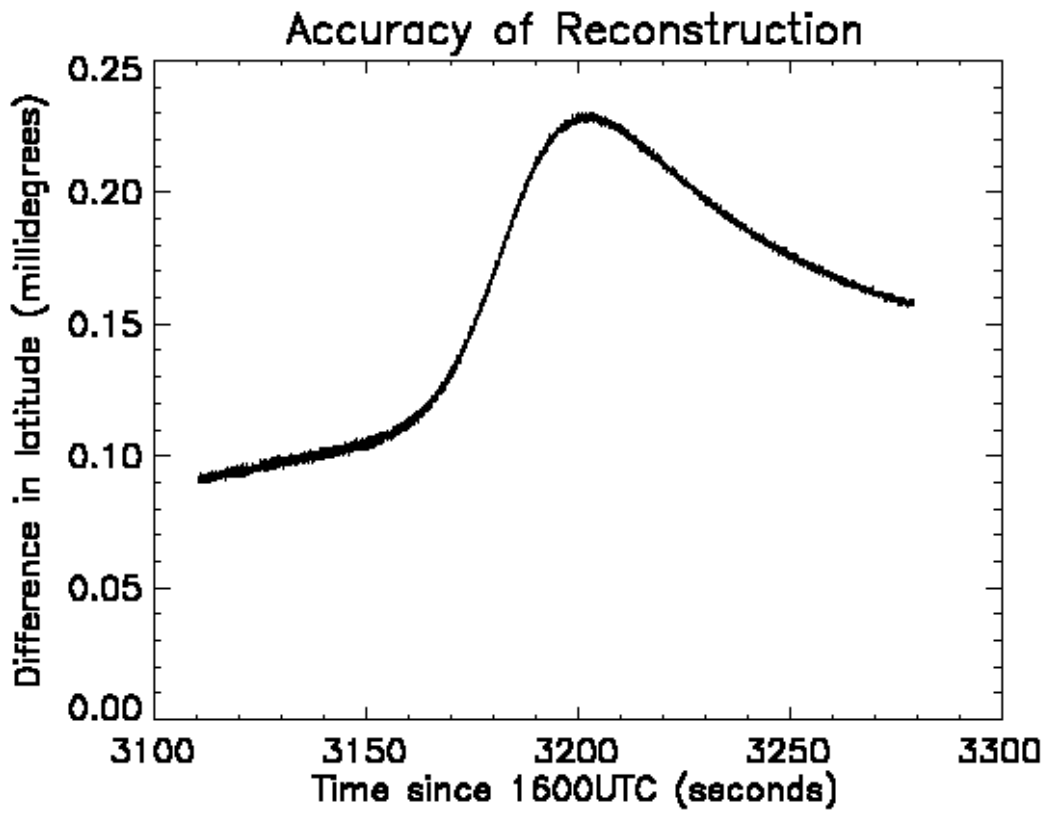
3.6 – Reconstructing the Reconstruction

[Magalhaes et al, 1999]

[E:/idl/mpf_nominal/model_atm.pro, E:/idl/mpf_nominal/get_acc_model.pro,
E:/idl/mpf_nominal/plot_model_results.pro]

To verify these results further, I modified this code to propagate a given entry state through a given atmospheric structure, returning the accelerations experienced by the spacecraft. This is the inverse problem to the one discussed above. This uses a simple first-order integration routine, admittedly with a 0.01s timestep. I used my solution for atmospheric density as a function of altitude and the JSR entry state for Mars Pathfinder. I have no knowledge of the aerodynamic properties of the Mars Pathfinder parachute, so cannot integrate the trajectory beyond the mortar firing. The results for predicted position are shown below. They are compared to the results of section 3.3.





Note that 0.1 millidegrees is 6 metres on Mars. The results appear good, but some aspects are puzzling. Why are the positions not identical at the start of the trajectories? I attribute it to a slight discrepancy between the time of the entry state and the time of the first acceleration measurements in the original trajectory reconstruction. A timing error of 0.01 seconds at the start of the trajectory corresponds to a lost distance of 70 m. Changes in the discrepancy in position after that after that might be due to my neglect of the spacecraft x and y-axis acceleration measurements in the original trajectory reconstruction. I have not studied these results in detail. Predicted velocities and accelerations should also be studied.

These techniques have provided consistent reconstructions of trajectory and atmospheric structure. Comparison with the PDS reconstructions shows that the reconstructions are correct.

4 - Error and Uncertainty

[Peterson (1965b) and scattered throughout the 1960s-era references]
[E:/idl/effects_of_errors/]

I have not attempted a formal error analysis of my solution procedures. Such an analysis is absolutely necessary for any interpretation of spacecraft data. I have been able to verify my reanalysis of the Mars Pathfinder data against the PDS data. This will not be possible for the first analysis of a dataset.

I recommend analytical and numerical studies of the effects of errors and uncertainties. Analytical studies will show why error or uncertainty in a given parameter is more important than in another. Numerical studies will provide an easy way of examining the effects of errors and uncertainties.

I have been able to make some simple simulations of the consequences of the some likely uncertainties using the Mars Pathfinder case as a framework:

4.1 – Uncertainty in Entry State Parameters

[E:/idl/effects_of_errors/entry_envelope.pro,
E:/idl/effects_of_errors/convert_entry_state.pro]

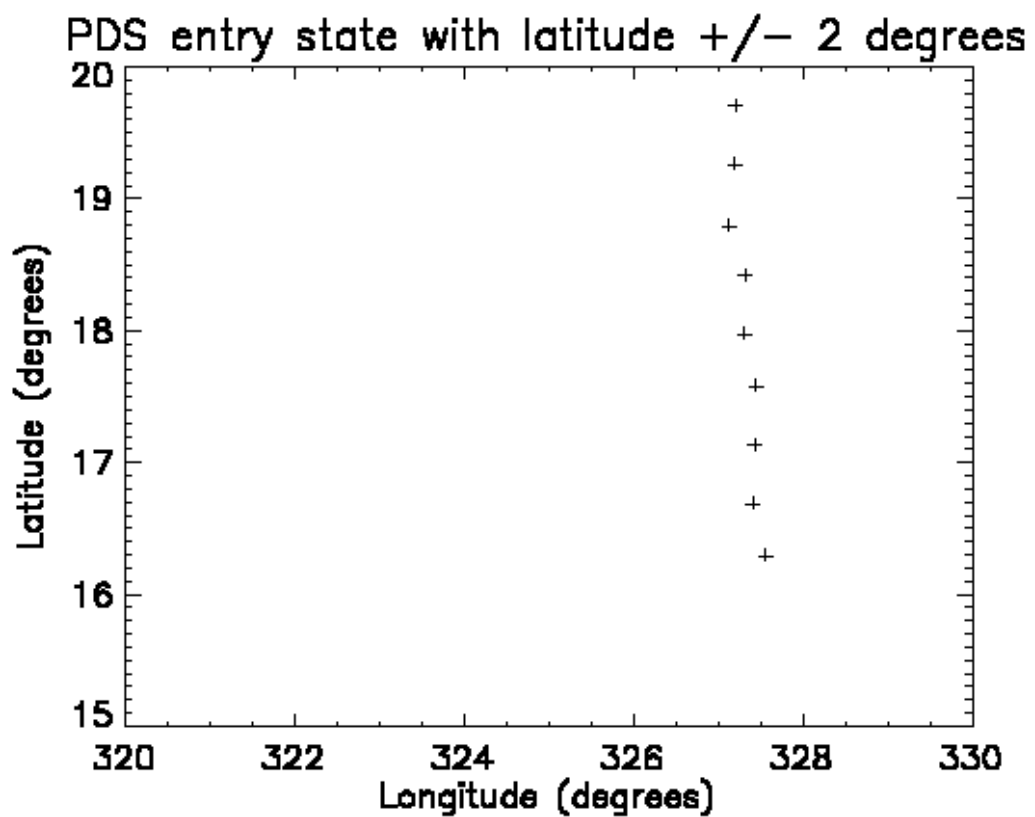
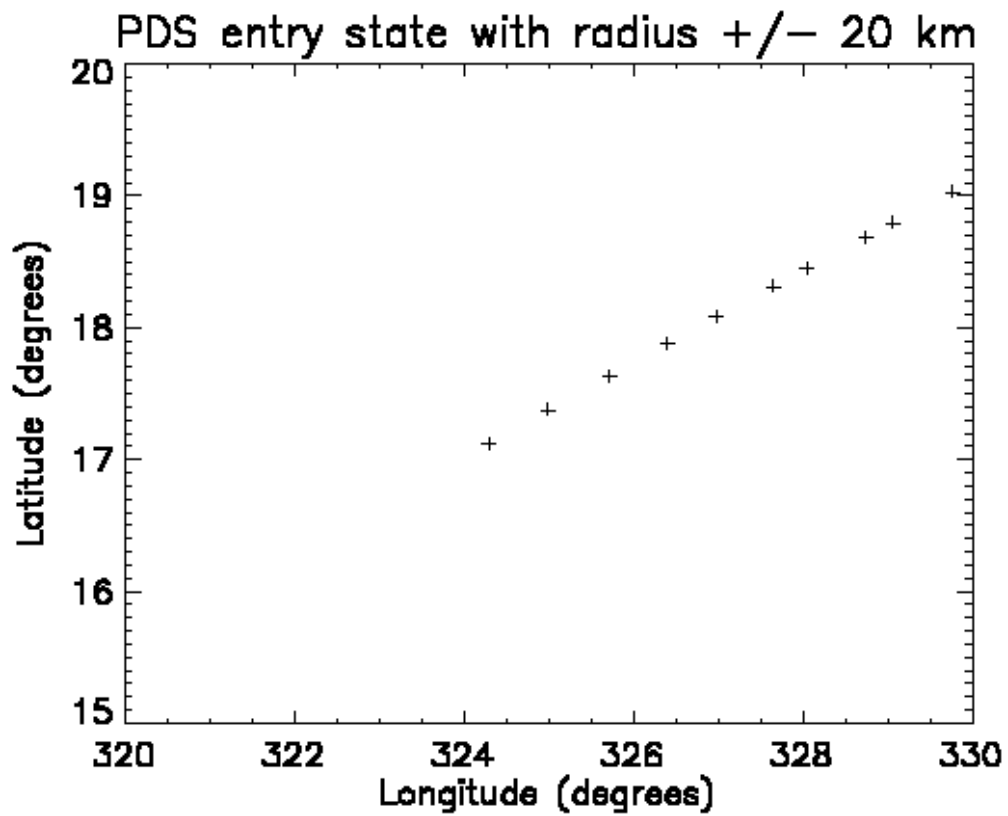
Adapting the code in section 3.6 makes it easy to see how landed position changes as a result of changed entry state. I took the PDS entry state and varied each parameter individually by what I thought was a suitable amount. I will not show any plots which vary more than one parameter, as the results become hard to interpret.

I have not changed the entry state in the code that reconstructs trajectory and atmospheric structure from the PDS accelerations. This is simply a result of pressures of time. Doing this will let you examine how your calculated $T(h)$ varies as a result of changing entry state within an uncertainty envelope. This is something that should be done.

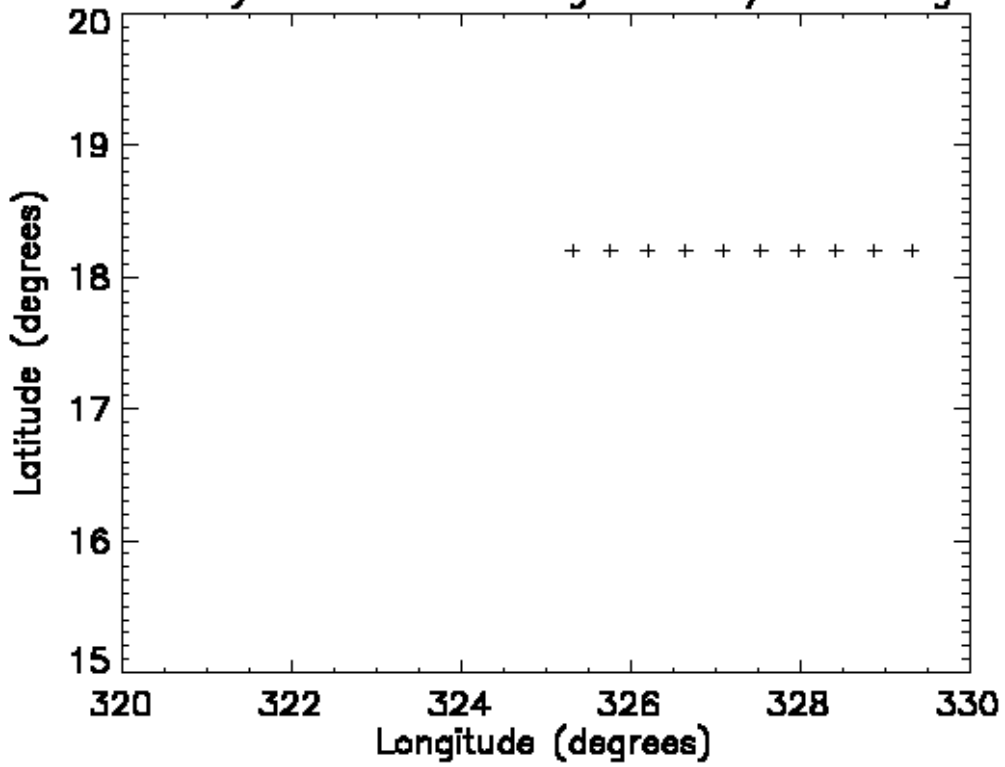
Instead, I dropped Mars Pathfinder into my reconstructed atmospheric structure and saw where it landed.

I am using the crudely modelled drag coefficient, my reconstructed atmospheric structure, and a timestep of 0.2 s. “The 'entry state' for 4-July-1997 16:51:12.28 UTC with 1-sigma uncertainties listed is $r = 3597.2 \pm 1.7$ km, $\theta = 23 \pm 0.04$ degrees N Areocentric latitude, $\phi = 343.67 \pm 0.01$ degrees East Longitude, $VR = 7444.7 \pm 0.7$ m/s, $\gamma = 16.85 \pm 0.02$ degrees, $\psi = 255.41 \pm 0.02$ degrees. r is the radial distance from the center of mass of the planet. VR is the entry speed, γ is the flight path angle below horizontal, and ψ is the flight path azimuth measured clockwise from North (all in a Mars-fixed, ie rotating, coordinate system).” Quoted from E:/mpam_0001/document/edladdrds.htm. I have used different uncertainties to give a reasonable spread across my plots.

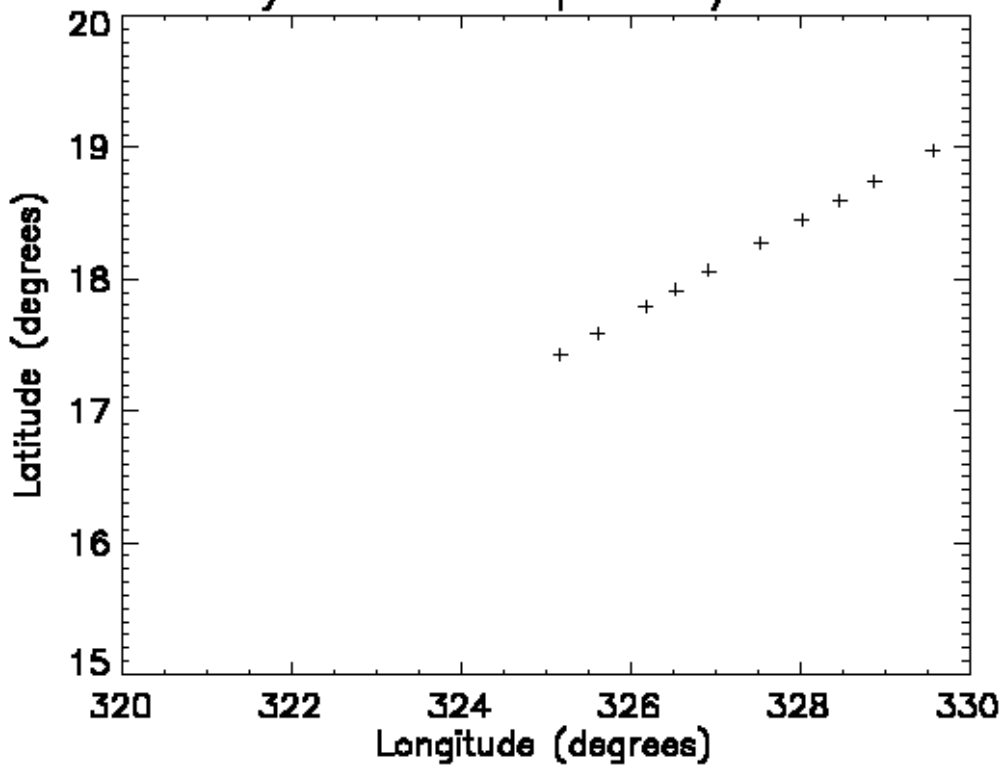
Changing the entry state time alone results in no change whatsoever in trajectory.

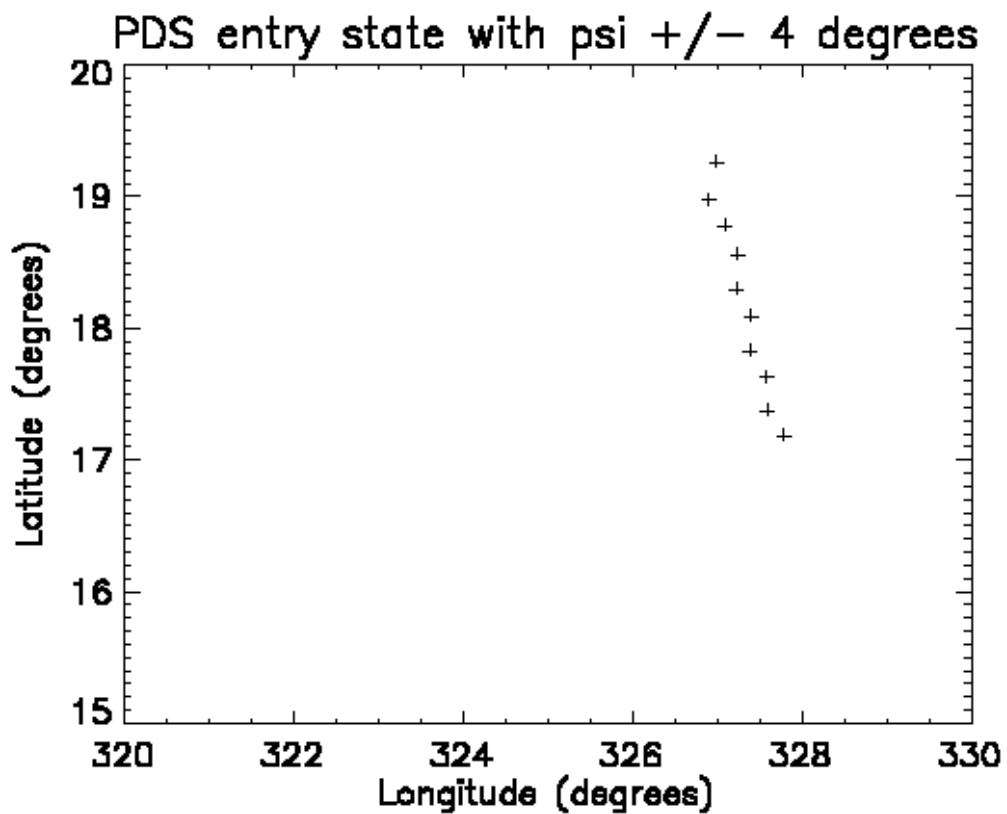
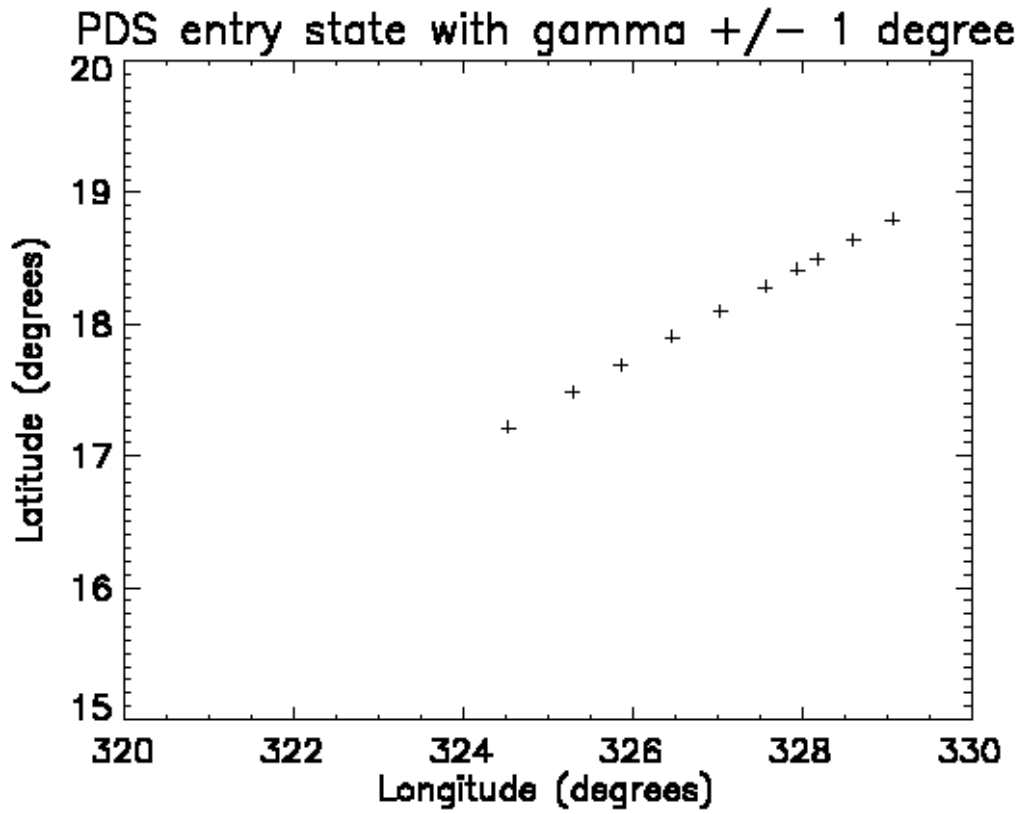


PDS entry state with longitude ± 2 degrees



PDS entry state with speed ± 2 km s⁻¹





I conclude that the most important parameters to know accurately are entry radius and flight path angle, γ . Uncertainties in entry latitude and longitude are reproduced

in uncertainty in landed position. Uncertainties in speed and azimuth angle, ψ , do not seem to have a large effect on landed position.

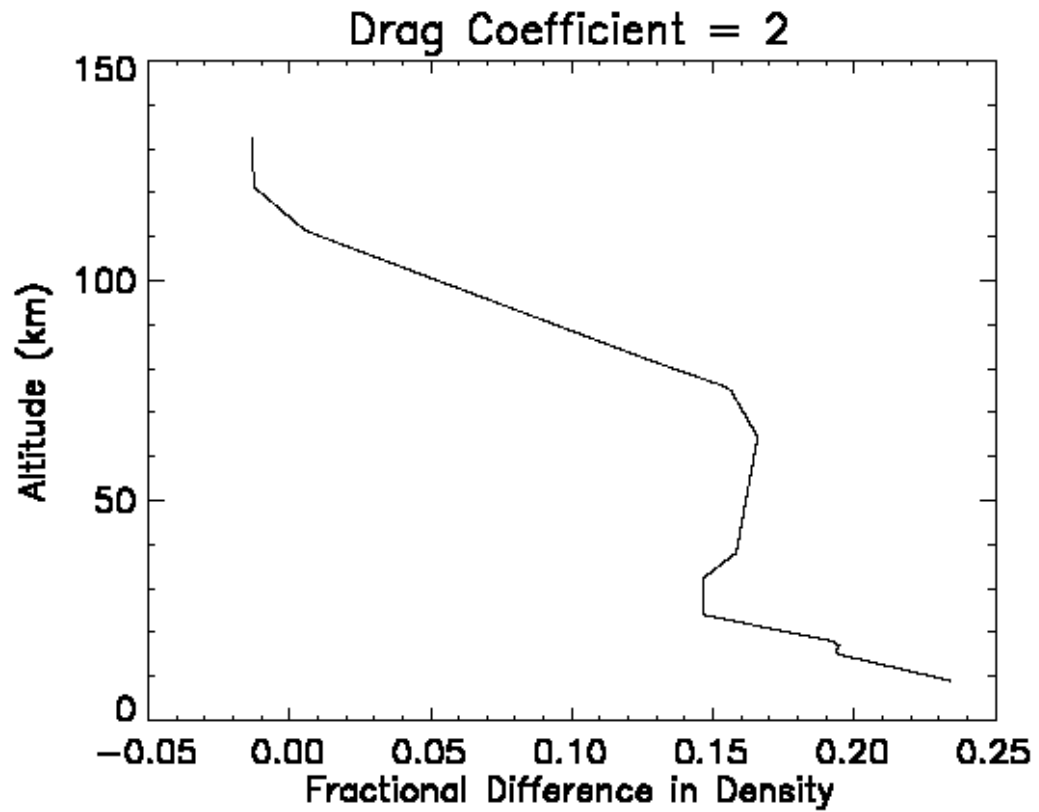
It is important to study the effects of these uncertainties on reconstructed atmospheric structure, in addition to the trajectory reconstruction looked at here.

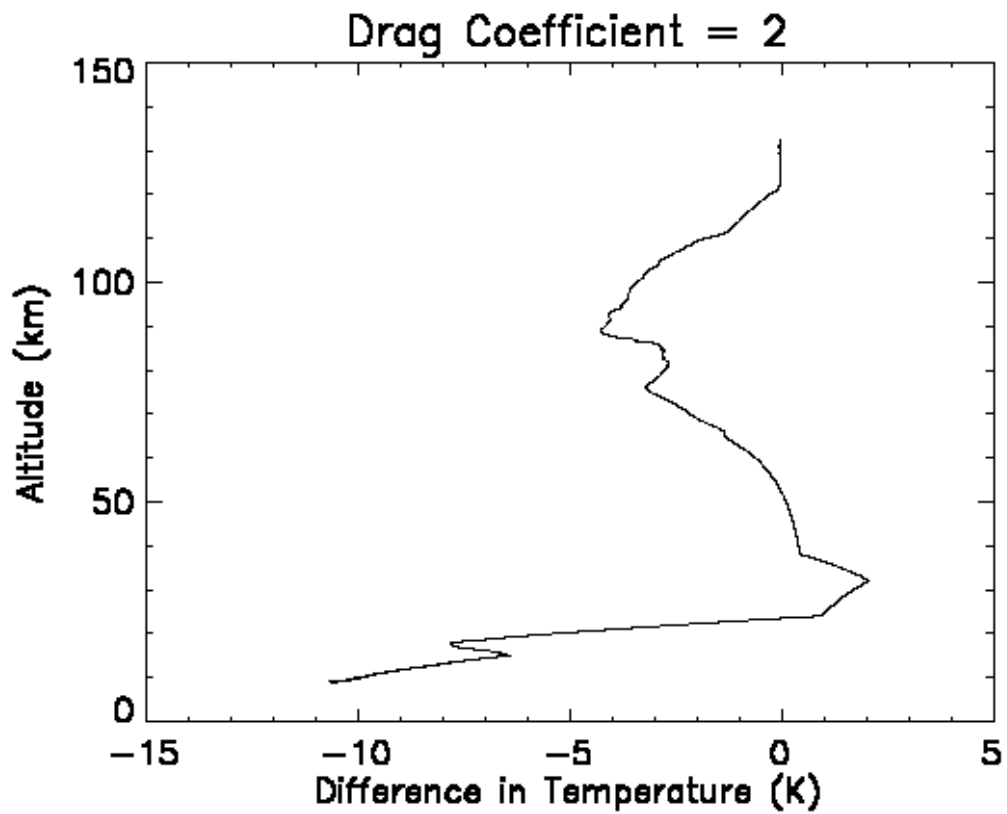
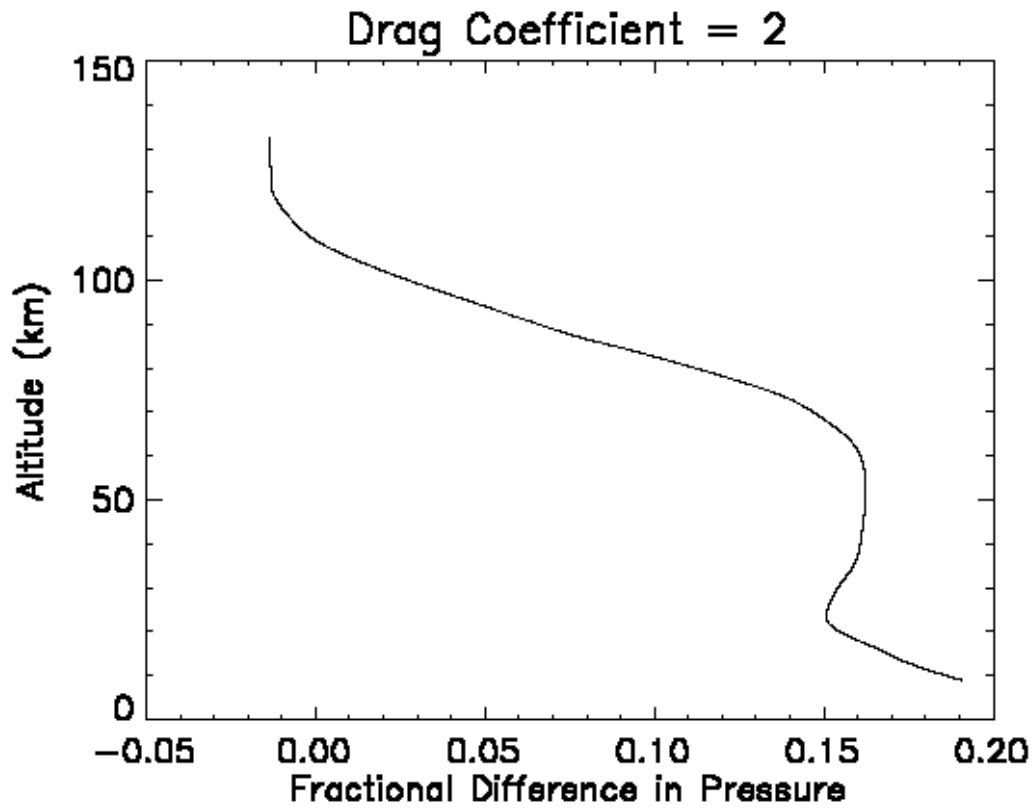
4.2 – Uncertainty in Aerodynamic Properties

[E:/idl/effects_of_errors/recon_atm.pro]

What are the effects on reconstructed atmospheric structure if the drag coefficient is poorly known?

I ran my atmospheric structure reconstruction code with the drag coefficient set everywhere to 2.0.





Density and pressure results are in error, compared to my nominal results using the crudely scanned drag coefficient, by tens of percent. The error in density obviously mimics the error I have introduced into the drag coefficient, as it should. The error in

pressure is a smoothed version of that. Since temperature is proportional to the ratio of pressure to temperature, this has the unexpected and pleasing effect that atmospheric temperatures are reconstructed very well indeed. **This has great potential for producing quick results to wave at your first press conference.** Given a direct landed measurement of atmospheric pressure, the density and pressure results can be corrected as well. It wouldn't hurt to have a direct measurement of landed temperature as well, since the error in temperature is large at low altitudes where the drag coefficient is far from 2.0.

If the drag coefficient is systematically in error by exactly 1%, then densities and pressures are systematically in error by exactly the same amount and the errors cancel out to give a perfect temperature reconstruction.

If the error in the drag coefficient is allowed to vary, then the results are worse. I have not been able to implement a convincing scheme for putting randomly varying errors of between, say, +/- 10%, onto my values for the drag coefficient and still keeping a smoothly varying curve for the drag coefficient as a function of altitude. More work to understand the effects of errors and uncertainties in the aerodynamic properties on the final results is needed...

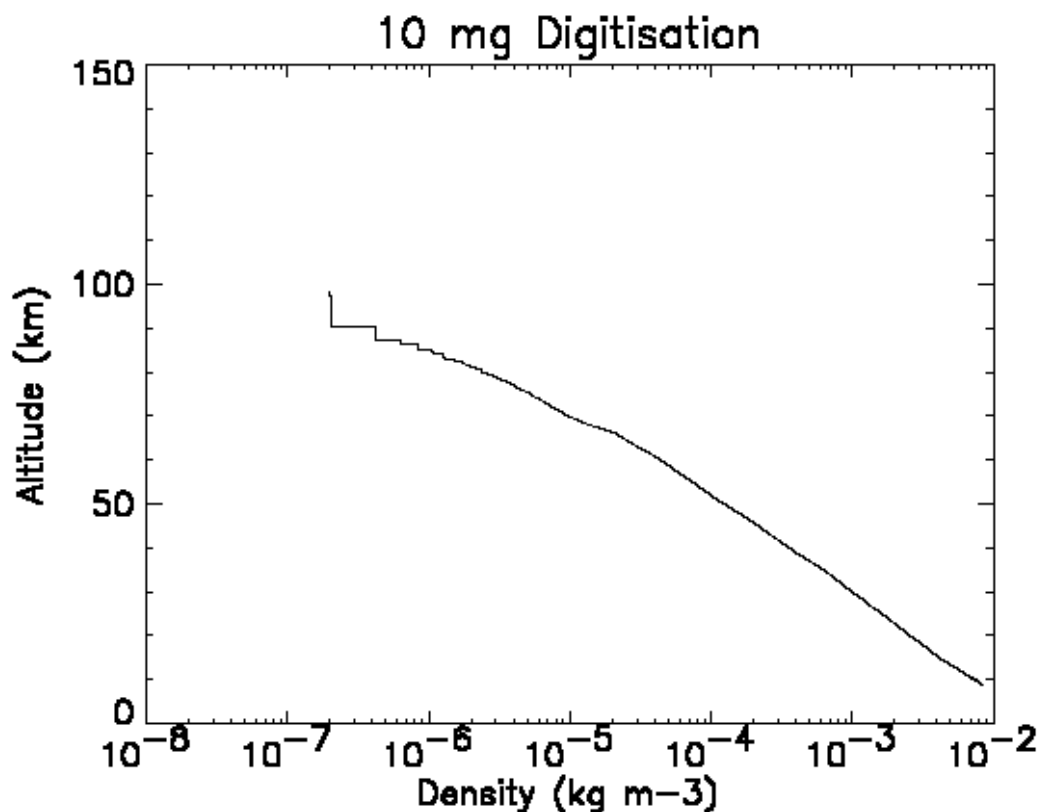
4.3 - Digitisation of acceleration measurements

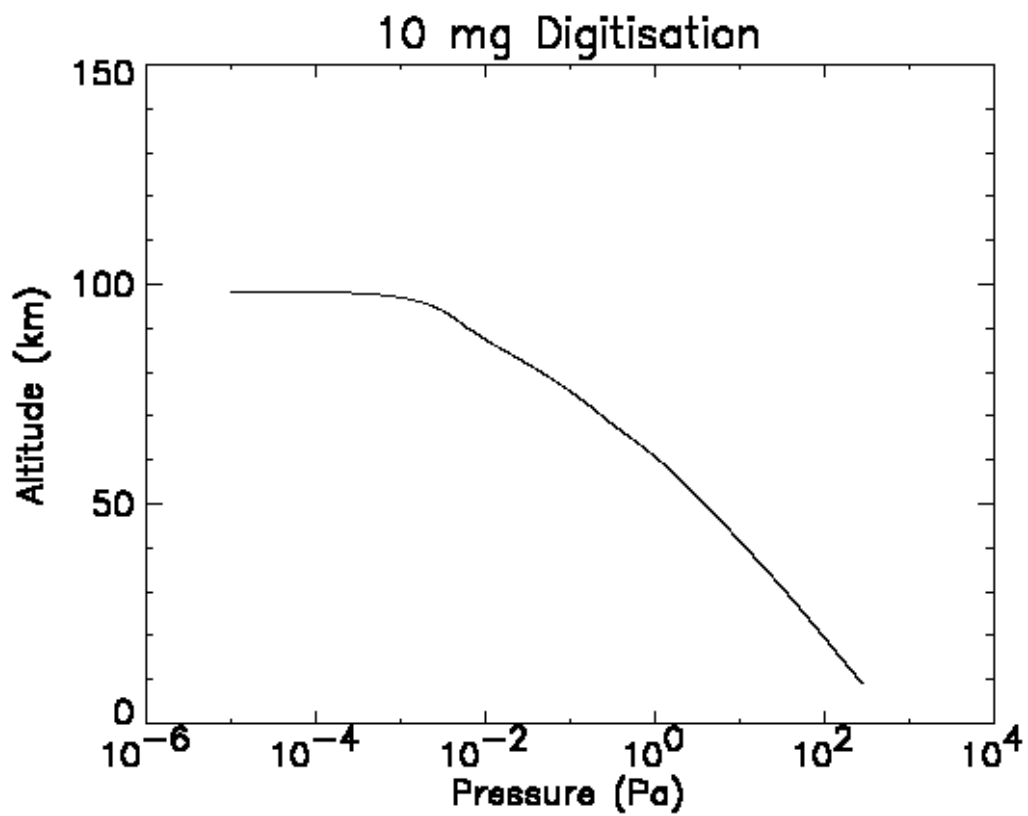
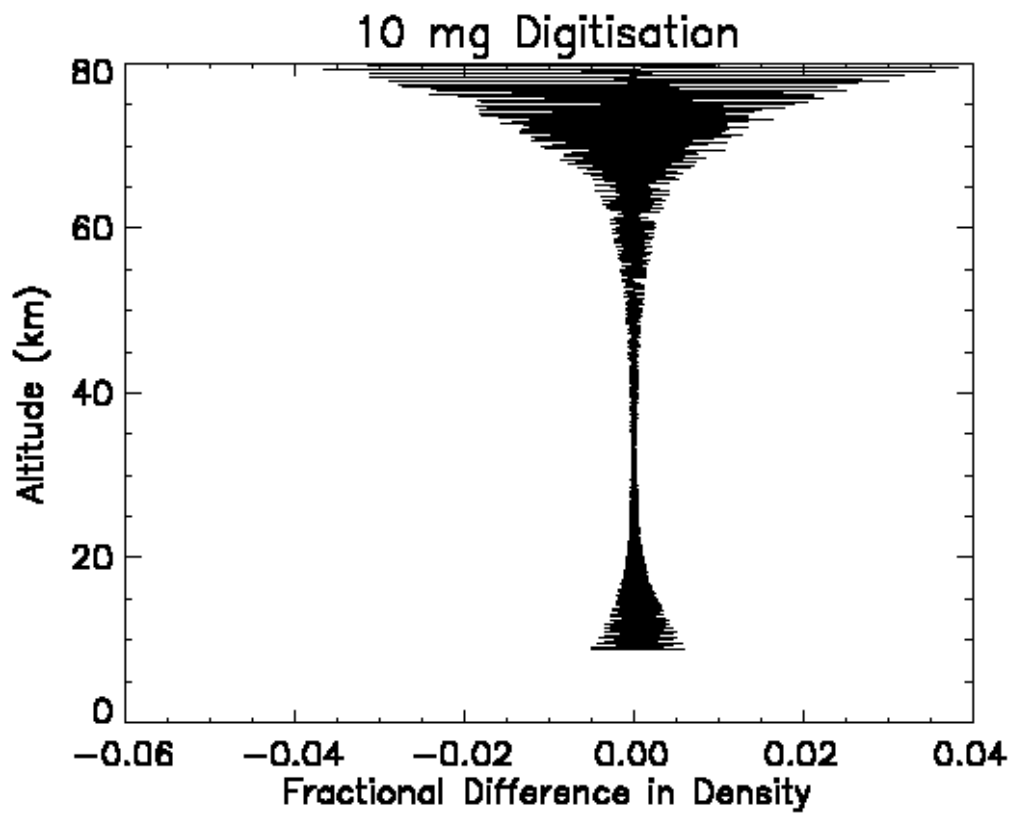
[E:/idl/effects_of_errors/extract_data.pro, E:/idl/effects_of_errors/corrupt_data.pro]

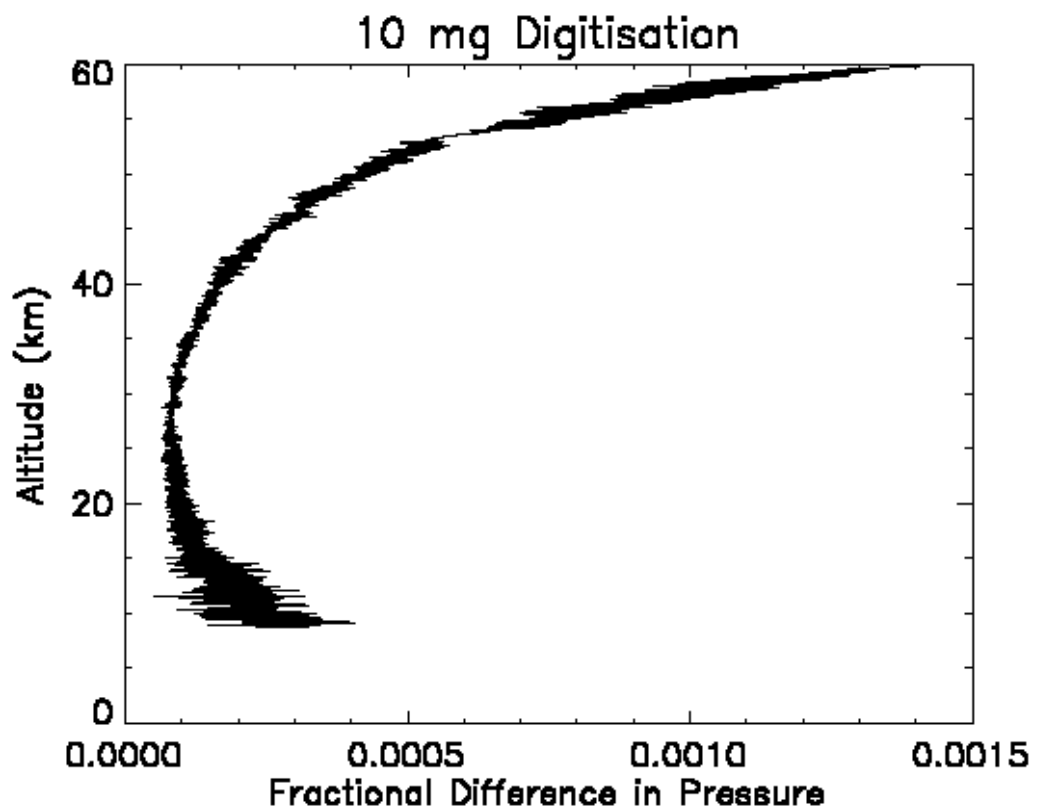
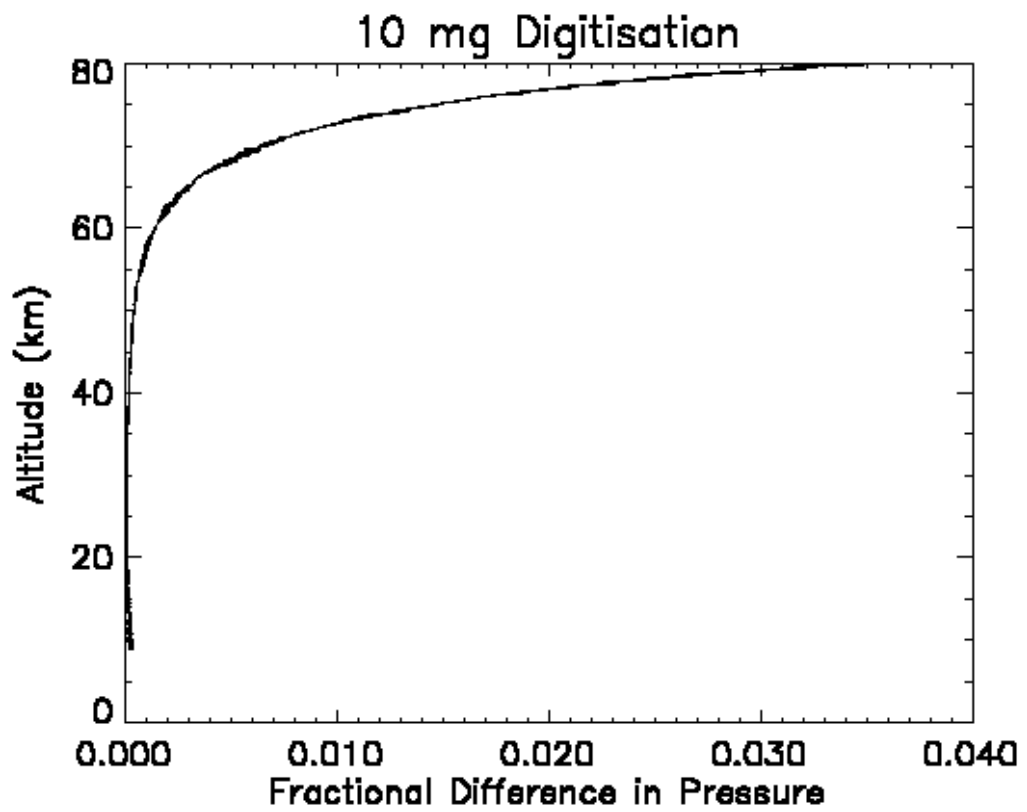
Data is degraded by digitisation. The Mars Pathfinder data was digitised to 14 bits and each accelerometer had the same three gain states. The first, with a dynamic range of ± 16 mg, had a digital resolution of $2 \mu\text{g}$; the second, with a dynamic range of ± 800 mg, had a digital resolution of $100 \mu\text{g}$; and the third, with a dynamic range of ± 40 g, had a digital resolution of 5 mg (Magalhaes et al, 1999).

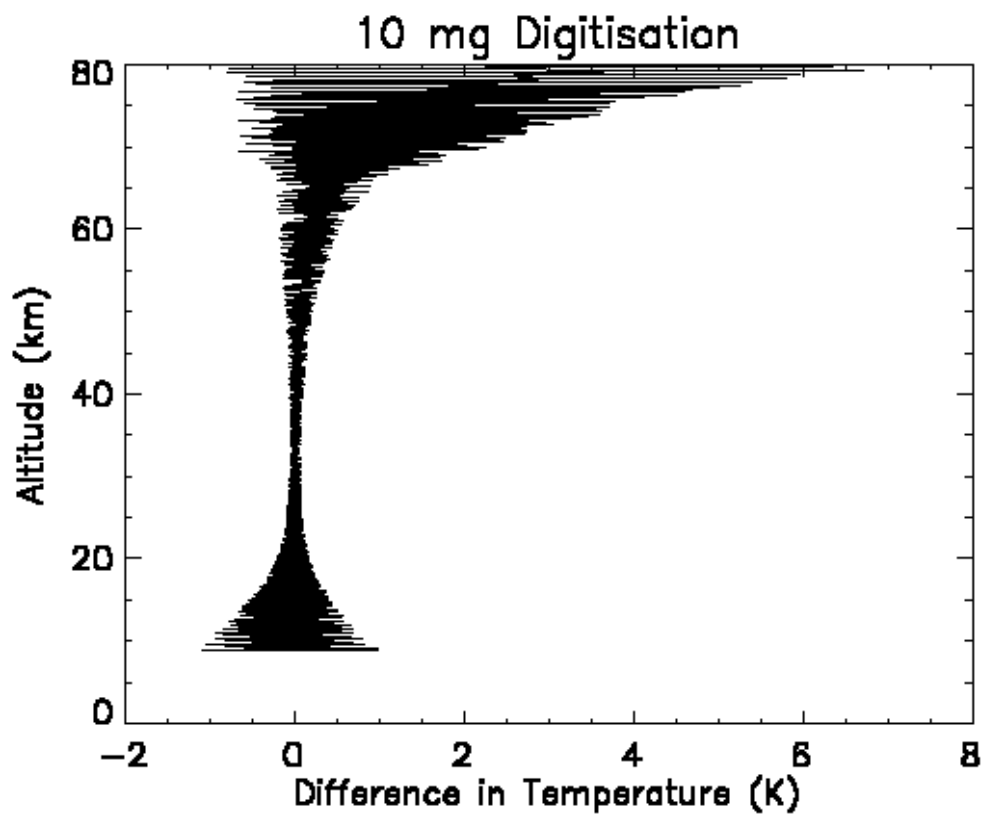
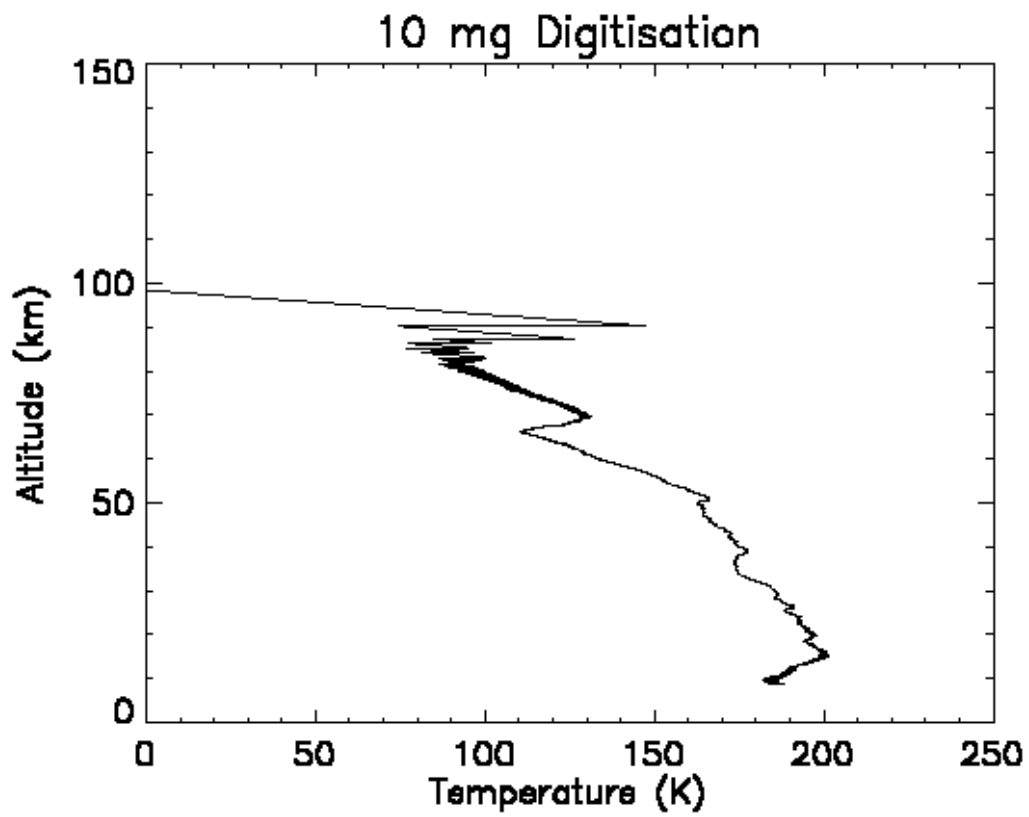
Roughly, the lowest gain state applied above about 110 km, the intermediate gain state between 110 km and 60 km, and the highest gain state below 60 km.

I artificially digitised the Mars Pathfinder accelerations to 10 mg and show the change in atmospheric temperature compared to my nominal reconstruction. Since this makes the highest altitude measurements meaningless, I used zero as my constant of integration in the integration for pressure. The error introduced by this is probably overwhelmed by the digitisation effects at high altitude and is negligible at lower altitudes. Changes in landed position are less than one-hundredth of a degree in both latitude and longitude.









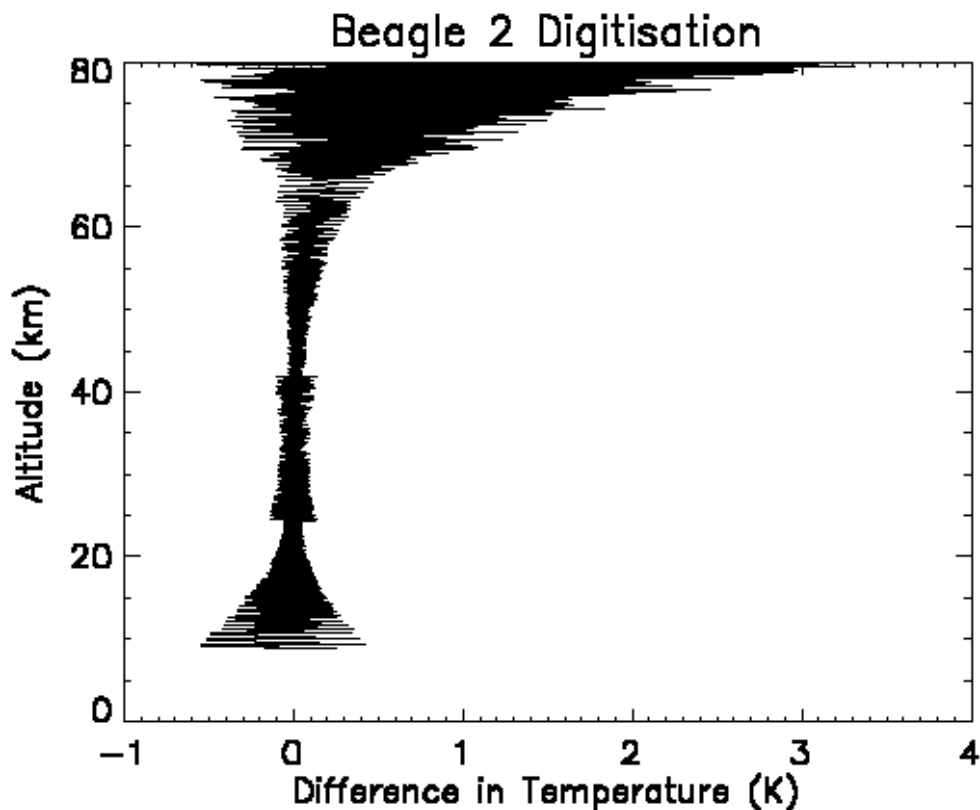
As you might expect, the only effect of increased digitisation is to make the results meaningless above a lower altitude threshold than before. The shape of the plot of pressure difference is interesting. The high altitude shape is caused by the use of zero as the constant of integration in the pressure integration. It can be improved by calculating a better constant of integration when the data become significantly larger than the digitisation. This would take a little bit of investigation. The shape of the plot of temperature difference does not change if a different digitisation is applied, it merely scales the horizontal axis differently.

The Beagle 2 digitisation will be:

Science x and y axis accelerometers	1 mg	+/- 2 g range
Science z axis accelerometer	15 mg	+/- 30 g range
System z axis accelerometer	5 mg	+/- 10 g range

14 bit resolution, 12 bit accuracy

Applying this digitisation the Mars Pathfinder data, I obtained results that were very similar to the 10 mg digitisation discussed above. I show only the plot of temperature difference compared to my nominal reconstruction.



4.4 – Reduced Sampling Rate

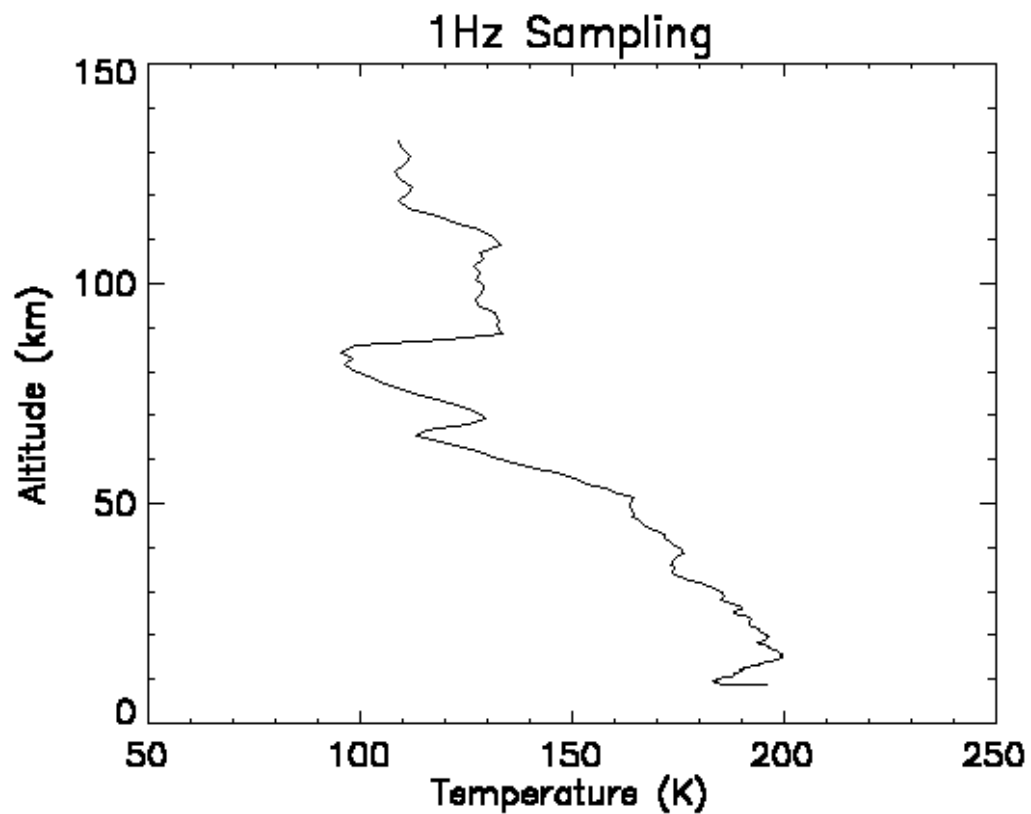
[E:/idl/effects_of_errors/extract_data.pro, E:/idl/effects_of_errors/corrupt_data.pro]

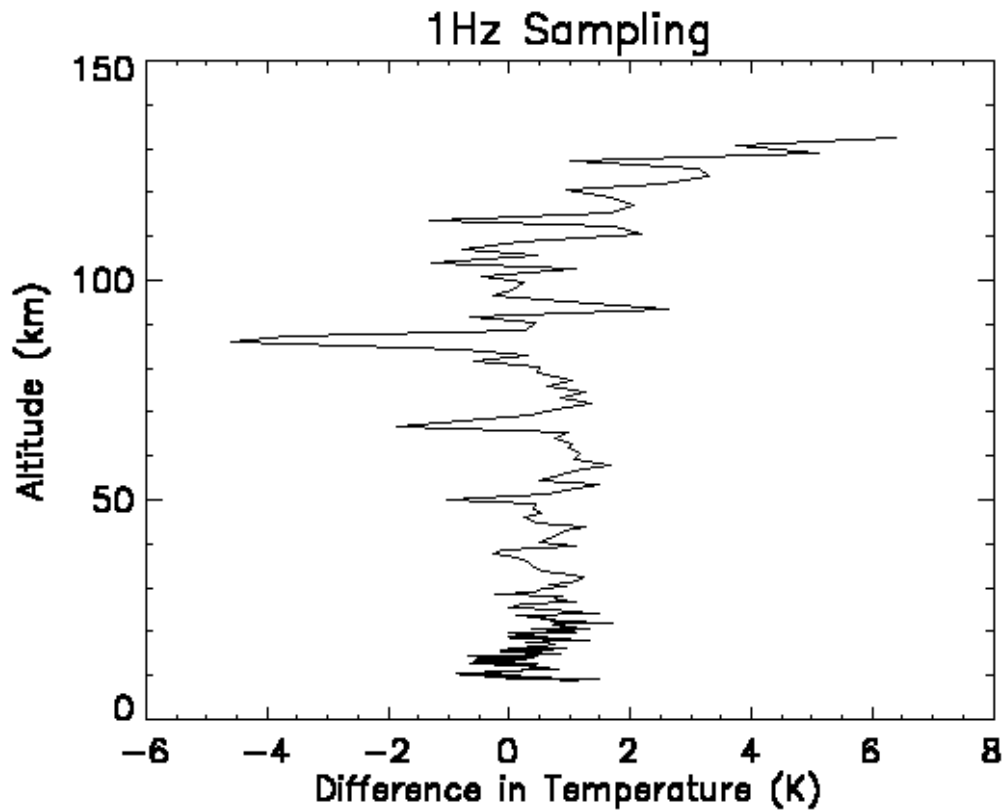
The Mars Pathfinder data is recorded at a frequency of 32 Hz. I do not know the sampling rate for the Beagle 2 data.

I increased my range to the highest 10 km for the calculation of the pressure constant of integration to allow for the smaller number of data points. See section 2.12.

Sampling the Mars Pathfinder data to 1 Hz and using it in the trajectory and atmospheric structure reconstructions, I obtain the following results.

The landed position is 19.05 degrees latitude and 326.42 degrees east longitude.
The PDS landed position is 19.09 degrees latitude and 326.48 degrees east longitude



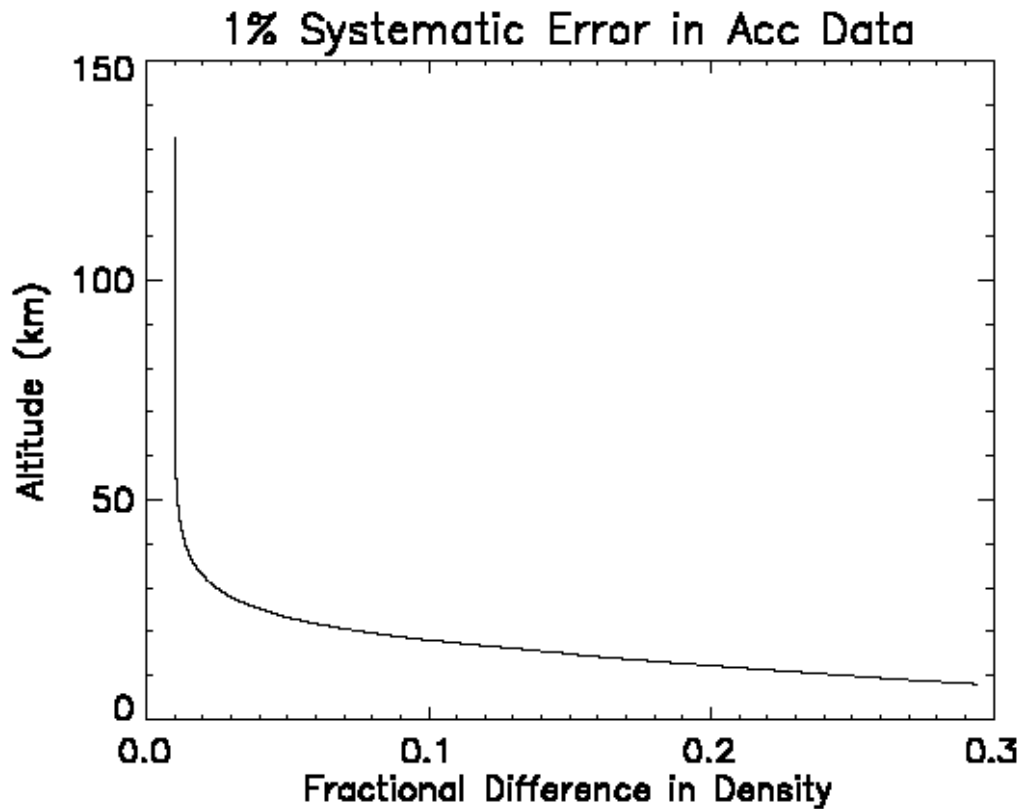


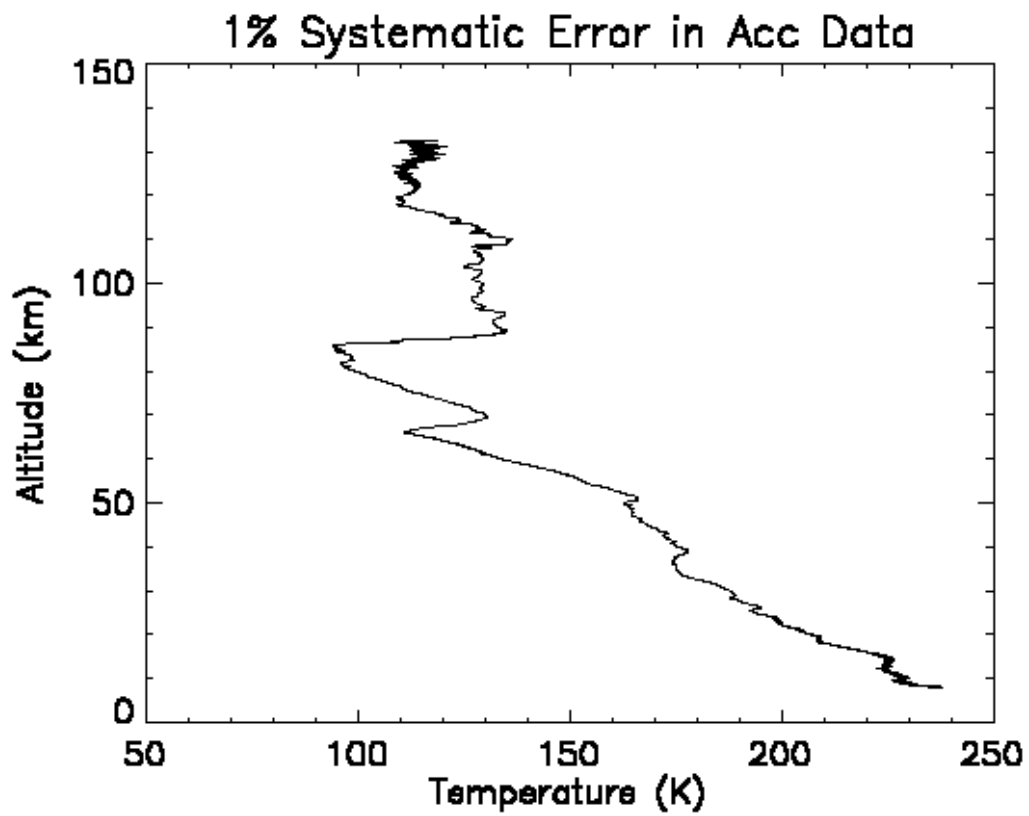
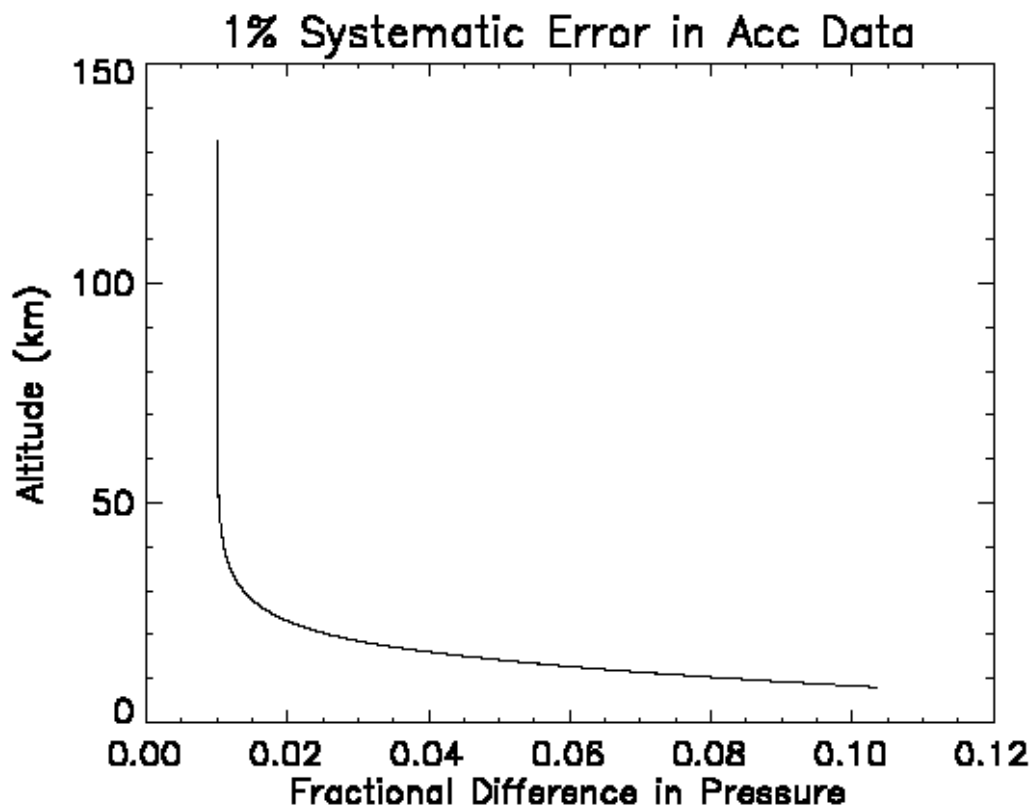
This temperature structure is compared to my nominal solution. The spike at 85 km is probably related to the gain state changes at that altitude, but I'm not certain. The error introduced by sampling at 1 Hz is less than 2 K below 100 km altitude, with one localised exception and below 7 K at all altitudes.

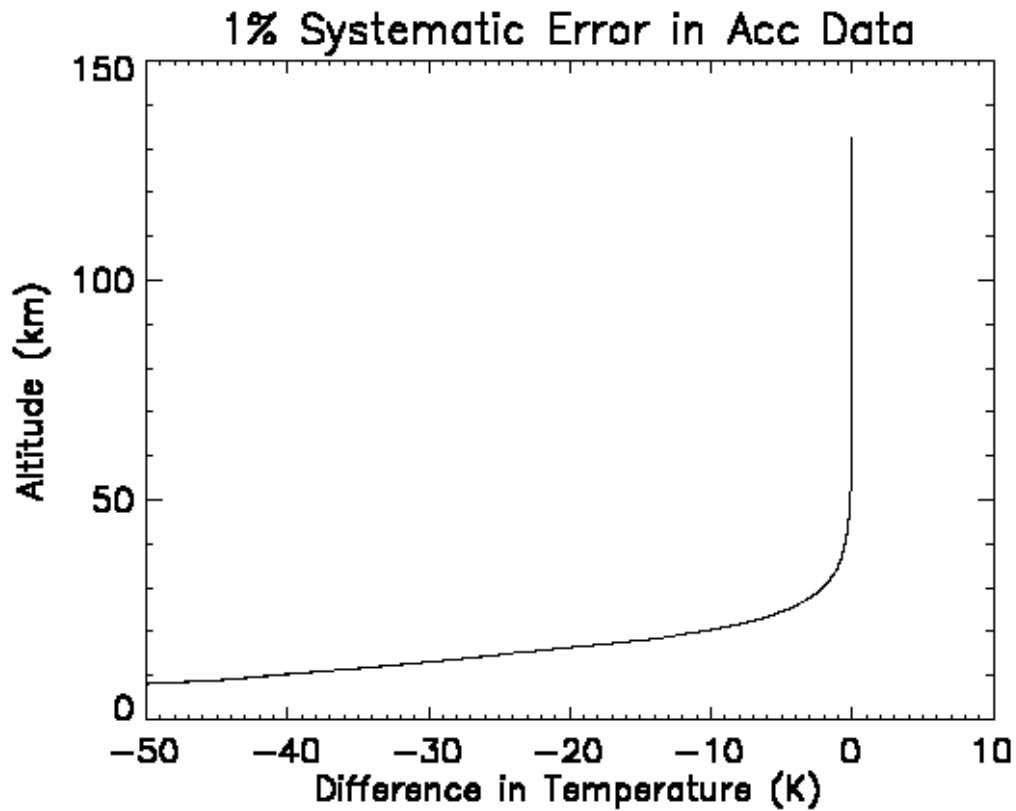
4.5 - Systematic offset in acceleration measurements

[E:/idl/effects_of_errors/extract_data.pro, E:/idl/effects_of_errors/corrupt_data.pro]

A systematic error in the acceleration measurements has serious consequences. I decreased all the Mars Pathfinder acceleration measurements by 1% and compared the results to my nominal reconstructions. Increasing the measurements systematically simply reverses the sign of the temperature offset.







My nominal reconstructed landed position is
 7.7 km below the surface
 19.00 degrees latitude
 326.28 degrees east longitude

The 1% systematic error can be seen in the high altitude density and pressure results. At lower altitudes, the accumulated errors in acceleration lead to an error in the velocity. Since density is inversely proportional to the square of velocity, this causes an error in density which increases rapidly as the spacecraft descends. Errors in pressure and temperature follow.

4.6 – Effect of the Atmosphere on the Trajectory

[E:/idl/effects_of_errors/entry_envelope.pro,
E:/idl/effects_of_errors/convert_entry_state.pro]

The effects of the atmosphere on landed position can be briefly summarized.

Reconstructed landed position using the code from section 4.1 is 18.2 degrees latitude and 327.3 degrees east longitude. [This is using the PDS entry state.]

Reconstructed landed position with atmospheric density set to zero is 16.9 degrees latitude and 323.6 degrees east longitude.

Reconstructed landed position with atmospheric density set to ten times greater than my nominal reconstructed Mars Pathfinder atmospheric structure is 19.2 degrees latitude and 330.2 degrees east longitude.

5 – Recommendations

The purpose of my work has been to prepare for the atmospheric entries of Beagle 2 on Mars and Huygens on Titan. Much of what I have actually done has been tested and demonstrated using Mars Pathfinder data and properties because that was what was available to me.

To enable full and rapid analysis of these datasets I recommend

- **Perform a formal error analysis of the reconstruction procedure**
- **Understand and prepare to apply the technique for constraining spacecraft attitude using acceleration ratios**
- **Understand the problem I am having with the PDS entry state**
- **Collaborate with an aerodynamicist to speed you along the learning curve**
- **Consider how additional constraints will affect the reconstruction**
- **Obtain aerodynamic information for those spacecraft**

The following information is required from the people building the spacecraft and designing its atmospheric entry:

Definition of the spacecraft frame

[diagram]

Location of the centre of mass of the spacecraft in this frame

[3 dimensional parameters and their uncertainties]

Location of test mass of each accelerometer in this frame

[3 dimensional parameters and their uncertainties]

Direction of the axis of each accelerometer in this frame

[3 dimensional parameters and their uncertainties]

Nominal mass of the spacecraft at and during entry and likely uncertainties in this parameter both at the time of entry AND after as much processing and head-scratching as needed has taken place.

[1 dimensional parameter and 2 uncertainties]

Chemical composition of the atmosphere as used to calculate aerodynamic properties.

An idealised composition with no uncertainties will probably be used for these calculations. Ask the compilers of this database how their database will change if they use various compositions within the permitted uncertainties. If your spaceflight improves knowledge of the planetary atmosphere, ask them again post-flight. Ask for a quantitative reply that you can use in formal uncertainty analyses.

Actual chemical composition of the atmosphere with uncertainties

This is needed to obtain the equation of state permitting the calculation of temperature from pressure and density.

Nominal entry state (UTC time and position and velocity in some well-defined frame) and likely uncertainties in these parameters at both the time of entry AND after as much processing and head-scratching as needed has taken place.

I assume that you know your accelerometers and what happens to information between the instruments and your computer on Earth.

An aerodynamic database consisting of the following black box:

Input:

Spacecraft mass

[1 dimensional parameter]

Atmospheric pressure

[1 dimensional parameter]

Atmospheric temperature

[1 dimensional parameter]

Relative velocity of the spacecraft to the atmosphere given in the spacecraft frame

[3 dimensional parameters]

Atmospheric composition

Only needed as a variable if it is likely to change during entry. This might affect Huygens. Viking told us that the martian atmosphere doesn't change much below 100 km.

Output:

Linear accelerations acting on the centre of mass of the spacecraft given in the spacecraft frame

[3 dimensional parameters and their uncertainties]

Angular accelerations acting about the centre of mass of the spacecraft given in the spacecraft frame.

[3 dimensional parameters and their uncertainties]

This request will confuse the people compiling the database. They will want to have dimensionless input parameters and dimensionless output parameters.

If the velocity of the spacecraft is replaced by a speed, an angle, and an assumption of axisymmetry, quantify how much error the assumption of axisymmetry introduces into the outputs. The actual spacecraft will not be ideally axisymmetric. Know how the angle is defined.

If atmospheric pressure and atmospheric temperature are replaced by two of Ma , Kn , and Re [or any other favourite of the aerodynamicist], you must know how to convert atmospheric pressure and atmospheric temperature into these quantities and vice versa.

Kn is the ratio of the molecular mean free path in the atmosphere to an arbitrary reference length. The molecular mean free path can be calculated, in principle, from the equation of state of the relevant chemical composition given atmospheric pressure and temperature. The arbitrary reference length must be known.

Ma is the ratio of speed of sound in the atmosphere to the spacecraft velocity relative to the atmosphere. The speed of sound can be calculated, in principle, from the equation of state of the relevant chemical composition given atmospheric pressure and temperature.

Re is the ratio of inertial forces to viscous forces. More usefully, it equals (fluid speed times fluid density times another arbitrary reference length) divided by the dynamic viscosity of the fluid. The dynamic viscosity may be referred to simply as the viscosity. It is not the kinematic viscosity. It can be calculated, in principle, from the equation of state of the relevant chemical composition given atmospheric pressure and temperature. The arbitrary reference length must be known.

Linear accelerations equal force times mass.

If the vector forces are replaced by force coefficients, then you must know how to convert forces into coefficients and vice versa. Signs are important here. Probably a coefficient, an arbitrary reference area, atmospheric density, relative speed, and two angles necessary to define the flow direction will combine to give a force. Know how to convert forces in unusual directions (such as along the flow direction) into forces along the spacecraft axes. The arbitrary reference area must be known. Signs of forces, coefficients, and relative velocity must be clearly understood.

I would expect to see a diagram, a definition and an equation for each force coefficient. I emphasise again that signs and direction conventions must be clearly understood.

Angular accelerations are related to torques by the moment of inertia matrix, which contains six independent parameters. Torques will probably be similar to forces in that they may be replaced by a moment coefficient. I don't know likely equations, but an arbitrary reference length (which may or not be the same as any other arbitrary reference length you are dealing with) may crop up. I would expect to see a diagram, a definition and an equation for each moment coefficient. I emphasise again that signs and direction conventions must be clearly understood.

6 - Bibliography and Resources

[E:/idl/biblio/biblio.txt, E:/idl/biblio/read_biblio.pro]

I have compiled a list of relevant references and useful resources, biblio.txt. read_biblio.pro provides a simple interfacing and searching capability. I shall summarise its contents with a view to pointing the reader at the good stuff. Important references are highlighted here with *.

Examine the bibliography file for the unphotocopied references to see if there's anything you like. Skim the references of any paper you read for anything that looks promising.

The Open University library is not a good resource for this field.

Cranfield University library is a good resource, as you might expect given their obvious interest in aerodynamics. Their website <http://www.cran.ac.uk/> allows you to search their catalogues remotely. When I visited them, they happily sold me a photocopy card and let me rummage around. They have a good collection of NASA technical reports and aerodynamics journals.

The British Library has an extensive collection of NASA technical reports, but I did not find their online catalogue, <http://blpc.bl.uk/>, to be very helpful. You'll have to visit and see what they've got on the shelves to know if it's better than Cranfield. As copyright libraries and universities with substantial engineering departments, Oxford and Cambridge University libraries are a potential resource if the British Library is inconvenient.

<http://techreports.larc.nasa.gov/>, a website at NASA-Langley, is a searchable archive of many NASA and NACA technical reports, internal publications, and peer-reviewed publications authored by NASA staff. Try searching in as many different ways as possible (author, title words, report number) before giving up on a reference. Many technical reports are available online as PDFs. The first link you find to a report might offer to sell you a hard copy. A later link might give you a free PDF. This service was having trouble with technical reports from NASA-Ames when I was using it. This is unfortunate, because Ames is one of the most important centres in this field.

<http://www.webofscience.com/>, now hideously renamed <http://wos.mimas.ac.uk/>, is a useful resource for peer-reviewed publications.

<http://adsabs.harvard.edu/> is less comprehensive in its coverage of aerodynamics than Web of Science, but it is useful for the scientific results. It lists conference abstracts, which Web of Science does not.

Try various databases of this kind. They all have full-text access and abstract-only access for a different set of sources. For example, Web of Science gives you JGR abstracts, ADSABS does not.

Cultivate an American connection. Someone at a NASA centre or a major US university might be able to get a reference from their library in a few minutes while you are wrestling with a delayed inter-library loan request.

Cultivate a friend at Cranfield University. If you can't use a paper purely because the authors have not defined a "pitching moment coefficient", an aerodynamicist will be able to help you out. I found lots of papers with numerical values for such things but no equation instructing the reader how to use it. This is because aerodynamicists know such things from childhood and assume that the reader does too.

Ralph Lorenz has some code for doing trajectory reconstructions. I had a look at it to help me understand what was going on. I wrote my own, rather than adapting his, so that I understood the process fully. I think he acquired it during his time at ESA? I have a copy. I haven't left one here since it's not my code. I'm sure he'll give you one if asked. You might find it helpful to see another version of the same technique if my code is confusing.

6.1 - Early Work and Overview

Chapman (1958) – Develops some basic equations and applies them analytically to an isothermal atmosphere.

Lees et al (1959) – Develops some basic equations and applies them numerically to some special cases.

* Seiff (1963) – The founding paper of this field. Not useful for developing equations. Very useful for understanding the basic approach, especially angle-of-attack oscillations and when to use direct pressure and temperature sensors. Immediately notices the horrendous problems caused by a systematic error in the accelerometer data.

Tobak and Peterson (1964) – I only have the cover page. It might be useful.

Beuf (1964) – Thoughts on an early entry vehicle that can characterise an atmosphere for future missions. Historical note – the martian surface pressure was unknown by a factor of about 100. How do you design a lander with such uncertainty? This precursor idea was the solution.

Seiff and Reese (1965b) – Same aims as Beuf (1964). At this stage, thinking is centred on a spherical spacecraft to reduce angle-of-attack problems. Later discovery of boundary layer separation (?) issues and instabilities brought the hybrid sphere-cone to its present dominance.

Seiff and Reese (1965a) – Shape optimisation. Probe attitude. Equations for error analysis on trajectory and atmospheric structure reconstruction.

* Peterson (1965a,b) – Key papers. Develops equations with clearly defined quantities and diagrams. Error analysis.

Sommer et al (1967b) – Results of a high-altitude balloon drop test. Spherical shape changes to a blunted cone without any explanation... First atmospheric structure reconstruction from measured accelerations? Some complicated analytical equations. I didn't photocopy the many figures.

Sommer and Boissevain (1967a) – pop sci version of the above. A good introduction to the above.

Seiff (1968) – Something of a summary of previous work and a look ahead to future work.

Sommer and Yee (1968) – Uncopied

Sommer and Yee (1969)– Piggybacking accelerometers onto a Viking parachute test. Revealed some instrument problems. Useful equations.

* Seiff et al (1973) – PAET results. Last time anyone every mentions shock layer radiometry as a measurement technique. Lots of details on instruments for the first time.

* Seiff (1990, 1991) – Reviews the development and implementation of this technique. Helpful for putting the early papers into context and summarises the results of Viking and Pioneer Venus.

* Young and Magalhaes (2001) – 16 December 2000. Al Seiff's obituary.

6.2 - Viking

Nier et al (1975) – How this technique will work in the thin martian atmosphere

* Seiff (1976) – Comprehensive discussion of Viking instrument and expected accuracies

* Nier et al (1976) – First results from another planet, Mars, with Viking 1

Seiff and Kirk (1976) – Viking 2

Euler, Adams, and Hopper (1977) – Not as useful as I expected

Inogoldby et al (1976) – Might be the big paper that explains how all the different data were combined to constrain atmospheric structure. Might have detailed equations. Uncopied

Hopper (1975) – Might be the big paper that explains how all the different data were combined to constrain atmospheric structure. Might have detailed equations. Uncopied

* Seiff and Kirk (1977)– Detailed analysis of VL1 and VL2 EDL measurements. Useful equations.

Seiff (1982) – Defines the standard martian atmosphere from Viking data.

Seiff (1993) – Viking radar altimetry of topography!

6.3 - Pioneer Venus

Seiff (1977) – Brief instrument descriptions

* Seiff et al (1979) – First results from Pioneer Venus

* Seiff et al (1980a) – Detailed instrument descriptions

Seiff et al (1980b) – Detailed analysis of results

Seiff and Kirk (1982) – Yet more analysis, primarily comparing to Venera results

Seiff et al (1985) – Defines the standard Venus atmosphere

Seiff and Kirk (1991) – Wiggles in the data and some error analysis

6.4 - Galileo

Seiff (1971) – Early thoughts on the special conditions at Jupiter

* Seiff and Knight (1992) – Detailed instrument description

* Seiff et al (1996) – First results from Jupiter

Atkinson et al (1996) – Winds from probe Doppler

Seiff et al (1997c) – Winds from accelerometer measurements

Seiff et al (1997a) – Better results from Jupiter

* Seiff et al (1998) – Detailed data analysis paper

6.5 - Mars Pathfinder

* Braun et al (1995) – Plots of force coefficients. Discusses aerodynamic properties.

Schofield et al (1997) – First results from MPF

* Seiff et al (1997b) – Detailed instrument description

Gnoffo et al (1998) – Surprisingly useless

* Spencer et al (1998a,b) – Engineer's trajectory and atmospheric structure reconstruction. Discusses major events during entry, observed accelerations, and reconstruction procedure in detail

* Magalhaes et al (1999) – Detailed data analysis paper. More detailed than usual.

6.6 - Others

Only the useful ones that I have are listed

Blanchard et al (1989) – Shuttle accelerometer data.

Journal of Spacecraft and Rockets (1999) – Special issue on Planetary Entry Systems

Smith et al (1993) – Defines the gravity field of Mars

Goldstein (1980) – Essential for understanding the Euler angles

Bradbury (1968) – Handy for coordinate transformations

Some potentially useful references that I do not have copied and have not mentioned yet are Cohen and Eggers (1965, 1973) and Brayshaw (1963).

I have no references for the Soviet Venus or Mars spacecraft. Their Venus spacecraft are definitely important, I don't know about their Mars ones.

6.7 – Correspondence

[E:/useful_correspondence/]

I emailed a variety of people with questions during this work. I'll summarise some conversations that you might benefit from knowing about. The useful_correspondence directory contains the text of emails from Engelund, Rivellini, and Schofield.

Julio Magalhaes – [Before coming to the OU] – Hello, can I have some advice?
No reply.

Tom Rivellini – Will Beagle 2 be spinning much after it lands? How much?
Yes, of course. No quantitative reply.

Tim Schofield – Can I have your trajectory and atmospheric structure code and the MPF aerodynamic database?
Ask Julio Magalhaes, ask Bobby Braun. Good luck. Calibrate thy instruments!

Julio Magalhaes – [cc'd by Tim Schofield on his email to me]
No reply.

Bobby Braun/Walt Engelund – Can I have the MPF aerodynamic database?
Sort of. Sent info necessary to reproduce figure 3 in Braun et al (1995). This is a subset of the full database and I wasn't able to use it usefully.

7 - Detailed Look at Archived Computer Programs

Top-level directory is currently “PGW65 on Ting” which is mapped as the E:/ drive. I assume that this directory will get moved around. Some programs use relative links, others use hard links to “E:/”. Search for this string in files before trying to use these programs without mapping the top-level directory to “E:/”.

A word of caution. Using IDL, I found that parameters passed to a slave procedure sometimes changed in the master procedure for no obvious reason.

Many of the plots which show differences between two datasets at a given altitude actually evaluate the difference at a given time, then plot the difference as a function of altitude in one dataset. Look at E:/idl/mpf_nominal/plot_results.pro for an example of this.

7.1 - E:/

Subdirectories:

biblio/, final_report/, idl/, imperial_talk/, misc/, mpam_0001/, non_openuni_stuff/, useful_correspondence/

biblio/ contains my bibliography file and an IDL procedure to read and search it, read_biblio.pro. The code is commented and there is a readme file.

final_report/ contains this file and all (?) of its images.

idl/ will be discussed later.

imperial_talk/ contains some images that I used to put together a presentation at Imperial College.

mpam_0001/ is the PDS Mars Pathfinder Atmospheric Structure Instrument / Meteorology Package available from <http://pds.jpl.nasa.gov/>. It is fully documented. I have deleted directories surf_edr and surf_rdr to decrease its size. These directories contained data from the landed meteorology part of the Mars Pathfinder mission.

misc/ is a dumping ground. It contains 98-1027.pdf, marspathfinderdescent.pdf, seiff_memorial.pdf, montalkintro.doc, meeting1.txt, meeting2.txt, meeting3.txt, inputs.txt, soln_proc.txt

98-1027.pdf, marspathfinderdescent.pdf, and seiff_memorial.pdf are PDF reprints of some of the references.

montalkintro.doc was used as part of a Monday morning presentation given to PSSRI on the age of lunar crater Giordano Bruno.

meeting1.txt (and 2 and 3) are summaries of meetings with John Zarnecki, Martin Towner, and Brijen Hathi during my stay at The Open University.

inputs.txt, and soln_proc.txt are rough notes made about how the reconstruction procedure works.

non_openuni_stuff/ is where I have kept up with necessary work that is not directly related to my time at The Open University. I may clear it out before I leave. Please ask me before deleting it. Its main contents are a funding proposal and a review of a paper.

useful_correspondence/ contains the text of emails from Engelund, Rivellini, and Schofield.

7.2 – E:/idl/

This is the main directory of interest.

It contains the following subdirectories:

old/, mpf_nominal/, effects_of_errors/, gyroscopes/, working/

old/ contains spare bits of code.

working/ contains rough versions of the programs in mpf_nominal/, effects_of_errors/, and gyroscopes/. You might find something useful in it. It contains three major files that have different names in their polished versions. extract_mpf_acc.pro is also called extract_data.pro, verify_mpf.pro is also called recon_traj.pro, and mpf_structure.pro is also called recon_atm.pro.

recon_traj.pro should be preceded by extract_data.pro each and every time it is run otherwise n.dat may be incorrect.

7.3 – E:/idl/mpf_nominal/

This contains all the pieces of code necessary to reconstruct the Mars Pathfinder trajectory and atmospheric structure as detailed below.

Run `extract_data.pro` to prepare the PDS data for trajectory reconstruction.

Run `recon_traj.pro` to reconstruct the trajectory and the information necessary for the atmospheric structure reconstruction

Run `recon_atm.pro` to reconstruct the atmospheric structure

The nearby figure shows this process as a flowchart. The primary input and output files are outlined twice. The primary procedures are outlined once.

`majorprogram.pro` -----C `minorprogram.pro` indicates that the minor program is called by the major program.

`program.pro` -----R `datafile.dat` indicates that `program.pro` reads `datafile.dat`

`program.pro` -----W `datafile.dat` indicates that `program.pro` writes `datafile.dat`

`dt.dat` is written twice (W2) by `extract_data.pro`. This feature is useful in section 7.4 when `dt` may change as a result of resampling the data.

The main reason for the convoluted diagram is that `get_n.pro` and `get_dt.pro` are called by both `recon_traj.pro` and `recon_atm.pro`.

Run `plot_results.pro` to display the results and compare against PDS reconstruction

Check that `plot_results.pro` outputs ‘`test_model_atm.dat`’

Run `model_atm.pro` to test consistency of trajectory and atmospheric structure reconstruction.

extract_data.pro	
Called by:	N/A
Calls:	N/A
Declares common blocks:	N/A
Reads from:	e:/mpam_0001/edl_erdr/r_sacc_s.tab
Writes to:	dt.dat, acc.dat, n.dat, dt.dat [again], deltat.dat, endstate.dat
Options:	endstate = 'touchdown' or 'mortar'
Purpose:	Prepare PDS data for trajectory reconstruction
recon_traj.pro	
Called by:	N/A
Calls:	get_n, get_dt, get_omega, setup_arrays, get_entry_state, set_initial, get_altlatlon, get_acc, derivs
Declares common blocks:	data_block, time, declare_arrays
Reads from:	acc.dat
Writes to:	aeroacc_res.dat, vrel_res.dat, aeroacc_res.dat, height_res.dat, t_res.dat, lat_res.dat, lon_res.dat, n.dat
Options:	initial_conditions = 'jsr' or 'pds'
Purpose:	Reconstruct trajectory and information necessary to reconstruct atmospheric structure
get_n.pro	
Called by:	recon_traj.pro, recon_atm.pro
Calls:	N/A
Declares common blocks:	N/A
Reads from:	n.dat
Writes to:	N/A
Options:	N/A
Purpose:	Return number to be used as array size
get_dt.pro	
Called by:	recon_traj.pro, recon_atm.pro, model_atm.pro
Calls:	N/A
Declares common blocks:	N/A
Reads from:	dt.dat
Writes to:	N/A
Options:	N/A
Purpose:	Return timestep in seconds
get_omega.pro	
Called by:	recon_traj.pro, model_atm.pro
Calls:	N/A
Declares common blocks:	N/A
Reads from:	N/A
Writes to:	N/A

Options:	N/A
Purpose:	Return planetary rotation rate in rad s^{-1}
setup_arrays.pro	
Called by:	recon_traj.pro, model_atm.pro
Calls:	N/A
Uses common blocks:	declare_array
Reads from:	N/A
Writes to:	N/A
Options:	N/A
Purpose:	Create many empty arrays to store results of trajectory reconstruction
get_entry_state.pro	
Called by:	recon_traj.pro, model_atm.pro
Calls:	get_omega
Declares common blocks:	N/A
Reads from:	N/A
Writes to:	N/A
Options:	N/A
Purpose:	Convert initial conditions into inertial cartesian frame
set_initial.pro	
Called by:	recon_traj.pro, model_atm.pro
Calls:	get_altlatlon
Uses common blocks:	declare_array
Reads from:	N/A
Writes to:	N/A
Options:	N/A
Purpose:	Put the initial conditions into the first element of the appropriate arrays
get_altlatlon	
Called by:	set_initial.pro, recon_traj.pro, derivs.pro, model_atm.pro
Calls:	N/A
Declares common blocks:	N/A
Reads from:	N/A
Writes to:	N/A
Options:	rmars. Altitude is referenced to this radius of Mars.
Purpose:	Transform positions from inertial cartesian frame to momentary spherical frame
get_acc.pro	
Called by:	recon_traj.pro, derivs.pro
Calls:	get_grav
Declares common blocks:	N/A
Reads from:	N/A
Writes to:	N/A
Options:	trustxy = 0 or 1

Purpose: Calculate accelerations in spacecraft frame using many pieces of information. Assumes option 1 for dealing with spacecraft attitude.

get_grav.pro

Called by: get_acc.pro, get_acc_model.pro

Calls: N/A

Declares common blocks: N/A

Reads from: N/A

Writes to: N/A

Options: model = 'gmm1' or 'mors_1006'
alt_ref = 'mpf_lander' or 'other'

Purpose: Return acceleration due to gravity in inertial cartesian frame given position in momentary spherical frame and time

update_arrays.pro

Called by: recon_traj.pro, model_atm.pro

Calls: N/A

Uses common blocks: declare_arrays

Reads from: N/A

Writes to: N/A

Options: N/A

Purpose: Increment various arrays after one timestep of integration

derivs.pro

Called by: recon_traj.pro

Calls: get_altlatlon, get_acc

Uses common blocks: data_block, time

Reads from: N/A

Writes to: N/A

Options: N/A

Purpose: Return velocity and acceleration in inertial cartesian frame between data points as needed for RK4 integration.

recon_atm.pro

Called by: N/A

Calls: get_n, get_endstate, get_dt, get_deltat, get_a, get_m

Declares common blocks: N/A

Reads from: aeroacc_res.dat, vrel_res.dat, height_res.dat, mpfcd.dat,

rho_res.dat, press_res.dat, temp_res.dat, out.gif

Options: pressure_condition = 'dsh' or 'none'
range_0 needed if 'dsh' used
gm, rmars, mean_molecular_mass,
universal_gas_constant

Purpose: Reconstruct atmospheric structure

get_endstate.pro

Called by: recon_atm.pro

Calls:	N/A
Declares common blocks:	N/A
Reads from:	endstate.dat
Writes to:	N/A
Options:	N/A
Purpose:	Track if data stops at touchdown or mortar firing
get_deltat.pro	
Called by:	recon_atm.pro
Calls:	N/A
Declares common blocks:	N/A
Reads from:	deltat.dat
Writes to:	N/A
Options:	N/A
Purpose:	Returns time interval between mortar firing and touchdown
get_a.pro	
Called by:	recon_atm.pro , model_atm.pro
Calls:	N/A
Declares common blocks:	N/A
Reads from:	N/A
Writes to:	N/A
Options:	N/A
Purpose:	Returns reference area of spacecraft
get_m.pro	
Called by:	recon_atm.pro , model_atm.pro
Calls:	N/A
Declares common blocks:	N/A
Reads from:	N/A
Writes to:	N/A
Options:	N/A
Purpose:	Returns mass of spacecraft
plot_results.pro	
Called by:	N/A
Calls:	get_n, get_endstate, get_dt, get_deltat
Declares common blocks:	N/A
Reads from:	e:/mpam_0001/edl_dds/edl_dds.tab, t_res.dat, height_res.dat, lat_res.dat, lon_res.dat, rho_res.dat, press_res.dat, temp_res.dat
Writes to:	test_model_atm.dat
Options:	N/A
Purpose:	Allow comparison between my reconstruction and the PDS reconstruction
model_atm.pro	
Called by:	N/A
Calls:	setup_arrays, get_entry_state, get_omega,

set_initial, get_altlatlon, get_acc_model, get_a, get_m,
 update_arrays
 Declares common blocks: declare_arrays
 Reads from: test_model_atm.dat, mpfcd.dat
 Writes to: model_t.dat, model_height.dat, model_lat.dat,
 model_lon.dat, model_n.dat
 Options: initial_conditions = 'jsr' or 'pds'
 dt, size_of_model_atm_arrays
 Purpose: Given a model atmosphere, an entry state and
 aerodynamic properties, integrate to find the trajectory

get_acc_model.pro

Called by: model_atm.pro
 Calls: get_grav
 Declares common blocks: N/A
 Reads from: N/A
 Writes to: N/A
 Options: N/A
 Purpose: Calculate accelerations in spacecraft frame using many
 pieces of information. Assumes option 1 for dealing
 with spacecraft attitude.

plot_model_results.pro

Called by: N/A
 Calls: get_n, get_endstate, get_dt, get_deltat
 Declares common blocks: N/A
 Reads from: t_res.dat, height_res.dat, lat_res.dat,
 lon_res.dat, model_t.dat, model_height.dat,
 model_lat.dat, model_lon.dat
 Writes to: N/A
 Options: N/A
 Purpose: Allow comparison between my reconstruction and my
 model reconstruction

To estimate the Mars Pathfinder drag coefficient I scanned in Figure 3 of Magalhaes
 et al 1999. I then used Ralph Lorenz's Datathief procedure
 [<http://www.lpl.arizona.edu/~rlorenz/datathief.pro>] to create thief.dat. steal_mpfcd.pro
 used thief.dat to estimate the drag coefficient at every kilometre between 0 and 200
 km. It stored this result in mpfcd.dat. mpfcd.dat is used by recon_atm.pro in the
 reconstruction of the atmospheric structure

7.4 – E:/idl/effects_of_errors/

This contains all .pro and .dat files from E:/idl/mpf_nominal/ with some additions and modifications. Note that I haven't updated the comments at the start of each file about what calls what for any files reproduced from E:/idl/mpf_nominal/.

Run entry_envelope.pro to look at the effects of uncertainties in entry state on landed position. This can also be used to examine the effects of the atmosphere on the trajectory.

Run recon_atm with a modified drag coefficient to look at the effects of uncertainties in drag coefficient on reconstructed atmospheric structure. Will need to precede with extract_data and recon_traj

Run extract_data, recon_traj, and recon_atm to look at the effects of digitisation, sampling frequency, and systematic errors on reconstructed trajectory and atmospheric structure. Will need to set desired corruptions to data in corrupt_data.

The modified files are:

recon_atm.pro has a couple of extra lines added to manipulate the drag coefficient and send the output to useful files

extract_data.pro has a couple of lines added to call corrupt_data

The additional files not found in E:/idl/mpf_nominal/ are:

entry_envelope.pro

Called by: N/A
Calls: get_omega, get_a, get_m, setup_arrays, convert_entry_state, set_initial, get_acc_model, update_arrays, get_atlatlon
Declares common blocks: declare_arrays
Reads from: test_model_atm.dat, mpfcd.dat
Writes to: N/A
Options: n, dt, size_of_model_atm_arrays, dist_width
7 values each of num_x, entry_x, sigma_x
Purpose: Modified from model_atm.pro to use a variety of entry states

convert_entry_state.pro

Called by: N/A
Calls: get_omega
Declares common blocks: N/A
Reads from: N/A
Writes to: N/A
Options: rot_factor
Purpose: Return entry state in inertial cartesian frame

plot_cd_results.pro

Called by: N/A

Calls: get_n, get_endstate, get_dt, get_deltat
 Declares common blocks: N/A
 Reads from: t_res.dat,height_res.dat, lat_res.dat, lon_res.dat,
 rho_res.dat, press_res.dat, temp_res.dat,
 press_cd.dat, rho_cd.dat, temp_cd.dat
 Writes to: N/A
 Options: dir
 Purpose: Allow comparison between my nominal reconstruction
 and a reconstruction with a different drag coefficient

corrupt_data.pro

Called by: extract_data.pro
 Calls: get_dt
 Declares common blocks: N/A
 Reads from: N/A
 Writes to: N/A
 Options: sampling = 'y' or 'n', systematic = 'y' or 'n',
 digitisation = 'y' or 'n'
 sampling_rate needed if sampling eq 'y'
 fudge_factor needed if systematic eq 'y'
 digcode needed if digitisation eq 'y'
 dig needed if digcode eq 'normal'
 Purpose: Modify the data to mimic various instrumental effects

7.5 – E:/idl/gyroscopes/

This contains programs that, in theory, can integrate option 3 for dealing with spacecraft attitude – knowledge of linear and angular accelerations.

Run `recon_gyro.pro` to reconstruct the trajectory and atmospheric density. You can reconstruct atmospheric density and temperature yourself if you're ever lucky enough to have such data.

Specify `n`, the number of datapoints, and `dt`, the timestep. Linear and angular accelerations are assumed to be stored in `acc.dat` and `wdot.dat` respectively. The procedure is similar to `recon_traj` and calls `get_acc_genl` in each timestep to transform accelerations into the inertial cartesian frame and calculate density.

There are lots of frame transformations in `get_acc_genl` involving the Euler matrix. `get_acc_genl.pro` calls `get_cd` to find out what the drag coefficient is. `get_cd.pro` currently returns a nominal drag-only value and should be adapted to use a large aerodynamic database if you have one. I have defined what the drag coefficient is exactly using an equation. Check that your definition of a drag coefficient agrees with mine.

`get_acc_genl.pro` then uses the aerodynamic information for the spacecraft `x`, `y`, and `z` axis force coefficients to estimate a density value for each of the three axes. Formally, these should be identical. Since the `z`-axis acceleration is likely to be known better than the others, I have only stored this density. Another option is to take the mean of the three densities, possibly weighted by their uncertainties.

Control returns to `recon_gyro.pro`, which moves everything forward by one timestep and goes round again. The way in which attitude is incremented is non-trivial.

Apart from these the files, the other pieces of code are trivial or familiar. Hence I haven't listed their properties here.

I haven't tested this fully, since I don't have a suitable dataset. User beware.

8 - References and Bibliography

Atkinson DH, Pollack JB, Seiff A (1996)

Galileo Doppler measurements of the deep zonal winds at Jupiter
SCIENCE 272 (5263): 842-843 MAY 10 1996

Beuf FG (1964)

A simple entry system experiment for martian atmospheric measurements
Document ID: 19640021177 N (64N31091) File Series: NASA Technical Reports,
AIAA paper 64-292, pp1 -14

Blanchard RC, Hinson EW, Nicholson JY (1989)

SHUTTLE HIGH-RESOLUTION ACCELEROMETER PACKAGE EXPERIMENT
RESULTS - ATMOSPHERIC DENSITY-MEASUREMENTS BETWEEN 60 AND
160 KM
JOURNAL OF SPACECRAFT AND ROCKETS 26 (3): 173-180 MAY-JUN 1989

Bradbury TC (1968)

Theoretical Mechanics
book - New York, Wiley [1968] xiii, 641 p. illus. 23 cm.

Braun RD, Powell RW, Engelund TC, Gnoffo PA, Weilmuenster KJ, Mitcheltree RA
(1995)

Mars pathfinder six-degree-of-freedom entry analysis
JOURNAL OF SPACECRAFT AND ROCKETS 32 (6): 993-1000 NOV-DEC 1995

Braun RD, Mitcheltree RA, Cheatwood FM (1997a)

Mars Microprobe Entry Analysis
1997 IEEE Aerospace Conference, Snowmass, CO, February 2-6, 1997, pp. 15

Braun RD, Spencer DA, Kallemeyn PH, Vaughan RM (1997b)

Mars Pathfinder Atmospheric Entry Navigation Operations
1997 AIAA Guidance, Navigation and Control Conference, New Orleans, Louisiana,
AIAA 97-3663, August 11-13, 1997

Braun RD, Mitcheltree RA, Cheatwood FM (1999a)

Mars Microprobe entry-to-impact analysis
JOURNAL OF SPACECRAFT AND ROCKETS 36 (3): 412-420 MAY-JUN 1999

Braun RD, Spencer DA, Kallemeyn PH, Vaughan RM (1999b)

Mars Pathfinder atmospheric entry navigation operations
JOURNAL OF SPACECRAFT AND ROCKETS 36 (3): 348-356 MAY-JUN 1999

Brayshaw JM (1963)

Mars atmosphere entry parametric study
NASA-CR-53020 JPL-TR-32-458

Cassidy DE (1967)

Unmanned entry into the Venusian atmosphere
NASA-CR-88181 TM-1013-6

Chapman DR (1958)
An approximate analytical method for studying entry into planetary atmospheres
NACA TN-4276 May 1958 <http://naca.larc.nasa.gov/reports/1958/naca-tn-4276/naca-tn-4276.pdf>

Cohen NB, Eggers AJ (1965)
Progress and problems in atmosphere entry
NASA-TM-X-56855 72p, also INTERNATIONAL ASTRONAUTICAL
FEDERATION, INTERNATIONAL ASTRONAUTICAL CONGRESS, 16TH,
ATHENS, GREECE, SEP. 13-18, 1965

Cohen NB, Eggers AJ (1973)
Progress and problems in atmosphere entry
AIAA Atmosphere Entry, Vol. 1 p110-128

Euler EA, Adams GL, Hopper FW (1977)
The design and reconstruction of the Viking Lander descent trajectories
American Astronautical Society and American Institute of Aeronautics and
Astronautics, Astrodynamics Specialist Conference, Jackson Hole, Wyo., Sept. 7-9,
1977, Paper. 45 p.

Fertig JK (1995)
Orbital Acrobatics around the nucleus of a comet
ESA Orbit Attitude Division, ESOC, Darmstadt, OAD Working Paper

Gnoffo PA, Braun RD, Weilmuenster KJ, Mitcheltree RA, Engelund WC, Powell RW
(1998)
Prediction and Validation of Mars Pathfinder Hypersonic Aerodynamic Data Base
7th AIAA/ASME Joint Thermodynamics and Heat Transfer Conference,
Albuquerque, New Mexico, AIAA 98-2445, June 15-18, 1998

Gnoffo PA, Braun RD, Weilmuenster KJ, Mitcheltree RA, Engelund WC, Powell RW
(1999)
Prediction and validation of Mars Pathfinder hypersonic aerodynamic database
JOURNAL OF SPACECRAFT AND ROCKETS 36 (3): 367-373 MAY-JUN 1999

Goldstein H (1980)
Classical Mechanics
book - Reading, Mass.. London. Addison-Wesley. c1980

Guglieri G, Quagliotti F (2000)
Low speed dynamic tests on a capsule configuration
AEROSPACE SCIENCE AND TECHNOLOGY 4 (6): 383-390 SEP 2000

Hankey WL (1988)
Re-entry Aerodynamics
book - Washington D.C.. American Institute of Aeronautics and Astronautics. 1988

Hopper FW (1975)

Trajectory, atmosphere, and wind reconstruction from Viking entry measurements
American Astronautical Society and American Institute of Aeronautics and
Astronautics, Astrodynamics Specialist Conference, Nassau, Bahamas, July 28-30,
1975, AAS 40 p. AAS PAPER 75-068

Inogoldby RN, Michel FC, Flaherty TM, Doty MG, Preston B, Villyard KW, Steele
RD (1976)
Entry data analysis for Viking landers 1 and 2
NASA-CR-159388 TN-3770218

Journal of Spacecraft and Rockets (1999)
Special Section: Planetary Entry Systems
Journal of Spacecraft and Rockets, v36, n3, p297 - 486

Kerzhanovich VV (1977)
Mars 6 - Improved analysis of the descent module measurements
Icarus, vol. 30, Jan. 1977, p. 1-25.

Lees L, Hartwig FW, Cohen CB (1959)
The use of aerodynamic lift during entry into the Earth's atmosphere
American Rocket Society Journal, September 1959, p633 - 641

Lodders K, Fegley B (1998)
The Planetary Scientist's Companion
Book - OUP

Loh WHT (1968)
Re-entry and planetary entry
Applied physics and engineering. an international series. vol. 2 , 3 Berlin. Springer.
1968 2 vol.. 24cm

Lorenz R (1994)
Descent and Impact Dynamics of the Huygens Probe
International Astronautical Federation conference in Jerusalem, October 1994, IAF-
94-A.1.004

Magalhaes JA, Schofield JT, Seiff A (1999)
Results of the Mars Pathfinder atmospheric structure investigation
Journal of Geophysical Research, Volume 104, Issue E4, April 25, 1999, pp.8943-
8956

Makinen T (1996)
Processing the HASI measurements
Advances in Space Research, Volume 17, Issue 11, p. 219-222.

Mitcheltree RA, Moss JN, Cheatwood FM, Greene FA, Braun RD (1997)
Aerodynamics of the Mars Microprobe Entry Vehicles
1997 Atmospheric Flight Mechanics Conference, New Orleans, LA, AIAA Paper 97-
3658, August 11-13, 1997, pp. 11

- Mitcheltree RA, Moss JN, Cheatwood FM, Greene FA, Braun RD (1999)
Aerodynamics of the Mars Microprobe entry vehicles
JOURNAL OF SPACECRAFT AND ROCKETS 36 (3): 392-398 MAY-JUN 1999
- Moss JN, Blanchard RC, Wilmoth RG, Braun RD (1998)
Mars Pathfinder Rarefied Aerodynamics: Computations and Measurements
36th AIAA Aerospace Sciences Meeting and Exhibit, Reno, Nevada, AIAA 98-0298,
January 12-15, 1998
- Moss JN, Blanchard RC, Wilmoth RG, Braun RD (1999)
Mars Pathfinder rarefied aerodynamics: Computations and measurements
JOURNAL OF SPACECRAFT AND ROCKETS 36 (3): 330-339 MAY-JUN 1999
- Nier AO, Hanson WB, McElroy MB, Seiff A, Spencer NW (1972)
Entry Science Experiments for Viking 1975
Icarus v16 p74-91
- Nier AO, Hanson WB, Seiff A, McElroy MB, Spencer NW, Duckett RJ, Knight TCD,
Cook WS (1976)
Composition and structure of the Martian atmosphere - Preliminary results from
Viking 1
Science, vol. 193, Aug. 27, 1976, p. 786-788.
- Peterson VL (1965a)
A technique for determining planetary atmosphere structure from measured
accelerations of an entry vehicle
NASA TN D-2669, Ames, 22p
- Peterson VL (1965b)
Analysis of the errors associated with the determination of planetary atmosphere
structure from measured accelerations of an entry vehicle
NASA-TR-R-225
- Queen EM, Cheatwood EM, Powell RW, Braun RD, Edquist CT (1999)
Mass Polar Lander aerothermodynamic and entry dispersion analysis
JOURNAL OF SPACECRAFT AND ROCKETS 36 (3): 421-428 MAY-JUN 1999
- Schofield JT, Barnes JR, Crisp D, Haberle RM, Larsen S, Magalhaes JA, Murphy JR,
Seiff A, Wilson G (1997)
The Mars Pathfinder atmospheric structure investigation meteorology (ASI/MET)
experiment
Science, Vol. 278, Iss. 5344, p. 1752 (1997)
- Seiff A (1963)
Some possibilities for determining the characteristics of the atmospheres of Mars and
Venus from gas-dynamic behavior of a probe vehicle
NASA TN D-1770, Ames, 35p
- Seiff A, Reese DE (1965a)
Use of entry vehicle responses to define the properties of the Mars atmosphere

Advances in the Astronautical Sciences, v19, p419 - 445

Seiff A, Reese DE (1965b)

Defining mars' atmosphere - a goal for the early missions.

ASTRONAUTICS AND AERONAUTICS, VOL. 3, FEB. 1965, P. 16-21. 9 REFS.

Seiff A (1968)

Direct measurements of planetary atmospheres by entry probes.

AMERICAN ASTRONAUTICAL SOCIETY, CONFERENCE ON ADVANCED SPACE EXPERIMENTS, ANN ARBOR, MICH., SEP. 16-18, 1968. AAS PAPER 68-187

Seiff A (1971)

Scientific questions and measurement approaches for a probe entering the atmosphere of Jupiter

ANNUAL MEETING ON JUPITER ORBITERS AND PROBES - A PRELIMINARY ASSESSMENT OF REQUIREMENTS AMERICAN ASTRONAUTICAL SOCIETY, ANNUAL MEETING, 17TH, SEATTLE, WASH., JUN. 28-30, 1971., AAS PAPER 71-148

Seiff A, Reese DE, Sommer SC, Kirk DB, Whiting EE, Niemann HB (1972)

PAET: An Entry Probe Experiment in the Earth's Atmosphere

Icarus, vol. 18, p.525-563

Seiff A, Kirk DB (1976)

Structure of Mars' atmosphere up to 100 kilometers from the entry measurements of Viking 2

Science, vol. 194, Dec. 17, 1976, p. 1300-1303

Seiff A (1976)

The Viking atmosphere structure experiment - Techniques, instruments, and expected accuracies

Space Science Instrumentation, vol. 2, Sept. 1976, p. 381-423.

Seiff A (1977)

Large Probe/Small Probe atmosphere structure experiment

Space Science Reviews (ISSN 0038-6308), vol. 20, no. 4, June 1977, p. 479-482.

Seiff A, Kirk DB (1977)

Structure of the atmosphere of Mars in summer at mid-latitudes

Journal of Geophysical Research, vol. 82, Sept. 30, 1977, p. 4364-4378.

Seiff A, Kirk DB, Sommer SC, Young RE, Blanchard RC, Juergens DW, Lepetich JE, Intrieri PF, Derr JS (1979)

Structure of the atmosphere of Venus up to 110 kilometers - Preliminary results from the four Pioneer Venus entry probes

Science, vol. 203, Feb. 23, 1979, p. 787-790

Seiff A, Lepetich JE, Juergens DW (1980a)

Atmosphere structure instruments on the four Pioneer Venus entry probes

IEEE Transactions on Geoscience and Remote Sensing, vol. GE-18, Jan. 1980, p. 105-111.

Seiff A, Kirk DB, Young RE, Blanchard RC, Findlay JT, Kelly GM, Sommer SC (1980b)
Measurements of thermal structure and thermal contrasts in the atmosphere of Venus and related dynamical observations - Results from the four Pioneer Venus probes
Journal of Geophysical Research, vol. 85, Dec. 30, 1980, p. 7903-7933.

Seiff A (1982)
Post-Viking models for the structure of the summer atmosphere of Mars
Advances in Space Research, vol. 2, no. 2, 1982, p. 3-17.

Seiff A, Kirk DB (1982)
STRUCTURE OF THE VENUS MESOSPHERE AND LOWER THERMOSPHERE
FROM MEASUREMENTS DURING ENTRY OF THE PIONEER VENUS
PROBES
ICARUS 49 (1): 49-70 1982

Seiff A (1983)
Thermal structure of the atmosphere of Venus
IN: Venus (Eds Hunten, Colin, Moroz). Tucson, AZ, University of Arizona Press, 1983, p. 215-279.

Seiff A, Schofield JT, Kliore AJ, Taylor FW, Limaye SS, Revercomb HE, Sromovsky LA, Kerzhanovich VV, Moroz VI, Marov MY (1985)
Models of the structure of the atmosphere of Venus from the surface to 100 kilometers altitude
Advances in Space Research (ISSN 0273-1177), vol. 5, no. 11, 1985, p. 3-58.

Seiff A (1990)
Entry-probe studies of the atmospheres of earth, Mars, and Venus - A review (Von Karman Lecture)
AIAA, Aerospace Sciences Meeting, 28th, Reno, NV, Jan. 8-11, 1990. 26 p. AIAA PAPER 90-0765

Seiff A, Kirk DB (1991)
Waves in Venus's middle and upper atmosphere - Implications of Pioneer Venus probe data above the clouds
Journal of Geophysical Research (ISSN 0148-0227), vol. 96, July 1, 1991, p. 11,021-11,032.

Seiff A (1991)
Atmospheres of earth, Mars, and Venus, as defined by entry probe experiments
Journal of Spacecraft and Rockets, v28, n3, 265-275

Seiff A, Knight TCD (1992)
The Galileo Probe Atmosphere Structure Instrument
Space Science Reviews (ISSN 0038-6308), vol. 60, no. 1-4, May 1992, p. 203-232

- Seiff A (1993)
MARS ATMOSPHERIC WINDS INDICATED BY MOTION OF THE VIKING
LANDERS DURING PARACHUTE DESCENT
JOURNAL OF GEOPHYSICAL RESEARCH-PLANETS 98 (E4): 7461-7474 APR
25 1993
- Seiff A, Kirk DB, Knight TCD, Mihalov JD, Blanchard RC, Young RE, Schubert G,
von Zahn U, Lehmacher G, Milos FS, Wang J (1996)
Structure of the atmosphere of Jupiter: Galileo probe measurements
Science, vol. 272, p. 844-845 (1996).
- Seiff A, Kirk DB, Knight TCD, Young LA, Milos FS, Venkatapathy E, Mihalov JD,
Blanchard RC, Young RE, Schubert G (1997a)
Thermal structure of Jupiter's upper atmosphere derived from the Galileo probe
SCIENCE 276 (5309): 102-104 APR 4 1997
- Seiff A, Tillman JE, Murphy JR, Schofield JT, Crisp D, Barnes JR, LaBaw C,
Mahoney C, Mihalov JD, Wilson GR, Haberle R (1997b)
The atmosphere structure and meteorology instrument on the Mars Pathfinder lander
JOURNAL OF GEOPHYSICAL RESEARCH-PLANETS 102 (E2): 4045-4056 FEB
25 1997
- Seiff A, Blanchard RC, Knight TCD, Schubert G, Kirk DB, Atkinson D, Mihalov JD,
Young RE (1997c)
Wind speeds measured in the deep jovian atmosphere by the Galileo probe
accelerometers
NATURE 388 (6643): 650-652 AUG 14 1997
- Seiff A, Kirk DB, Knight TCD, Young RE, Mihalov JD, Young LA, Milos FS,
Schubert G, Blanchard RC, Atkinson D (1998)
Thermal structure of Jupiter's atmosphere near the edge of a 5- μ m hot spot in the
north equatorial belt
JOURNAL OF GEOPHYSICAL RESEARCH-PLANETS 103 (E10): 22857-22889
SEP 25 1998
- Smith DE, Lerch FJ, Nerem RS, Zuber MT, Patel GB, Fricke SK, Lemoine FG (1993)
AN IMPROVED GRAVITY MODEL FOR MARS - GODDARD MARS-MODEL-1
JOURNAL OF GEOPHYSICAL RESEARCH-PLANETS 98 (E11): 20871-20889
NOV 25 1993
- Sommer SC, Boissevain AG (1967a)
Atmosphere definition with a free-falling probe
ASTRONAUTICS AND AERONAUTICS, VOL. 5, FEB. 1967, P. 50-54. 7 REFS
- Sommer SC, Boissevain AG, Yee L, Hedlund RC (1967b)
The structure of an atmosphere from on-board measurements of pressure,
temperature, and acceleration
NASA TN D-3933, Ames, 56p
- Sommer SC, Yee L (1968)

An experiment to determine the structure of a planetary atmosphere
AMERICAN INST. OF AERONAUTICS AND ASTRONAUTICS, ANNUAL
MEETING AND TECHNICAL DISPLAY, 5TH, PHILADELPHIA, PA., OCT. 21-
24, 1968. AIAA PAPER 68-1054

Sommer SC, Yee L (1969)

An experiment to determine the structure of a planetary atmosphere
Journal of Spacecraft and Rockets, v6, n6, p704-710

Spencer DA, Braun RD (1996)

Mars Pathfinder atmospheric entry: Trajectory design and dispersion analysis
JOURNAL OF SPACECRAFT AND ROCKETS 33 (5): 670-676 SEP-OCT 1996

Spencer DA, Blanchard RC, Braun RD, Kallemeyn PH, Peng CY, Thurman SW
(1998a)

Mars Pathfinder Atmospheric Entry Reconstruction
Monterey, California, AAS 98-146, February 9-11, 1998

Spencer DA, Blanchard RC, Braun RD, Thurman SW (1998b)

Mars Pathfinder Atmospheric Entry Reconstruction
<http://techreports.jpl.nasa.gov/1998/98-0048.pdf>, Spacecraft Mechanics, Monterey,
California, USA, February 9, 1998

Spencer DA, Blanchard RC, Braun RD, Kallemeyn PH, Thurman SW (1999)

Mars Pathfinder entry, descent, and landing reconstruction
JOURNAL OF SPACECRAFT AND ROCKETS 36 (3): 357-366 MAY-JUN 1999

Tobak M, Peterson VL (1964)

Angle-of-attack convergence of spinning bodies entering planetary atmospheres at
large inclinations to the flight path
NASA-TR-R-210

Underwood JC (1993)

A 12 Degree of Freedom Parachute/Payload Simulation of the Huygens Probe
12th AIAA Aerodynamic Decelerator Systems Technology Conference and Seminar
(RAeS/AIAA) London, England, May 10-13, 1993, AIAA paper 93-1251

Vaughan RM, Kallemeyn PH, Spencer DA, Braun RD (1998)

Navigation Flight Operations for Mars Pathfinder
Monterey, California, AAS 98-145, February 9-11, 1998

Vaughan RM, Kallemeyn PH, Spencer DA, Braun RD (1999)

Navigation flight operations for Mars Pathfinder
JOURNAL OF SPACECRAFT AND ROCKETS 36 (3): 340-347 MAY-JUN 1999

Vinh NX, Busemann A, Culp RD (1980)

Hypersonic and planetary entry flight mechanics
Ann Arbor, Mich.. University of Michigan Press. c1980, 357p.. 27cm, ISBN
0472093045

Yinh NX, Brace FC (1974)

Qualitative and quantitative analysis of the exact atmospheric entry equations using Chapman's variables

International Astronautical Federation, International Astronautical Congress, 25th, Amsterdam, Netherlands, Sept. 30-Oct. 5, 1974, 36 p. IAF PAPER 74-010

Young RE, Magalhaes JA (2001)

In Memoriam Alvin Seiff (1922 - 2000)

Icarus v152 n1 pp1-3 (2001)